Joffe

Physics Library
QC
.P5812
v.56
no.3

THE PHYSICAL REVIEW

VOLUME 56 *Second Series* NUMBER 3

AUGUST 1, 1939

Published for the

AMERICAN PHYSICAL SOCIETY

by the

AMERICAN INSTITUTE OF PHYSICS
Incorporated

LANCASTER, PA., AND NEW YORK, N. Y.

UNIVERSITY OF MICHIGAN LIBRARIES

THE PHYSICAL REVIEW

A journal of experimental and theoretical physics established by E. L. Nichols in 1893

Published by the American Institute of Physics for the

American Physical Society

OFFICERS

President

JOHN T. TATE
University of Minnesota
Minneapolis, Minnesota

Vice President

JOHN ZELENY
Yale University
New Haven, Connecticut

Secretary

W. L. SEVERINGHAUS
Columbia University
New York, New York

Treasurer

G. B. PEGRAM
Columbia University
New York, New York

Local Secretary for the Pacific Coast

PAUL KIRKPATRICK
Stanford University
California

Editor

JOHN T. TATE
University of Minnesota
Minneapolis, Minnesota

BOARD OF EDITORS

JOHN T. TATE, *Editor* — J. W. BUCHTA, *Assistant Editor*

Associate Editors

K. T. BAINBRIDGE	A. L. HUGHES	W. BLEAKNEY
H. P. ROBERTSON	T. H. JOHNSON	G. BREIT
H. B. WAHLIN	F. A. JENKINS	D. M. DENNISON

Manuscripts for publication should be submitted to John T. Tate, University of Minnesota, Minneapolis, Minnesota.

Proof and all correspondence concerning papers in the process of publication, should be addressed to the Publications Manager, American Institute of Physics, 175 Fifth Avenue, New York, New York.

Subscription Price

United States and Possessions and Canada $15.00
Foreign $16.50

Back Numbers

Complete set: Series 2,[1] Vol. 1, 1913–Vol. 54, 1938—$390.00
Yearly rate: $16.50
Single copies: $1.50 each prior to July, 1929; $.75 each after July, 1929.

Subscriptions and orders for **back numbers** should be addressed to Prince and Lemon Streets, Lancaster, Pennsylvania, or to the American Institute of Physics, 175 Fifth Avenue, New York, New York.

Advertising is not accepted for the *Physical Review* but attention is called to the *Review of Scientific Instruments* and the *Journal of Applied Physics*, companion publications of the Institute, and media through which the field of physics can be reached most effectively. Rates and other information will be furnished on request.

Changes of address and complaints of failure to receive the *Physical Review* in the case of members of the American Physical Society, should be addressed to the Treasurer; in the case of other subscribers, to the Publications Manager. New copies can be sent free in response to complaints of non-delivery only if notice of non-delivery is received within three months of date of issue.

[1] For Series 1 inquire of Physics Department, Cornell University, Ithaca, N. Y.

The Physical Review is published semi-monthly at Prince and Lemon Streets, Lancaster, Pennsylvania.

Entered at the Post Office at Lancaster, Pennsylvania, as second class matter.

Acceptance for mailing at special rate of postage provided for in section 1103, Act of October 3, 1917, authorized September 6, 1945.

THE
PHYSICAL REVIEW
A Journal of Experimental and Theoretical Physics Established by E. L. Nichols in 1893
VOL. 56, NO. 3 AUGUST 1, 1939 SECOND SERIES

The East-West Symmetry of the Cosmic Radiation at Very High Elevations Near the Equator and Evidence that Protons Constitute the Primary Particles of the Hard Component

THOMAS H. JOHNSON AND J. GRIFFITHS BARRY, *Bartol Research Foundation of the Franklin Institute, Swarthmore, Pennsylvania and The Carnegie Institution of Washington, Washington, D. C.*

(Received May 29, 1939)

The east-west symmetry of the soft component of the cosmic radiation has been investigated near the equator by sending triple coincidence counters into the stratosphere with free balloons. The data were transmitted to a ground station by radio signals. Direct comparisons between eastern and western intensities were made on flights in which the orientation of the instrument was determined by means of a photo-cell actuated by light from the sun. On other flights we have studied the fluctuations which would be introduced into the counting rates by the rotation of the balloon if the radiation were asymmetric. The results show that the asymmetry is less than about seven percent, a value far below what would have been expected if all of the primary radiation were positive. Analysis shows that less than about ten percent of the intensity at a depth of one meter of water is attributable to unbalanced positives. Contrasting this result with that found from the asymmetry at sea level that the mesotrons of the hard component are produced entirely by positive primaries, it becomes necessary to conclude that the mesotrons are produced in the upper atmosphere, not by the primary electrons of the soft component, but by an independent primary component consisting probably of protons or some other more massive positive ion. Reasons based upon the electrical properties of space are advanced to show that it is reasonable to expect to find protons of high energy in the primary cosmic radiation.

INTRODUCTION

IT is generally recognized that the cosmic radiation in the atmosphere consists of two components, the soft component, constituting most of the intensity at high elevations, and the hard component which predominates at sea level. The soft component is fully accounted for[1] by the assumption that its primaries are electrons of the energies required to pass through the earth's magnetic field but the interpretation of the hard component is more difficult. Its particles are mesotrons of intermediate mass and there are at least three reasons for thinking that these particles are created in the atmosphere by some other type of primary particle. In the first place the energies of the mesotrons at sea level are incompatible with the latitude effect if the mesotrons are themselves the primary particles. If one computes the energy distribution of these rays at the top of the atmosphere by adding to the energies of the rays found at sea level that which is known to be lost in passing through the atmosphere, about half of the primary rays would have an energy less than 15 Bev and would not be able to reach the earth at the equator. The observed latitude effect on the other hand is less than ten percent.[2] Secondly, mesotrons are

[1] R. Serber, Phys. Rev. **54**, 317 (1938); H. Snyder, Phys. Rev. **53**, 960 (1938); J. F. Carlson and J. R. Oppenheimer, Phys. Rev. **51**, 220 (1937).

[2] This argument was first advanced in a slightly different form by Bowen, Millikan and Neher, Phys. Rev. **53**, 217 (1938). See also L. W. Nordheim, Phys. Rev. **53**, 694 (1938).

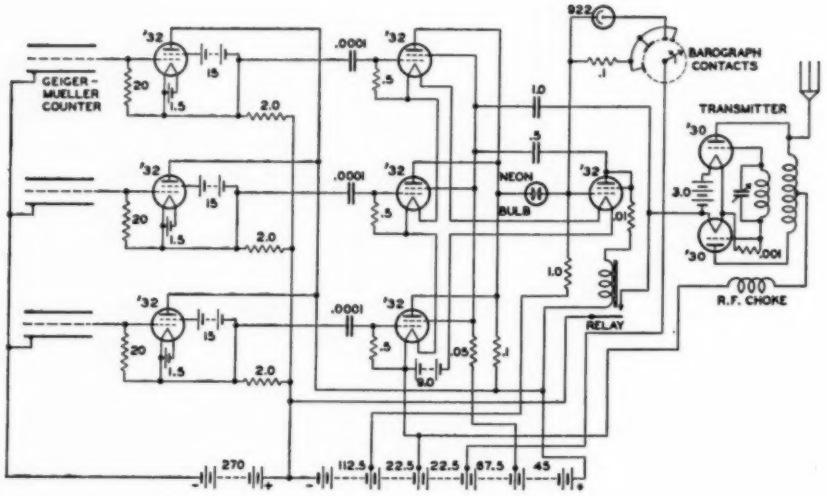

FIG. 1. Circuit used in the balloon apparatus. Capacities are given in microfarads, resistances in megohms, vacuum tubes by RCA, and G. E. Vapor Lamp Company.

probably unstable and would not survive a long journey through space. The mean life found from the experiments[3] corresponds with a path through space of only 150 km in the case of particles of 10 Bev energy. Thirdly, the equality of the numbers of positives and negatives found in the cloud-chamber experiments[4] is incompatible with the east-west asymmetry unless the mesotrons are secondaries produced in the atmosphere. There is at the most but a slight preponderance of positives at sea level whereas the asymmetry indicates that practically all of the primary particles of the hard component are positive.[5] There can thus be little doubt that the mesotrons are secondaries produced in the atmosphere and the problem arises to determine what type of particles compose their primary radiation.

If the electrons of the soft component were also the primaries of the hard component, it would be necessary to suppose that these are largely positrons in order to explain the sea-level asymmetry. In that event the soft component should also show a considerable asymmetry. On the other hand, if the mesotrons are produced by some other type of primary particle, the soft component primaries might be equally positive and negative and show no east-west asymmetry. The first attack on this question was made by one of us[6] in 1934 by measuring the east-west asymmetry of small showers produced in two centimeters of lead at an atmospheric depth of six meters. In those experiments it was shown that the asymmetry was less than a percent or two, compared with a fifteen-percent asymmetry of the penetrating component at the same station, although it was known from the variation of the same type of shower with latitude that the primary rays involved were field sensitive. However, in view of possible uncertainties attending those experiments in regard to which component was chiefly involved in the effects measured and in regard to the directional selectivity of the instrument, the matter obviously deserved further study.

EXPERIMENTS

Following a period of development of the radio balloon technique[7] we have at last succeeded in measuring the asymmetry of the

[3] For a discussion of these experiments and their interpretation see H. Euler and W. Heisenberg, *Ergebn. d. Exakt. Naturwiss.*, 1938. See also T. H. Johnson and M. A. Pomerantz, Phys. Rev. **55**, 104 (1939).

[4] P. M. S. Blackett, Proc. Roy. Soc. **A159**, 1 (1937).

[5] A resumé of these experiments and their interpretation was given by T. H. Johnson, Rev. Mod. Phys. **10**, 193 (1938).

[6] T. H. Johnson, Phys. Rev. **47**, 318 (1935).

[7] T. H. Johnson, J. Frank. Inst. **223**, 339 (1937); Phys. Rev. **54**, 151 (1938); Curtiss, Astin, Stockmann, Brown and Korff, Phys. Rev. **53**, 23 (1938).

cosmic radiation near the equator at high elevations where the intensity is largely that of the soft component.[8] The flights were sent up from the Barro Colorado Island Laboratory of the Institute for Research in Tropical America, located in the Panama Canal Zone 20° north of the geomagnetic equator. In that latitude the band of energies contributing to the asymmetry is nearly as great as at the equator itself. Out of a total of ten flights, four resulted in complete records from which direct comparisons could be made of the intensities in the eastern and western directions at depths of less than one and one-half meters of water. Two of the remaining flights yielded exceptionally good cosmic-ray data but the orientation record was lacking. These data have been useful nevertheless for a study of the possible fluctuations which would be introduced by the rotation of the balloon if the radiation were asymmetric.

On all of these flights the cosmic rays were detected by a train of three coincidence counters with the principal axis of the train inclined 60° from the zenith. Each counter was four inches long and one-half inch in diameter and the extreme counters were separated one and one-half inches from center to center. Half or more of the counter area was sensitive for a range of zenith angles of about 20° and a range of azimuths of about 90°. The counters were filled to a pressure of 15 cm Hg with a mixture of ten percent hydrogen and ninety percent neon, and their operating potential was about 500 volts. A vacuum tube circuit (Fig. 1) already described by one of us[9] was used for stabilizing the discharges, and with this arrangement the recovery time was so short that no appreciable inefficiency was experienced at the counting rates attained in the stratosphere. With the triple coincidences the accidental rate was also low and amounted, according to tests made at the start of each flight, to less than two or three percent of the counting rates observed in the stratosphere. The coincidence selection stage employed the usual Rossi parallel plate connection with neon tube coupling to the output stage. The pulses resulting from coincidences were prolonged to produce radio signals of sufficient duration for satisfactory recording by means of two capacity coupled feedbacks to the screen grid circuit of the selection stage from the plate of the output tube and from the relay contact, respectively. The resulting pulses were about one-quarter of a second long, a time which depended entirely upon the circuit and was quite independent of the amplitude of the input pulse as long as the latter was sufficient to produce the initial flash in the neon tube. The barograph has also been described elsewhere.[10] In addition to the usual contacts for indicating the barometric pressure and the temperature the barographs used for this series of flights were also provided with a third contact for indicating the orientation. This contact was fixed in position but was connected to the output tube through a photo-cell upon which the rays of the early morning sun could fall when the counter train was pointing eastwards. The corresponding signal was transmitted only during the eastern half of the rotation cycle. The radio transmitter consisted of two RCA 30 tubes in push pull with capacity tuning in the grid circuit, and was operated from a 135-volt plate battery. All B-voltages were supplied by Burgess V30FL batteries and the additional high voltage for the counters by National Carbon Company X-180 batteries. The entire apparatus with batteries and rigging weighed about nine pounds.

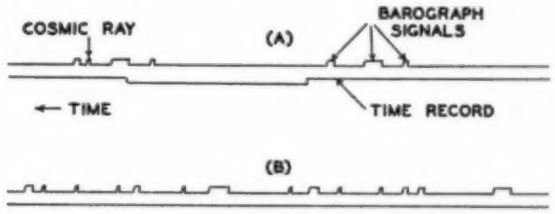

FIG. 2. Two portions of a flight record covering about ten seconds; (*A*) near sea level and (*B*) in the stratosphere.

The recording apparatus located at the ground station consisted of a National 1–10 super-regenerative receiver with one stage of radio-frequency amplification. The output from the power stage was rectified with a diode and then

[8] A brief preliminary report of these experiments has already been published. T. H. Johnson and J. G. Barry, Phys. Rev. **55**, 503 (1939).

[9] T. H. Johnson, Rev. Sci. Inst. **9**, 218 (1938).

[10] T. H. Johnson and S. A. Korff, Rev. Sci. Inst. **10**, 82 (1938).

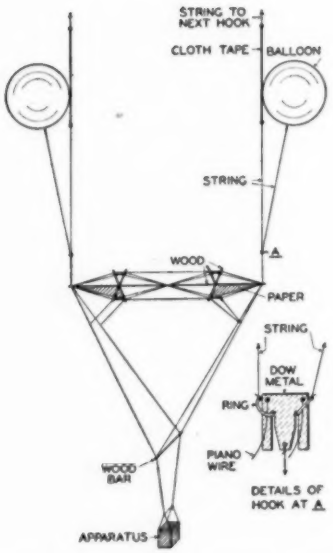

FIG. 3. Suspension used for attaching apparatus to the balloons for the asymmetry experiments. The ten-foot spacing bar was rotated by paper vanes attached at each end. The lower suspension allowed the apparatus to hang vertically. The hooks shown in the insert permitted the fragments of the exploded balloons to fall away. The radio transmitter, not shown, hung above the apparatus.

passed through two stages of direct coupled amplification to a magnetic recording pen which traced a line on a paper tape. Two portions of the record of one of the flights are shown in Fig. 2.

For the asymmetry studies the apparatus was suspended by two strings of balloons separated by a ten-foot spacing rod, Fig. 3. Paper vanes were attached to the ends of this rod so that as the balloons ascended the entire rigging rotated slowly in azimuth. The lower suspension was designed to keep the instrument vertical in spite of unequal forces from the two strings of balloons, after one of the balloons had burst. Each balloon was attached by means of a special release hook, the details of which are shown in the insert, so that after the bursting the remnants of the balloon fabric fell away from the rigging, eliminating the uncertain factor in the final weight of the equipment. It was thus possible to calculate the inflations so that the flights would come into static equilibrium after the bursting of the first balloon and several flights were realized in which the balloons remained at one level for several hours. On most of these flights six balloons have been used, inflated so that with five balloons the instrument would just float. The average ceiling pressure was 30 mm Hg and the initial rising velocity was about 500 ft. per minute. At this speed the rotation varied irregularly from one-half to three revolutions per minute, but after the bursting of the first balloon the rotational speed decreased to about one revolution in five minutes. Most of the data were obtained with the lower rotational speeds.

Unfortunately none of the four flights for which the record was complete stayed at the ceiling for a long period of time and it has been necessary to combine all of the data recorded on these flights at elevations above a depth of one and one-half meters of water. The data are not sufficient to show how the asymmetry varies with elevation, but they are consistent in regard to the average asymmetry for the higher levels. A resumé of these data is given in Table I. The average asymmetry calculated from the four flights is

$$\alpha = 2(j_w - j_e)/(j_w + j_e) = 0.072. \qquad (1)$$

No very reliable estimate of the probable error of the final average can be made other than to note the variations from one flight to another.

On two other flights the orientation signal failed to operate satisfactorily although the cosmic-ray data were remarkably good. One of these flights remained at a pressure of 35 mm for seven hours with a continuous counting rate of about 120 counts per minute; the other remained for four hours at a pressure of 49 mm. Subsequent experience under similar circumstances showed that the rotation of the balloon

TABLE I. *Resumé of data.*

Flight No.	Minimum Depth (Meters of Water)	East Counts	East Time (min.)	East Rate j_e	West Counts	West Time (min.)	West Rate j_w	α
110	0.40	1100	28.3	38.9	1523	35.4	43.0	0.10
112	0.45	277	10.5	26.3	413	14.9	27.6	.048
113	0.60	464	18.5	25.1	680	24.6	27.6	.095
B	0.33	554	19.3	28.7	740	23.8	31.1	.080
Average weighted according to the total counts								0.072*

* The discrepancy between this value and that published in our preliminary account (reference 8) arises from the fact that in our earlier reductions we did not realize the existence of certain spurious counts which occurred on the western half of the rotation cycle during the time when the photo-cell signal would have been transmitted if the cell had been illuminated. During that brief period the dark current through the cell raised the potential of the output tube grid and made the circuit less selective against single and double discharges. Since the period when these pulses could be recorded was known it was a simple matter to make this correction.

during this level portion of the flight must have continued at the rate of about one revolution in four minutes. Hence if there were an asymmetry in the radiation the rotation should introduce a fluctuation into the counting rate when broken down into periods short compared with that of the rotation. The data for one hundred ten-second periods from each of three flights have been analyzed with the results contained in Table II. Two of these flights are those referred to above and the third was flight 110 for which the orientation data were also available. If the time for the transmission of a signal could be neglected and the fluctuations were of a purely statistical nature the sums of the squares of the deviations from the average should be equal to the total number of counts recorded. The actual fluctuations were somewhat less than would have been expected on this basis and a correction was required for the dead time following each pulse during which a second pulse would have failed to record. If the dead time be designated by τ and the true counting rate, which would have been recorded if τ were equal to zero, by $\bar{N}$, then the average number of counts recorded in unit time is obviously

$$\bar{M}=\bar{N}/(1+\bar{N}\tau). \quad (2)$$

Similarly if in a given interval of unit length the actual number of counts which would have been recorded with $\tau=0$ is N, then the probable number of counts actually recorded is

$$M=N/(1+N\tau). \quad (3)$$

Thus the squares of the deviations of the observed counts from the average of the observed counts may be written as

$$(M-\bar{M})^2=(N/(1+N\tau)-\bar{N}/(1+\bar{N}\tau))^2 \doteqdot (N-\bar{N})^2(1-4\bar{N}\tau). \quad (4)$$

Thus the mean square deviation averaged over a large number of intervals, n, is given by

$$(1/n)\sum_n (M-\bar{M})^2 \doteqdot \bar{N}(1-4\bar{N}\tau) \doteqdot \bar{M}(1-3\bar{M}\tau). \quad (5)$$

The last column of Table II contains the mean of the squares of the deviations to be expected statistically in the case where $\tau=0.0085$ of the interval, a value obtained from the measurement of the width of the pulses on the actual records.

TABLE II. *Analysis of data.*

Flight No.	Depth (Meters of Water)	Average Counts per ten sec. Interval	Mean of the Squares of 100 Deviations	Mean Square Deviation Expected from Statistics
103	0.47	14.1	9.0	9.0
104	0.66	13.7	8.2	8.9
110	0.40	4.30	3.8	3.8

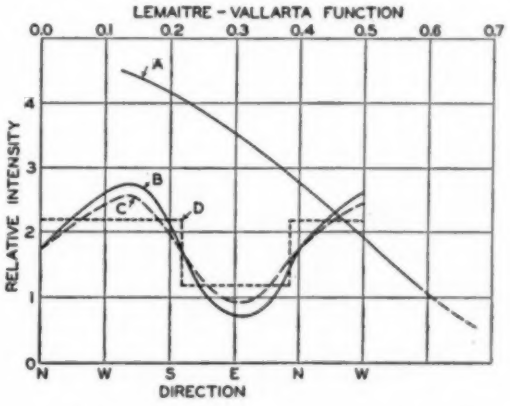

FIG. 4. Curves showing the asymmetry to be expected at 60° from the zenith and at a depth of $\frac{3}{4}$ meter of water calculated on the assumption that all of the soft component primary rays are positive. Curve A is the intensity at a depth of $1\frac{1}{2}$ meters of water in the vertical direction plotted as a function of the low energy limit expressed in terms of the Lemaitre-Vallarta function (scale above). Curve B is the azimuthal variation of the intensity at zenith angle 60° and depth $\frac{3}{4}$ meters, calculated from curve A (scale below). Curve C is that which would be measured, instead of B, with counters of the aperture used in the experiments. The square lines D represent the intensities as they are averaged by our method of taking observations.

It is seen that the expected values are in close agreement with those found from the data and there is thus no evidence of an azimuthal asymmetry from the fluctuations. If there had been a sinusoidal variation of intensity with azimuth of amplitude N_1 counts per interval this would have introduced a contribution to the mean square deviation of amount $\frac{1}{2}N_1^2$, and if we say that this contribution must have been less than ten percent of total mean square deviation in order not to have shown itself in the results we may conclude, in the case of flight 103 for example, that $N_1<1.3$ counts per interval or about ten percent of the average counting rate. The peak asymmetry is thus less than twenty percent, and the difference between the

average counting rates on the eastern and western sides of the meridian, corresponding to the asymmetry given by (1), must be less than 13 percent. The fluctuational analysis is thus not in disagreement with the direct measurements.

Discussion

In order to perceive the significance of the observed asymmetry in relation to that which would be expected if all of the primaries were positive, the following calculation has been based upon the balloon flight data of Bowen, Millikan and Neher.[11] The vertical intensity at a depth of one and one-half meters of water has been determined from the experimental curves by the method of Gross[12] and plotted in curve A, Fig. 4 as a function of the low energy limit expressed in terms of the Lemaitre-Vallarta parameter. The same curve should also represent the intensity at the 60° inclined direction at a depth of $\frac{3}{4}$ meter if the intensity is a function of $h \sec\theta$. Making use of Lemaitre and Vallarta's determinations[13] of the azimuthal variation of the low energy limit for the latitude of 20°, curve A has been converted into curve B which should represent the azimuthal variation of intensity if all of the primaries were positive. Because of the finite aperture of our counter train which admits rays from a range of azimuths, the curve C represents what would have been observed if the observations had been precisely correlated with azimuthal angle. Since we have observed only the average counting rates on the eastern and western halves of the cycle our results are to be compared with the squared lines, D. Thus if all of the primaries were positive we would have expected to find an asymmetry of 0.60 instead of the value 0.072 as given by Eq. (1). Since this calculation is based upon the observed latitude effect the discrepancy cannot be attributed to neutral rays but is to be accounted for by the presence of negative primaries. If j^+ and j^- represent the intensities per unit range of the energy in this region of the primary spectrum, produced by positive and negative primaries, respectively, and if K designates the total intensity produced by neutral rays and rays whose energies exceed the upper limit of the asymmetric component, and if ΔE is the average range of energy contained in the asymmetric component, our results can be represented by the equation

$$2(j^+ - j^-)\Delta E/(j^+\Delta E + j^-\Delta E + 2K) = 0.072, \quad (6)$$

whereas if j^- were zero in this region of the spectrum and a positive intensity $j^{+\prime}$ accounted for all of the variation of intensity with latitude, then we should have expected the asymmetry to be represented by

$$2j^{+\prime}\Delta E/(j^{+\prime}\Delta E + 2K) = 0.60 \quad (7)$$

where $j^{+\prime}$ must be chosen equal to $j^+ + j^-$ in order to preserve the same latitude effect in both instances. It thus follows by simple arithmetic that

$$j^-/(j^+ + j^-) = 0.44$$

and

$$j^+/(j^+ + j^-) = 0.56. \quad (8)$$

That part of the intensity produced by positives unbalanced by negatives is thus of the order of twelve percent of the total field sensitive intensity in this region of the spectrum. A part, if not all, of this intensity can be accounted for by the hard component and we must conclude that the soft component is very nearly balanced as regards the numbers of primary rays of the two signs of charge.*

In drawing the conclusion that an absence of an asymmetry is indicative of a balance between positives and negatives in the primary beam it is of course necessary to assume that there has been no appreciable alteration in the direction of the rays from that of their primaries after entry into the atmosphere. Inasmuch as no

[11] Bowen, Millikan and Neher, Phys. Rev. **53**, 855 (1938).
[12] See reference 4, page 197.
[13] See reference 4, page 218.

* The following argument that some of the asymmetry may be attributable to the soft component was pointed out in conversation by L. W. Nordheim. Since at a depth of one meter the soft component has multiplied to about thirty times the number of primary rays and if the hard component has not undergone an appreciable multiplication then the number of primary hard component rays, equal to ten percent of the total radiation at a depth of one meter, is $0.1 \times 30 = 3$ times the number of primary soft rays. But the total energy, and therefore the total number of rays in the hard component, cannot be more than about ten percent of the total radiation. Therefore it is necessary to assume, either that the asymmetry is less than is indicated by the figures in Eq. (1), or that the hard component has undergone a multiplication of the order of thirty-fold at a depth of one meter, or that part of the asymmetry may be attributed to the soft component.

heavy matter lay above the counters no appreciable scattering could be readily accounted for.† The possibility of a spread of direction due to magnetic deflection of the secondary electrons of lower energies is discussed in the following paper[14] where it is shown that this effect cannot account for an average deflection of more than about five degrees. Furthermore the correction for this effect would be of a second order, for the rays produced by primaries from nearer the horizon would tend to increase the asymmetry while those from nearer the vertical would tend to diminish it. At the elevation of our measurements the variation of intensity with zenith angle is not rapid and the two effects would tend to balance each other. Thus there seems to be no escape from the conclusion that the soft component is composed of very nearly equal numbers of positives and negatives.

Contrasting this property of the soft component with the fact revealed by sea-level asymmetry measurements that the hard component is produced by primaries which are nearly all positive, it seems impossible to attribute the hard component to the soft component electrons as primaries, and it becomes necessary to suppose that some other type of primary particle produces the mesotrons.[15] Since the primaries of the hard component cannot be electrons, and, for the reasons cited in the introduction, they cannot be mesotrons, the next possibility in order is that they are protons, a suggestion which has been frequently made as an explanation of the asymmetry.[16] Although no protons which could be primaries are found in the cosmic radiation at sea level,[17] their absence may well be attributed to a nuclear absorption in which the mesotron production may be an important process. The cross section for nuclear collisions should be at least of the order of $\pi r_0^2 = 2.5 \times 10^{-25}$ for which the absorption coefficient is 1.0 per meter of water, and only one ray in 25,000 would reach sea level. Absorption coefficients of this order have already been found for large bursts, for slow neutrons, and for nuclear explosions. At least the latter two phenomena might be interpreted as resulting from primary protons.

It may also be pointed out that the well-known difficulty in explaining the 40° position of the knee of the latitude effect is removed by the assumption that the primary rays of the hard component are protons. The critical energy with which protons are admitted at 40° latitude is 6.4 Bev and the maximum kinetic energy that a proton of this energy could impart to a mesotron of one-tenth the proton mass in a head-on collision is 3.1 Bev. This figure is in more satisfactory agreement with the energy lost by ionization in passing through the atmosphere than the value 7.5 Bev obtained from the primary electron hypothesis, so that the latitude of the knee may be that where the mesotrons of maximum energy are just able to penetrate the atmosphere.

Reasons for expecting to find protons in the primary cosmic radiation, regardless of the nature of the initial cosmic-ray particle or of the process by which it acquired its initial energy, have already been advanced by one of us.[18] At the source we assume the existence of matter in the familiar static form in which protons are positive and electrons are negative, and we may assume that either (a) electrons or (b) protons acquire an initial energy of the order of cosmic-ray energies. In case (a) the electron current charges the source to a high positive potential and in the electrostatic field thus created the electrons lose part of their energy and protons or other positively ionized particles are accelerated. When equilibrium is finally established the two currents will just balance one another and at all distances from the source

$$\rho^+ v^+ = \rho^- v^-, \tag{9}$$

where ρ^+ and ρ^- are the average space densities

† Even the shower rays from lead, observed in cloud-chamber experiments at sea level, lie within about 30° of the primary direction and in air this spread would be considerably less.

[14] T. H. Johnson, Phys. Rev. **56**, 226 (1939).

[15] The fact that electrons at sea level do not produce mesotrons was already indicated by the shower studies of Janossy (Proc. Camb. Phil. Soc. **34**, 614 (1938)) and by the cloud-chamber photographs of Anderson and of Street and Fussell (privately communicated). The latter evidence is not entirely clear however since there have been instances where shower particles have failed to multiply as much as would have been expected if they were electrons. The independence of the soft and hard component primaries was pointed out by one of us on the basis of the symmetry of showers in 1935 (reference 16).

[16] T. H. Johnson, J. Frank. Inst. **220**, 25 (1935); Phys. Rev. **54**, 385 (1938). Protons have also been invoked on other grounds by various writers.

[17] C. G. Montgomery, D. D. Montgomery, W. E. Ramsey and W. F. G. Swann, Phys. Rev. **50**, 403 (1936).

[18] T. H. Johnson, Phys. Rev. **54**, 385 (1938); J. Wash. Acad., June, 1939.

of positive and negative particles and v^+ and v^- are their average velocities at the same distance. At great distances from the source the space charge density of the positives and negatives must also balance for otherwise potential differences irreconcilable with the observed passage of charged particles through space would develop. This consideration leads to the condition,

$$\rho_\infty{}^+ = \rho_\infty{}^-, \tag{10}$$

where $\rho_\infty{}^+$ and $\rho_\infty{}^-$ are the charge densities at some suitably large distance from the source. Combining (9) and (10) we obtain

$$v_\infty{}^+ = v_\infty{}^-. \tag{11}$$

The ultimate velocities of the two types of particles are equal and their ultimate energies must therefore be in proportion to their respective rest masses. Thus the protons should have two thousand times more energy than the electrons and they alone should be able to reach the earth at the equator. In case (b) the considerations and the final result are identical with those of case (a) and the conclusion is the same regardless of which particle received the original energy. The ionic conductivity of intergalactic space and the production of positive and negative electron pairs add some complexities to these considerations which have not as yet been fully investigated, but which do not seem necessarily to invalidate the explanation of the proton component. Such considerations may also provide an explanation of the soft component primary electrons.

ACKNOWLEDGMENTS

Finally we wish to acknowledge the encouragement and financial assistance given to us by the Carnegie Institution of Washington upon the recommendation of ex-President Merriam and his Committee for the Coordination of Cosmic Ray Studies upon which so much of the success of this work has depended. We have also made full use of the facilities of Bartol Research Foundation in the preparation of the instruments, and for certain elements of the expenses. For this assistance we are indebted to Dr. W. F. G. Swann. The work in the Canal Zone was greatly facilitated by the earnest cooperation of Mr. James Zetek, Director of the Barro Colorado Island Laboratory and by Colonel S. B. Akin of the U.S.A. Signal Corps.

AUGUST 1, 1939 PHYSICAL REVIEW VOLUME 56

The Angular Dispersion of the Cosmic Radiation in the Upper Atmosphere Resulting from Deflections of Low Energy Particles in the Earth's Magnetic Field

T. H. JOHNSON

Bartol Research Foundation of the Franklin Institute, Swarthmore, Pennsylvania, and Research Associate of the Carnegie Institution of Washington, Washington, D. C.

(Received May 29, 1939)

In order to estimate the diffuseness of the soft component of the cosmic radiation with respect to the direction of the primary particles for the interpretation of east-west asymmetry measurements a calculation has been made of the angular spread of secondary rays produced by deflections in the earth's magnetic field for the idealized case where the primary particles are incident unidirectionally from the vertical. Both radiation and ionization losses have been considered and it is found that at a depth of one meter of water rays whose energies exceed 15 Mev lie within thirty degrees and half of the intensity is within five degrees of the original direction. The beam broadens at higher elevations or when lower energies are included. The correction to the recent east-west asymmetry measurements at very high elevations because of this effect is wholly negligible.

IN the interpretation of cosmic-ray directional effects at sea level one may assume with close approximation that the rays which enter the instrument have the same direction as the pri-

maries which produced them.[1] At higher elevations where the loss per cm is less the rays may bend through considerable angles before they come to rest and it is necessary[2] to consider if such deflections might have an effect upon the observed asymmetries and zenith angle distributions. In order to estimate the possible magnitude of this effect in relation to the interpretation of asymmetry measurements made recently[3] at a depth of about one-tenth of the atmosphere the angular distribution in the east-west vertical plane at the equator has been calculated for this depth in the case where the primary rays are incident vertically and the electrons are produced and lose energy in accordance with the theory of the radiation and ionization processes.[4] In the first approximation it is assumed that all electrons have the vertical direction at the point where they are produced by photons in the multiplicative process and the deflections suffered thereafter are investigated. In the second approximation the deflections of the electrons one stage back of the final one have been taken into consideration and it is shown that these do not contribute appreciably to the final spread of the beam.

The energy loss in unit distance may be represented by the well-known approximation

$$-dE/ds = p(E+\alpha), \tag{1}$$

in which s is the orbital distance expressed in appropriate units, p is the pressure in atmospheres and α is the energy lost by ionization in one unit of path length at atmospheric pressure.

If ρ is the radius of curvature of the orbit of an electron at any point and ρ_α that when the electron's energy is α, Eq. (1) may be written

$$-d\rho/ds = p(\rho+\rho_\alpha). \tag{2}$$

Eq. (2) can be solved analytically if either one of two approximations are made. (*a*) It may be assumed that p is constant along the orbit and the solution will be appropriate for electrons produced with low energies near the ends of their range, for in this case the total variation of p along the orbit will be small; or (*b*) it may be assumed that ρ_α is small compared with ρ and the solution will be appropriate for high energies. In this approximation the variation of p along the orbit is taken into consideration.

Approximation (*a*)

With p=constant Eq. (2) may be integrated giving

$$\rho = \rho_\alpha(2e^{-ps}-1), \tag{3}$$

where s is measured in the direction of motion from the point on the trajectory where $\rho=\rho_\alpha$. The deflection at a final point s_f on the orbit with respect to the direction at the original point s_0 is given by

$$\theta = \int_{s_0}^{s_f}(1/\rho)ds = (1/p\rho_\alpha)\log((2-e^{ps_0})/(2-e^{ps_f})). \tag{4}$$

From (3) and (4) the initial radius of curvature is expressed as a function of the angle of deflection and the distance traversed ($Hx_0=s_f-s_0$) by

$$\rho_0/\rho_\alpha = (e^{pHx_0}-1)/(1-e^{-p\rho_\alpha\theta}), \tag{5}$$

a relation which will be useful in discussing the distribution function. Here H represents the height of the homogeneous atmosphere expressed in the units of s. In terms of the deflection and the final radius of curvature the initial radius has the value

$$\rho_0/\rho_\alpha = \rho_f e^{p\rho_\alpha\theta}/[\rho_\alpha+\rho_f(1-e^{p\rho_\alpha\theta})]. \tag{6}$$

The length of the orbit Hx_0 is given as a function of the same variables by

$$x_0 = (1/Hp)\log[\rho_\alpha/(\rho_\alpha+\rho_f(1-e^{p\rho_\alpha\theta}))]. \tag{7}$$

From Eq. (5) is derived the Jacobian for the transformation from the ρ_0, x_0 system to the θ, x_0 system;

$$\partial(\rho_0, x_0)/\partial(\theta, x_0) = \partial\rho_0/\partial\theta = \rho_0^2 pe^{-p\rho_\alpha\theta}/(e^{pHx_0}-1). \tag{8}$$

The Jacobian for the transformation from the

[1] Calculations of the deflections of secondaries at sea level have been made by I. S. Bowen, Phys. Rev. **45**, 349 (1934) and by B. Rossi and A. Garbasso, Rendi. Lincei. **15**, 62 (1932).

[2] The necessity of considering the possible reductions in east-west asymmetry arising from this effect has been brought to the writer's attention by W. F. G. Swann, to whom acknowledgment is gratefully made.

[3] See the previous paper by T. H. Johnson and J. G. Barry.

[4] W. Heitler, *The Quantum Theory of Radiation* (Oxford).

x_0, ρ_0 system to the θ, ρ_f system is obtained from Eqs. (6) and (7).

$$\partial(x_0, \rho_0)/\partial(\theta, \rho_f) = \rho_f\rho_\alpha e^{p\rho_\alpha\theta}/[\rho_\alpha+\rho_f(1-e^{p\rho_\alpha\theta})]^2. \quad (9)$$

We also note for future reference that any ray which is deflected through an angle θ and has a final radius of curvature greater than $\rho_{f\,\min}$ must have come from an orbital distance greater than $Hx_{0\,\min}$ where

$$x_{0\,\min}=(1/Hp)\log \rho_\alpha/[\rho_\alpha+\rho_{f\,\min}(1-e^{p\rho_\alpha\theta})], \quad (10)$$

while a ray which deflects through angle θ and starts with a radius less than $\rho_{0\,\max}$ must have come from an orbital distance less than $Hx_{0\,\max}$ where

$$x_{0\,\max}=(1/Hp)\times\log[\rho_\alpha+\rho_{0\,\max}(1-e^{-p\rho_\alpha\theta})/\rho_\alpha]. \quad (11)$$

Approximation (*b*)

Neglecting ρ_α and assuming that the elevation above the end point of the orbit is equal to the orbital distance, as is very nearly true for rays incident vertically, Eq. (2) takes the form

$$\partial\rho/\rho=-pe^{-(s_f-s)/H}ds=pHe^{-x}dx, \quad (12)$$

where again $x=(s_f-s)/H$ and p is the pressure at the final point on the orbit where $x=0$. By integration of (12) one obtains

$$\rho=\beta\rho_\alpha\exp[-pHe^{-x}], \quad (13)$$

where $\beta=\exp[pHe^{-s_f/H}]$ and s_f is measured from the point on the orbit where $\rho=\rho_\alpha$.

The deflection at the end point $x=0$ with respect to the direction at the level x_0 where the ray was produced is given by

$$\theta=\int_{s_0}^{s_f}(1/\rho)ds=(H/\beta\rho_\alpha)\int_0^{x_0}\exp[pHe^{-x}]dx$$

$$=(H/\beta\rho_\alpha)\int_{pHe^{-x_0}}^{pH}(e^t/t)dt, \quad (14)$$

$$=(H/\beta\rho_\alpha)F(x_0) \quad (15)$$

where

$$F(x_0)=x_0+Hp(1-e^{-x_0})+H^2p^2(1-e^{-2x_0})/2.2!+\cdots. \quad (16)$$

From (13) and (15), the original radius of curvature ρ_0 is given in terms of the deflection and orbital distance by

$$1/\rho_0=\theta\exp[pHe^{-x_0}]/HF(x_0) \quad (17)$$

and the Jacobian for the transformation from the ρ_0, x_0 system to the θ, x_0 system is

$$\partial(\rho_0, x_0)/\partial(\theta, x_0)=\partial\rho_0/\partial\theta=\rho_0^2\exp[pHe^{-x_0}]/HF(x_0). \quad (18)$$

We also note for future reference that if the final radius of curvature $\rho_f=\beta\rho_\alpha e^{-pH}$ is to be greater than a certain minimum value $\rho_{f\,\min}$ then a ray deflected through angle θ must have come from a height greater than,

$$x_{0\,\min}=F^{-1}(\rho_{f\,\min}\theta e^{pH}/H), \quad (19)$$

where F^{-1} is the inverse of the function F.

Let us now consider the number of electrons produced with an initial radius of curvature in the range ρ_0 to $\rho_0+d\rho_0$ in the element of path x to $x+dx$ where the atmospheric pressure is pe^{-x}. If we limit the discussion to those levels above that where the cosmic-ray intensity has its maximum we may assume with close approximation to the fact that the cosmic-ray intensity and therefore the photon intensity is increasing approximately in proportion to the pressure. At levels not too far above that of the maximum where the degree of multiplicity is large we may also assume that as regards its energy distribution the photon intensity has attained an equilibrium and as Carlson and Oppenheimer[5] and Nordheim[6] have shown, may be represented by an inverse square of the energy. Thus the variation of the photon component with elevation and with energy may be represented by the function

$$\Gamma(\epsilon, x)d\epsilon=(Ape^{-x}/\epsilon^2)d\epsilon. \quad (20)$$

The probability that a photon of energy ϵ will produce an electron of energy in the range E to $E+dE$ while traversing the path distance Hdx_0

[5] J. F. Carlson and J. R. Oppenheimer, Phys. Rev. **51**, 220 (1937). According to these authors the lower energy particles are distributed about as E^{-1} whereas the E^{-2} distribution is a suitable approximation for high energies. The angular distribution is not especially sensitive to the choice of this distribution and the E^{-2} law has been used.

[6] L. W. Nordheim, Phys. Rev. **51**, 1110 (1937).

is given by the well-known approximation

$$P(\epsilon, E)dEdx=(\sigma Hpe^{-x_0}/\epsilon)dx_0dE, \quad (21)$$

where σ is approximately proportional to log ϵ and, for the range of energies whose contribution to the electron intensity is appreciable, may be regarded as constant. The number of electrons produced in the energy range dE and path dx_0 is

$$\int_{\epsilon=E}^{\infty} P(\epsilon, E)\Gamma(\epsilon, x_0)dx_0dEd\epsilon = (ae^{-2x_0}/E^2)dx_0dE \quad (22)$$

and since the radius of curvature ρ_0 is proportional to the energy E the number of electrons

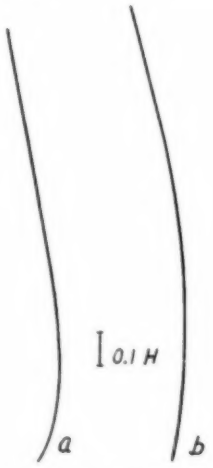

FIG. 1. Typical orbits terminating at a pressure of 0.1 atmosphere. (*a*) An orbit calculated with Approximation (*a*) terminating with an energy of 0.1α. (*b*) An orbit calculated with Approximation (*b*) for the case where the electron has an energy α at the same level as that of orbit (*a*).

produced in the range dx_0 with radii between ρ_0 and $\rho_0+d\rho_0$ is

$$N(\rho_0, x_0)d\rho_0dx_0=(be^{-2x_0}/\rho_0^2)d\rho_0dx_0. \quad (23)$$

Transforming this distribution from the ρ_0, x_0 system to the θ, x_0 system the approximation (*a*) gives by Eq. (8)

$$N(\theta, x_0)d\theta dx_0 = (bpe^{-p\rho_\alpha\theta}e^{-2x_0}/(e^{pHx_0}-1))dx_0d\theta \quad (24)$$

and the approximation (*b*) gives by Eq. (18)

$$N(\theta, x_0)d\theta dx_0=\{(b/H) \times\exp[pHe^{-x_0}-2x_0]/F(x_0)\}dx_0d\theta. \quad (25)$$

The required distributions of intensity with respect to direction are found by integrating Eq. (24) or (25) over all values of x_0. Since we wish to take into consideration only those electrons whose energies exceed a certain lower limit for which the radius of curvature is $\rho_{f\,\min}$ this integral is made to extend upwards from a minimum value of x_0 given by (10). Likewise if we wish to use approximation (*a*) and Eq. (24) only if the rays are produced with an energy less than a certain maximum value for which the radius is $\rho_{0\,\max}$ the integral of (24) may be made to extend to an upper limit $x_{0\,\max}$ given by Eq. (11). Approximation (*b*) may then be used for the remainder of the high energy particles by carrying out the integration of Eq. (25) from a lower limit $x_{0\,\min}$ given by Eq. (19) in which the minimum final radius is equal to the maximum initial radius used in determining the upper limit of the integral of Eq. (24).

In carrying out the calculations it is first of all necessary to fix upon an appropriate unit of length for which Eq. (1) will be valid. The cross section for radiative collisions is appreciably lower for electrons of energy less than 10^9 volts than the constant value pertaining to high energy particles, and there is some variation of cross section with energy so that the energy losses cannot be expressed accurately by an equation of the type of Eq. (1). The variation of the cross section with energy is small, however, and if the unit of length is chosen with respect to the band of energies which contributes largely to the spread of the beam the approximation involved in the use of Eq. (1) will be a close one. Since low energies predominate in the spreading effect it will be necessary to use a somewhat longer unit of distance than that usually chosen for discussion of the multiplicative process and in the following calculations the value of 475 meters of air at atmospheric pressure has been used, corresponding to the cross section for radiative losses by rays of energy 20 Mev. The ionization loss per unit distance is then $\alpha=3.3\times10^5\times475=15\times10^7$ ev* and in the equatorial field of 0.3 gauss the radius of curvature is $\rho_\alpha=167\times10^4$ cm $=35$ units. The height of the

* This figure is based upon 100 ions per cm in air at 1 atmos. If Brode's value of 60 ions is used the spread represented in Fig. 2 will be increased by 66 percent.

homogeneous atmosphere in the same units is given by $H=17$. Orbits calculated with approximations (a) and (b) are shown in Fig. 1 for the case where the terminal pressure is $p=0.1$ atmosphere. Orbit (a) has the terminal radius $\rho_f=0.1$ and orbit (b) has been drawn so that the ray has the energy α at the same level in both orbits.

In computing the distribution of intensity shown in Fig. 2 rays whose terminal energies are

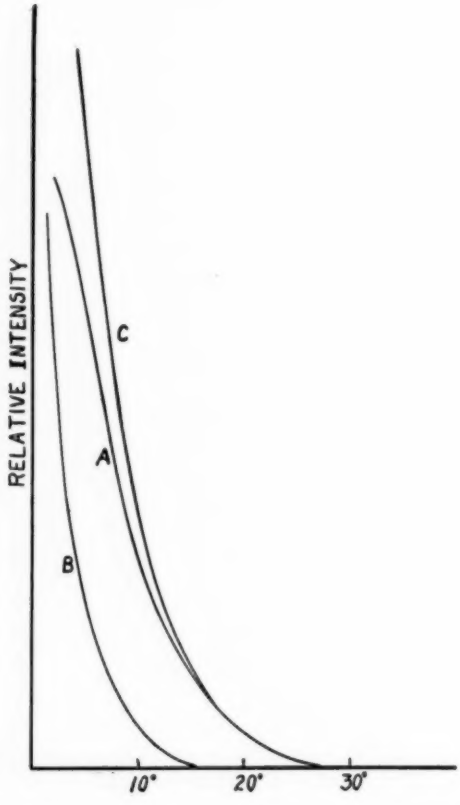

FIG. 2. The first-order angular spread at a depth of 0.1 atmosphere for secondaries produced by primaries incident unidirectionally from the vertical. Curve A, the contribution of electrons produced with an energy less than α, calculated by Approximation (a). Curve B, the contribution of electrons of terminal energy greater than α, calculated by the Approximation (b); and curve C, the total intensity of electrons of all energies.

greater than 0.1α have been included. This is approximately the energy limit to which a coincidence train of thin walled counters will respond. Curve A represents the contribution to the intensity by rays whose initial energies were less than α, and whose final energies were between 0.1α and α. This curve has been computed with Approximation (a). Curve B represents the contribution of rays of final energy greater than α and has been computed by means of Approximation (b). The distribution of the total intensity represented by curve C is not sensitive to the choice of the limit to which each approximation is used; no very important differences in the final result appeared when this limit was taken as $0.6\ \rho_\alpha$, ρ_α, or ∞. In each case the intensity falls to zero for angles greater than 30° and half of the intensity lies within 5°. Since the primary rays have been considered exactly vertical the distribution rises abruptly for zero deflection.

SECOND-ORDER CALCULATION

In order to estimate the error in the results of the first-order calculation arising from the neglect of deflections occurring along electron trajectories of earlier stages of the multiplicative process, deflections which would have been communicated to photons and then passed on to the final electrons, a second-order calculation can be made in which the distribution in angle found from the first-order calculation is considered as applying to the electrons one stage before the final one. Here of course the deflections are half-positive and half-negative so that they may add to or subtract from the deflection in the final stage. If we designate quantities pertaining to the stage before the final one by primed symbols and restrict the calculations to Approximation (a) the distribution of electrons in this stage with respect to deflection θ' and final radius of curvature ρ_f' deduced with the help of Eqs. (6), (7), (9) and (23) is

$$N'(\rho_f', \theta')d\rho_f'd\theta' = (b/\rho_f'\rho_\alpha)e^{-p\rho_\alpha\theta'} \times[1+(\rho_f'/\rho_\alpha)(1-e^{p\rho_\alpha\theta'})]^{2/H_p}d\rho_f'd\theta'. \quad (26)$$

The probability that one of these electrons of energy $E_f' = k\rho_f'$ will produce a photon of energy ϵ to $\epsilon+d\epsilon$ while traversing the path element Hdx is approximately $Hpe^{-x}dxd\epsilon/\epsilon$ and the total number of photons of energy ϵ produced by electrons of all energies in the angle range θ' to $\theta'+d\theta'$ is

$$[Hpe^{-x}N'(\rho_f', \theta')/\epsilon]d\epsilon d\theta' d\rho_f' dx. \quad (27)$$

In equilibrium this number must equal the number of photons of the same energy converted in the same path element into electron pairs. The latter quantity may be expressed by $\sigma Hpe^{-x}\Gamma(\epsilon, \theta', x)d\epsilon d\theta' dx$ where $\Gamma(\epsilon, \theta', x)d\epsilon d\theta$, is the number of photons of energy in the range ϵ to $\epsilon+d\epsilon$ and in the angle range $d\theta'$. Thus

$$\Gamma(\epsilon, \theta', x) = (1/\epsilon\sigma)\int_{\epsilon/k}^{\infty} N'(\rho_f', \theta')d\rho_f'. \quad (28)$$

This distribution of photons must now be considered as the primary radiation for the production of the electrons in the final stage. The number produced with energy between E and $E+dE$ in path element dx_0 and in the angle range $d\theta'$ is

$$N(E, x_0, \theta')dEdx_0d\theta' \cdot$$

$$= \frac{Hpe^{-x_0}}{\sigma}\int_{\epsilon=E}^{\infty} [\Gamma(\epsilon, \theta', x_0)/\epsilon]d\epsilon dx_0 dEd\theta'. \quad (29)$$

The number of electrons starting off in the direction θ' to $\theta'+d\theta'$ with radius in the range ρ_0 to $\rho_0+d\rho_0$ at the distance x_0 above the detector is thus

$$N(\rho_0, x_0, \theta')d\rho_0 dx_0 d\theta' = \frac{kHpe^{-x_0}}{\sigma} dx_0 d\rho_0 d\theta'$$

$$\times \int_{\epsilon=k\rho_0}^{\infty} \frac{d\epsilon}{\epsilon^2}\int_{\epsilon/k}^{\infty} N'(\rho_f', \theta')d\rho_f. \quad (30)$$

Transforming this to the θ, x_0 system by means of Eqs. (5) and (8) and integrating over all values of x_0, the number of electrons which have started at angle θ' and are deflected through angle θ is

$$N(\theta, \theta')d\theta d\theta' = kHp^2/\sigma e^{-p\rho_0\theta} d\theta d\theta'$$

$$\times \int_{x_0 \text{ min}}^{\infty} (e^{-x_0}/(e^{pHx_0}-1)dx_0\rho_0^2$$

$$\times \int_{k\rho_0}^{\infty} \epsilon^{-2}\int_{\epsilon/k}^{\infty} N'(\rho_f', \theta')d\rho_f' d\epsilon, \quad (31)$$

where ρ_0 is given by (5).

Graphical integration of Eq. (31) for various values of θ' shows that the spread of the beam in θ is essentially that shown by Fig. 2 if θ' is less than 0.1 but for values of θ' greater than 0.1 the spread in θ becomes rapidly less and for $\theta'=0.3$ half of the intensity lies within $\theta=0.05$ (3°). Thus the first-order calculation is correct within a factor of two and since the deflections in previous stages are half-positive and half-negative the distribution shown by Fig. 2 is doubtless correct to within fifty percent.

At higher elevations the orbits bend through larger angles and the distribution will have a proportionately wider spread. At larger zenith angles the variation of pressure along the orbit is less and the Approximation (*a*) will be more nearly correct for all energies. However the distribution in angle of the secondaries will not be appreciably different from that indicated in Fig. 2. If lower energies are included in the secondary beam the distribution spreads out to wider angles and, conversely, the secondaries will have more closely the direction of their primaries if the lowest energies are excluded.

Further Experiments on the Recoil of the Nucleus in Beta-Decay

H. R. CRANE AND J. HALPERN
University of Michigan, Ann Arbor, Michigan

(Received June 5, 1939)

Experiments on the recoil of the nucleus in the disintegration of Cl^{38} have been continued. The fact (which has been reported in earlier publications) that momentum is not conserved in the system consisting only of the nucleus and the emitted electron has been confirmed. By measuring the momenta of the electron and nucleus it has been possible to ascertain the direction of emission of the neutrino with respect to the direction of the electron in each case. Theoretical predictions according to both the Fermi and the K-U theory are plotted for comparison. The experimental data agree slightly better with the Fermi than with the K-U theory, but it is not safe to attach much significance to the results obtained on this aspect of the problem, because of the possibilities for rather large experimental errors. An investigation into the manner in which droplets in the cloud chamber are produced by the recoil atom has been carried out. Evidence is offered which indicates that the products resulting from dissociation of the gas molecules act as centers for condensation. This effect, in addition to ionization, accounts for the droplets observed.

INTRODUCTION

ABOUT a year ago[1,2] we reported our first results on the observation of the recoil of the atom resulting from the emission of a beta-particle by radiochlorine. In many of the cases observed the momentum of the atom was found to be much greater than the momentum of the emitted beta-particle, and this was considered as evidence that a third particle participates in the event; that is, evidence in the same sense that the apparent failure of the law of the conservation of energy is evidence for the participation of a third particle in the beta-disintegration. Since our last report we have repeated the experiment[3] with some improvements in technique and have obtained good confirmation of the important features of the results. It was our hope that with improved accuracy and a larger number of tracks we might be able to draw some conclusions about the direction of emission of the neutrino with respect to that of the electron. We have found that if the results indicate anything at all in this respect they favor slightly the predictions of the Fermi theory. The principal new fact which has appeared is that the production of droplets in the cloud chamber by the recoil atom is not due only to ionization, but is due in part to dissociation of molecules. The assumption that the atom makes a pair of droplets for each 30 ev energy is therefore not justified, and the calibration of the scale of energies has to be made in a different way, which will be described.

EXPERIMENTAL METHOD

The method used in the experiment may be reviewed briefly as follows. Radiochlorine, Cl^{38}, is produced by bombarding $MgCl_2$ with deuterons in the cyclotron, and is converted into ethyl chloride, C_2H_5Cl, which is a gas at ordinary temperatures. This is more satisfactory than ethylene dichloride, which we used in the earlier experiments, because of its greater volatility. Ten to 20 cc of ethyl chloride gas, made up partly of a nonradioactive and partly of the radioactive sample is introduced into the cloud chamber, which already contains air saturated with ethyl alcohol vapor at atmospheric pressure. The Cl^{38} atoms then disintegrate in the gas. The electric clearing field of the cloud chamber is short-circuited for a fraction of a second before each expansion, so as to allow the ions (and molecules) along the paths of the beta-rays to diffuse out into paths a few millimeters wide before the condensation occurs. It is by this means possible to count the individual droplets along the beta-ray path, and also to count the

[1] J. Halpern and H. R. Crane, Phys. Rev. **53**, 676(A) (1938).
[2] H. R. Crane and J. Halpern, Phys. Rev. **53**, 789 (1938).
[3] H. R. Crane and J. Halpern, Phys. Rev. **55**, 1123(A) (1939).

droplets in the spherical cluster at the point of origin of the track, which is presumably due to the recoil nucleus. The arrangement of the stereoscopic camera and the method of analyzing the photographs is the same as that described in our previous paper.

Results

The tracks obtained with the ethyl chloride vapor mixture are plotted in Fig. 1. Because the assumption that the energy of the recoil atom is 30 ev per droplet pair produced is no longer believed to be valid, we have been forced to adopt another method of normalizing the ordinate scale in terms of energy of the recoil atom. Fortunately we obtained one track of good quality in which the electron carried away nearly the entire energy of the disintegration. In this case we know the energy of the recoil atom, because the neutrino has nearly zero energy, and therefore its direction is unimportant. In other parts of the diagram (lower electron momentum) the highest of the points ought to correspond to cases in which the neutrino and electron were emitted in nearly the same direction, provided all directions are permitted, and provided there is a large number of points in the diagram. As a result of this reasoning, we have drawn the solid curves in Fig. 1 in the following way: We make the assumption that the energy of the neutrino is in all cases $W_0 - E_e$ where W_0 is the upper limit of energy of the beta-ray spectrum of Cl^{38} and E_e is the energy of the particular beta-ray. The momentum of the neutrino will then be $(W_0 - E_e)/C$ on the assumption that it has zero rest mass. This will not be altered appreciably, however, by assuming a rest mass as large as that of the electron. We calculate the energy of the recoil atom as a function of the momentum of the beta-particle for the two limiting cases: (1) that the electron and neutrino are emitted in the same direction and (2) that they are emitted in opposite directions. These limits are shown as curves (1) and (2) in Fig. 1, the ordinate scale being adjusted to fit the point at 11 mc, in which case the momentum of the electron alone determines the energy of the recoil atom.

Evidence that momentum is not conserved in the two-particle system

Without going any further in the experiment, we can see in Fig. 1 strong indications that momentum is not conserved in the system consisting only of the emitted beta-particle and the nucleus. This is best shown by those cases in which the beta-particle had a small momentum and in which the recoil atom produced a large number of droplets. Fortunately it is not necessary here to know the absolute relation between the number of droplets and the energy of the recoil atom. The mere fact that as large a cluster is often associated with a beta-particle of 3 or 4 mc momentum as with a beta-particle of nine or ten mc momentum indicates that conservation of momentum in the two-particle system is not possible, and the simplest assumption to make is that a third particle participates in the event

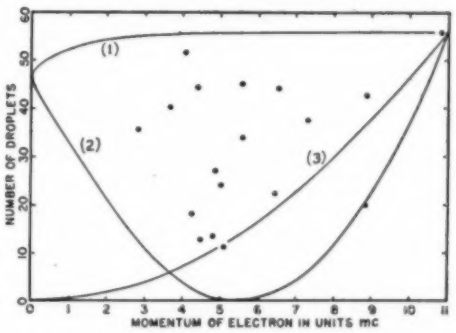

FIG. 1. Plot of the number of droplets in the cluster against the momentum of the emitted beta-particle. Each point in the diagram represents an individual disintegration, and the number of droplets in each cluster has been corrected for the number of droplets which is due to the escaping beta-particle, so that the number plotted represents only those due to the recoil atom. The curves shown have been calculated for the two limiting cases, (1) that in which the electron and neutrino escape in the same direction and (2) that in which they escape in opposite directions. Curve (3) shows what we should expect if momentum were conserved between the beta-particle and the nucleus (no neutrino).

Direction of emission of the neutrino

On the assumption that a neutrino participates in the disintegration, and that the above formulae for its energy and momentum are correct, we should be able to calculate the angle, ϕ, between the directions of emission of the neutrino and the electron for any one of the points in the diagram, Fig. 1. This would also have to be based upon some assumption as to the relation

between the number of droplets and the energy of the recoil atom. We have calculated the angle ϕ for all the cases in the diagram, on the simple assumption that the energy of the recoil atom is proportional to the number of droplets produced. We are aware that the relation is more complicated than this, but since it is not possible to determine it, the assumption that was made will have to suffice for a first approximation. Fig. 2 shows the distribution of the cases with respect to ϕ. On the same diagram theoretical curves for the distribution according to the K-U and Fermi theories are shown. Formulae for these have been given by Bloch and Moller[4] and by Hebb.[5] According to Bloch and Moller's formula, which is given in a convenient form for our purpose, the probability that the neutrino will be emitted within the solid angle $d\Omega$ at an angle ϕ with respect to the direction of the electron is

$$\text{K-U}: \quad \frac{1}{4\pi}\left(1-\frac{v}{c}\cos\phi\right)d\Omega$$

$$\text{Fermi}: \frac{1}{4\pi}\left(1+\frac{v}{c}\cos\phi\right)d\Omega$$

for a given velocity, v, of the electron. In plotting these we have transformed them into terms of the probability of emission within the angular interval $d\phi$ at an angle ϕ, in order to place the curves in the same diagram as our experimental values. The formulae become

$$\text{K-U}: \quad \tfrac{1}{2}\sin\phi\left(1-\frac{v}{c}\cos\phi\right)d\phi$$

$$\text{Fermi}: \tfrac{1}{2}\sin\phi\left(1+\frac{v}{c}\cos\phi\right)d\phi.$$

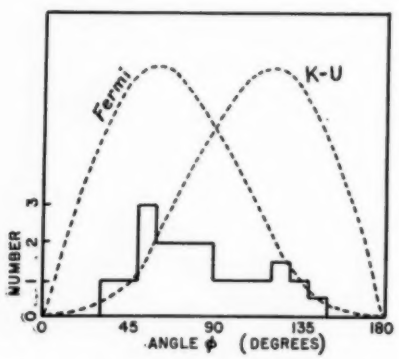

FIG. 2. Distribution of the angle between the directions of emission of the neutrino and the electron. The theoretical predictions based upon the K-U and the Fermi theories are given for comparison.

In the experimental data with which we are concerned, v/c ranges from 0.94 to 0.995. Rather than subdivide the data according to v/c, we have taken an arbitrary value, 0.98, to serve for all the data. The choice of this value is of little importance in determining the important features of the curves. It is seen in Fig. 2 that the experimental distribution is in slightly better agreement with the Fermi than with the K-U theory. Very little weight can be placed in this evidence, however, in view of the many possibilities for systematic error, and in view of the small number of points in the diagram. It is unsafe to draw any conclusions from this part of the experiment.

THE ROLL OF MOLECULAR DISSOCIATION IN THE PRODUCTION OF DROPLETS

In the course of our recent experiments two facts become apparent: (1) The number of droplets in a cluster was often more than could be accounted for by ionization by the recoil atom[6, 7] and (2) the number of droplets in the clusters (ordinate scale in Fig. 1) was influenced by the composition of the gas present in the chamber. We now believe that we have good evidence showing that droplets are caused by certain neutral molecules which are formed as a result of the dissociation of O_2, N_2, etc. by the recoil atom, and that this effect accounts for the two facts mentioned above. The existence of this effect is fortunate, because it increases the sensitivity of the experimental method.

It is well known that a heavy, slowly moving particle can be very efficient in bringing about dissociation of the molecules of a gas through which it passes. The amount of dissociation will be large compared to the amount of ionization when (to say it in simple language) the time of interaction with the gas molecule is short com-

[4] F. Bloch and C. Moller, Nature **136**, 911 (1935).
[5] M. H. Hebb, Physica **5**, 701 (1938).
[6] L. Wertenstein, Phys. Rev. **54**, 306 (1938).
[7] H. R. Crane and J. Halpern, Phys. Rev. **54**, 306 (1938).

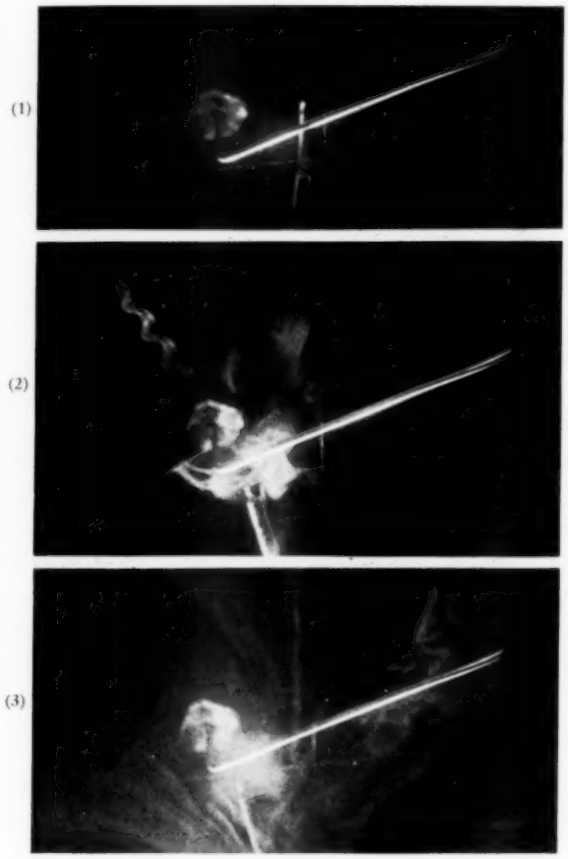

FIG. 3. Series of three consecutive photographs showing the effect of introducing a minute quantity of NO_2 into the cloud chamber. (1) (Top photograph.) The small capillary containing NO_2 turned into position ready to be broken by the cutter which is attached to the piston of the chamber. (2) Gas issuing from the broken capillary at the time of the first expansion of the chamber. The sinusoidal form of the main gas stream is due to vibration of the wire which holds the capillary. (3) The next expansion, showing that the cloud is spreading to the entire chamber.

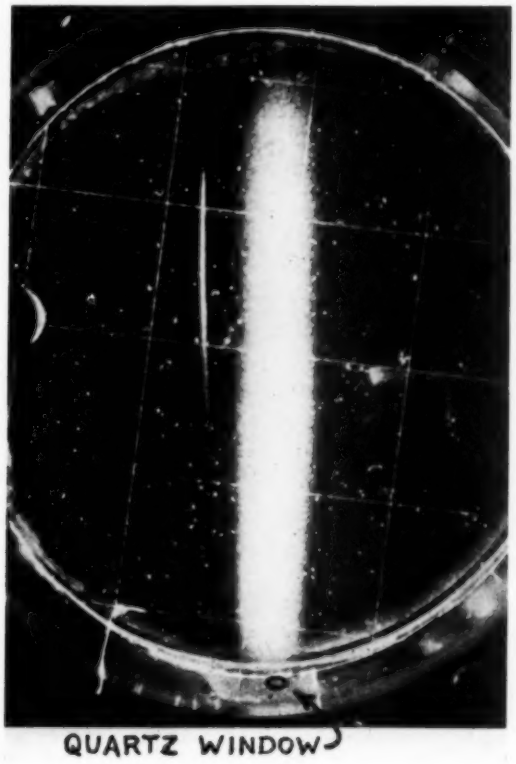

FIG. 4. Photograph of cloud chamber expansion which was made a few seconds after a narrow pencil of ultraviolet light was projected across the chamber. Before the expansion all the ions were drawn out of the space, so the effect shown here is due to neutral molecules. The small streak which appears at the side is an alpha-particle track.

pared to the periods of oscillation of the nuclei in the molecule and long compared to the classical periods of rotation of the electrons in the atomic orbits. The perturbation of the electrons will then be predominately adiabatic, while molecular excitation will occur, frequently to the dissociation level. In air, practically all of the atoms O and N thus set free will combine with other molecules to form NO_2, N_2O, O_3 etc. The combination will have to occur in triple collisions, to satisfy momentum and energy conservation, but at atmospheric pressure triple collisions are so frequent that the chemical reaction will be completed in a time which is short compared to the sensitive time of the cloud chamber. In our experiment there is also alcohol vapor, (C_2H_5OH) and ethyl chloride (C_2H_5Cl) in the cloud chamber, which increase the number of possible reactions. It is our belief that some, at least, of the molecules formed as a result of the dissociation, act as centers for the condensation of droplets in the cloud chamber.

TABLE I. *Resumé of results obtained upon the introduction into the cloud chamber of minute quantities of various gases.*

SUBSTANCE INTRODUCED	ESTIMATED CONCENTRATION IN CHAMBER	RESULT
NO_2	10^{-8}	dense cloud
N_2O	10^{-7}	medium cloud
CO_2	10^{-7}	no cloud
H_2O		no cloud
air		no cloud
HNO_3	10^{-10}	very dense cloud
NH_3	10^{-8}	very little cloud

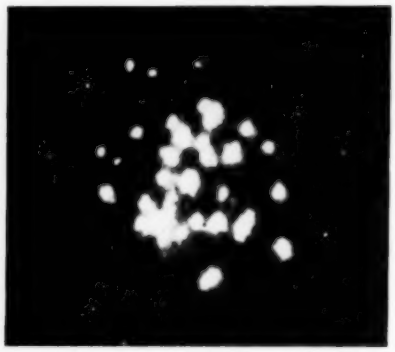

FIG. 5. Spherical cluster of droplets due to the recoil atom. In this case the ions have been drawn away, and the droplets which appear must therefore have condensed upon neutral molecules.

Experiments with NO_2, CO_2, N_2O, HNO_3, H_2O and air

The following experiments were tried to test the possibility mentioned above. A piece of drawn-out glass tubing about 1/10 mm inside diameter was filled with NO_2 gas at atmospheric pressure and a piece about 1 cm long was sealed off. This was placed in a clamp in the center of the cloud chamber. After the chamber had cleared and had become sensitive to electron tracks, the end of the capillary was clipped off just at the time of an expansion, by means of a cutter which was moved by the piston of the chamber. The stream of gas issuing from the capillary produced a dense cloud, and on the next expansion the cloud filled the entire chamber. A typical series of three photographs is shown in Fig. 3.

The release of like quantities of CO_2, H_2O vapor, and air, caused no appreciable cloud. N_2O caused a cloud, but not such a dense one as that caused by NO_2. The most potent agent for producing condensation which we found was nitric acid vapor. For testing this we cut a small round hole in the glass top-plate of the chamber and closed it with a rubber cork. The chamber was then cleared and adjusted so that good electron tracks were obtained. A fine glass filament (less than 0.1 mm diameter) was then wet with nitric acid. The cork was removed, and the filament quickly lowered into the chamber and out again without touching any part, and the cork replaced. Upon the next expansion an exceedingly dense cloud appeared, which soon filled the entire chamber. This was due to the nitric acid, and not to anything else which might have entered the chamber when the cork was removed, because the same motions were carried out without dipping the glass in the acid, and no cloud was produced. In each case in which a cloud was produced, it was not found possible to clear the chamber by repeated expansions (up to about 20 were tried). The chamber was opened, dried thoroughly with a stream of air and put together with fresh alcohol after each experiment.

A resumé of the substances tried, and the results are given in Table I. The question arose as to whether the cloud was caused by a fairly high concentration of the substance in a local region near the point where it was introduced. We therefore repeated the experiments, allowing time for the substance to diffuse throughout the chamber before bringing about the expansion. The results were the same.

Experiments with ultraviolet light

The question of concentration of the substance introduced in the air in the chamber has to be considered rather carefully. We must be sure that a droplet can grow around a *single molecule* of the substance. If the concentration were high, the condensation of a droplet might be initiated by the accidental grouping together of several molecules of the substance. If this were so, the result would have no bearing upon the case in which the substance is produced by the recoil atom in the beta-disintegration, because there the concentration is so small that two molecules of the substance would almost never come together in the same incipient droplet.

In order to liberate an extremely small amount of atomic oxygen in the chamber we resorted to the use of ultraviolet light. A quartz window 2 mm in diameter was cemented to the side wall of the chamber. A few seconds before the expansion a small arc was made just outside the window by touching a pair of copper wires together. The arc carried about two amperes for about a quarter of a second. The result was very striking, and is shown in Fig. 4. Photographs were taken with various intervals of time, from one to ten seconds, between the spark and the expansion, and at all times the electrical clearing

field was left on the chamber, so we are sure that none of the effects observed are due to ions. The only effect of varying the time interval was a variation in the width of the clouded strip in the chamber, due to diffusion. The extremely small amounts of the compounds synthesized by the weak ultraviolet light make it seem reasonably certain that the effect observed is not an effect of the concentration of the substances, but is due to the action of individual molecules in initiating the formation of droplets.

Isolation of droplet clusters produced by uncharged molecules

With this encouragement we proceeded to a more direct test. We repeated the experiment on the recoil of the atom resulting from the decay of Cl^{38}, with all conditions the same as before except that the electrical clearing field was not removed from the chamber at the time of expansion. The expectation was that if a Cl^{38} atom should disintegrate a short time (fraction of a second) before the expansion, the *ions* would be drawn out of the chamber by the electric field, while *uncharged* molecules would remain, and would move about only by diffusion. Many isolated clusters like the one shown in Fig. 5 were observed. In this case the ions comprising the electron track have been drawn away. The ions produced by the recoil atom have also been drawn away, and what remains is presumably due to neutral molecules, which have had time enough to diffuse into a cluster a few millimeters in diameter. A plot of the number of droplets in the clusters of this type which we obtained is shown in Fig. 6. The shape of this is complicated by the existence of the lower energy component[2] in the chlorine beta-ray spectrum. The clusters due to the lower component cannot be sorted out as they could in the other data, because of the absence of the electron track. The plot does show, however, that in some cases as many as 40 droplets are due to neutral molecules, whereas the total number of droplets (due to ions and molecules) extends up to only about 60. This indicates the great importance of the effects of dissociation.

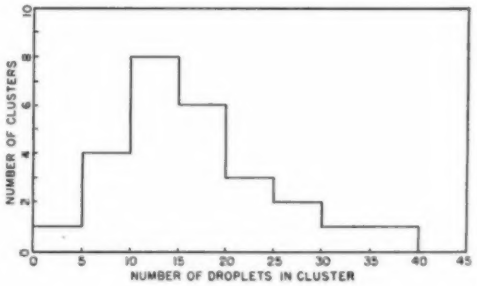

FIG. 6. Plot of the number of droplets in the clusters which were due to neutral molecules.

CONCLUDING REMARKS

A few remarks about the possibilities for extension of this experiment may be set down at this point. Since the number of droplets produced for a given energy of the recoil atom is dependent upon the chemical composition of the gas in the cloud chamber, it might be possible to find a gas mixture which would give many more droplets than we obtained in this experiment. Besides increasing the accuracy of the measurements on Cl^{38}, this might allow us to work with other radioactive elements, in which the energy of recoil is smaller.

The principal unknown in the method is, and always has been, the relation between the number of droplets and the energy of the recoil atom. Because of the complexity of the chemical reactions which can give rise to droplets, it is difficult to think of an auxiliary experiment in which this relation could be measured.

It may be pointed out that the fact that individual molecules of certain polar compounds can make their presence known in a cloud chamber, may have interesting applications in other kinds of research, such as physical chemistry.

The authors are grateful for the financial support of this work which was made available from the Rackham Endowment Fund. Professor J. M. Cork and the other members of the staff of the University of Michigan cyclotron have been very generous in supplying the radiochlorine for this experiment.

Delayed Gamma-Rays from Uranium Activated by Neutrons

J. C. Mouzon and R. D. Park
Duke University, Durham, North Carolina

(Received May 25, 1939)

A cloud chamber in a magnetic field was operated in conjunction with a source of neutrons in such a way as to observe gamma-rays emitted during the bombardment of uranium by neutrons and the number emitted about ½ second after bombardment in alternate expansions of the chamber. Although the energy distribution of the gamma-rays seems to be about the same in the two expansions, the total number of gamma-rays emitted during bombardment is considerably greater than those emitted ½ second after bombardment. This means that more gamma-rays are obtained which are coincident (or nearly so) with fission than gamma-rays associated with a period of as much as several seconds.

IN continuing the work previously reported[1] on gamma-rays from the uranium-neutron reaction a comparison has been made between gamma-rays emitted during bombardment and those emitted about ½ second after bombardment. Delayed gamma-rays from the uranium-neutron reaction have been reported by Roberts, Meyer and Wang.[2]

Apparatus

The neutrons used in these experiments are produced in the deuteron-deuteron reaction by the bombardment of a heavy-ice target with deuterons of about 350 kilovolts energy giving neutrons of 2.5 Mev. The high potential source is an unrectified transformer set capable of producing something over 500 kilovolts built up by cascading discarded x-ray transformers. At the present time three x-ray transformers are being used: two 115-kv units and one 300-kv unit. The three units are mounted on separate insulating platforms and are inclosed in corona shields. A coil wound for 110 volts was added to each high potential end of the transformers, and the old primary windings were discarded. The new 110-volt primary and tertiary windings make it possible to cascade these transformers in the usual commercial fashion. This scheme provides a moderate voltage at a minimum cost.

The three-section accelerating tube is of the same general design as Crane's[3] with the exception that it is mounted horizontally. Textolite insulating supports carry only the vertical load. Atmospheric pressure on the end of the tube provides a force of about 3000 lb. which holds the tube together.

The voltage is distributed over the three sections by means of leads to appropriate points on the transformers.

The grounded end of the accelerating tube projects through an 8″ brick wall into the control room. A motor driven set of contactors automatically controls the operation of the transformers, ion source, cloud chamber and camera.

Figure 1 shows a more or less typical photograph taken during the bombardment of the uranium, in which appears an electron track whose energy is about 5 Mev. The heavy recoil proton tracks will also be noted. (Air and alcohol were used in the chamber in all this work.)

Measurements

Two different experiments have been performed in which delayed gamma-rays from the uranium-neutron reaction have been observed by means of their recoil electrons and photo-electrons in a horizontal cloud chamber placed in a magnetic field. Three arrangements of the heavy-ice target and uranium with reference to the cloud chamber are shown in Fig. 2. (For simplicity the coils of the magnet are not shown.) Fig. 2(A) is the set-up used in the previous work on gamma-rays. In an effort to obtain a large yield of delayed gamma-rays the arrange-

[1] J. C. Mouzon, R. D. Park and J. A. Richards, Jr., Phys. Rev. **55**, 668 (1939).
[2] Roberts, Meyer and Wang, Phys. Rev. **55**, 510 (1939).
[3] H. R. Crane, Phys. Rev. **52**, 11 (1937).

ment in Fig. 2(B) was used. Uranium nitrate in thin rubber envelopes was wrapped around the target tube so as to subtend a very large angle. In view of the fact that cloud-chamber photographs were to be made after the bombardment of the heavy-ice target by deuterons had ceased, no lead was necessary between the target and chamber to absorb soft x-rays.

A test run without the beam on was first made and out of about 240 pictures only one electron track of energy as much as 2.1 Mev was observed, its energy being 2.14 Mev. (Only the horizontal projections of the tracks are measured.) A series of 890 photographs was then made with a one-second delay after a 1–2-second bombardment of the uranium. Only 15 recoil electron tracks with energies greater than 2.1 Mev were found. Seven of these had energies of 3 Mev or more. From these measurements compared to those on gamma-rays emitted during bombardment one might conclude that most gamma-rays are emitted immediately on or a very short time after the absorption of neutrons by the uranium nuclei. However, because of the uncertainty in the relative neutron intensities in these two experiments, this conclusion might be questioned. A further cause of uncertainty is the fact that if the majority of the delayed gamma-rays have a half-life of the order of several seconds, then the time of bombardment of 1–2 seconds was not sufficient to activate the uranium fully.

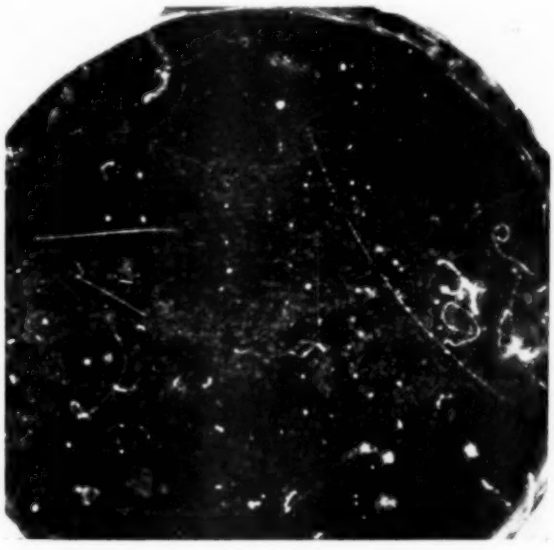

FIG. 1. A typical photograph of a high energy recoil electron track due to a gamma-ray from the uranium-neutron reaction. The energy of this electron is about 5 Mev.

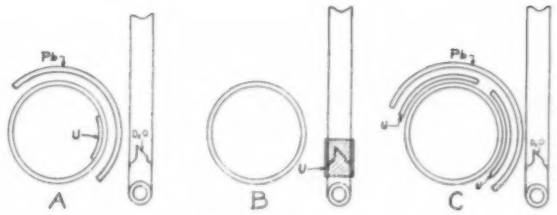

FIG. 2. Relative positions of heavy-ice target, uranium, and cloud chamber in three experiments. Arrangement (A) refers to the previous work on gamma-rays. (B) and (C) refer, respectively, to the first and second experiments on delayed gamma-rays.

A second experiment designed to make a direct comparison between delayed gamma-rays and the gamma-rays emitted during bombardment was performed. The control apparatus was adjusted so that alternate photographs (and corresponding cloud chamber expansions) could be made during and $\frac{1}{2}$ second after the bombardment of the uranium. The ion beam was on about three seconds at the time the direct photographs were made, and an eleven second bombardment preceded the delayed photographs. The time between photographs was about 30 sec. This alternate method of bombardment made certain that the average neutron intensity was the same during the two bombardments of the uranium. Fig. 2(C) shows the relative positions of the deuterium target, uranium and cloud chamber. The lead around cloud chamber served to absorb the soft x-rays from the tube. About 600 direct and the same number of delayed photographs were taken. The uranium was then removed and a check run made to get an idea of the number of gamma-rays due to radiative capture of the neutrons in lead and the other material present. Integral curves of the results of these measurements are plotted in Fig. 3 showing the energy distribution of the gamma-rays. The curves A and C correspond to the photographs taken while the ion beam was on with and without the uranium present, respectively. Curve B shows the energy distribution of delayed gamma-rays with uranium present, and curve D (based on only two tracks) gives the delayed gamma-ray distributio without

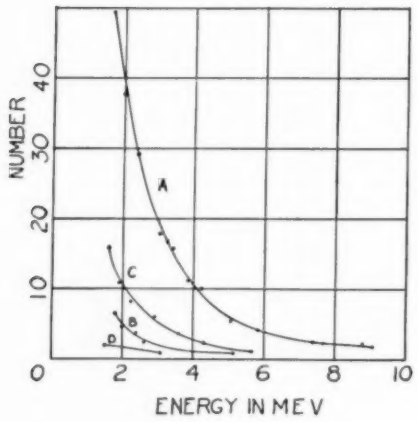

FIG. 3. Energy distributions of gamma-rays *vs.* total number of tracks. (These are integral curves.) A. Cloud chamber expanded during bombardment of uranium. B. Expansion delayed ½ sec. after bombardment of uranium ceased. C. Cloud chamber expanded with ion beam on but with uranium removed giving gamma-rays due to radiative capture of neutrons in the material around the chamber. D. Cloud chamber expansion ½ sec. after the ion beam was shut off with no uranium present. All curves correspond to the same number of photographs and to approximately the same neutron intensity.

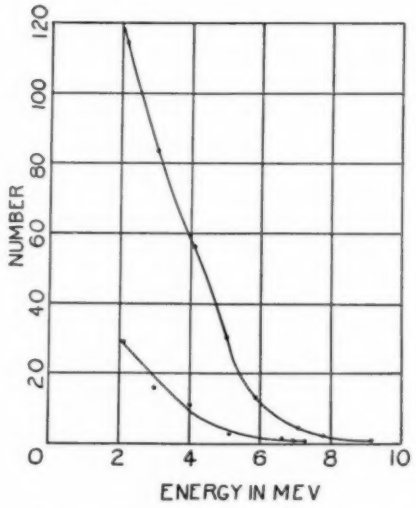

FIG. 4. Energy distribution of gamma-rays from the earlier experiment. Gamma-rays observed with and without uranium present are shown in the upper and lower curves, respectively.

uranium. Curves C and D were adjusted to correspond to the same neutron yield and the same number of photographs as curves A and B. An estimate of the neutron yields was made by counting recoil protons in the nondelayed pictures with and without the uranium.

RESULTS

For comparison the energy distribution of the gamma-rays previously studied is reproduced in Fig. 4. The marked similarity between the upper curves of Fig. 3 and Fig. 4 will be noted, showing good agreement between the two experiments. The data for Fig. 3(A) were taken with the uranium outside the cloud chamber, while the data for the upper curve of Fig. 4 were taken with the uranium contained in a 0.85-mm lead envelope inside the chamber. By comparing curves A and B of Fig. 3, it appears evident that the majority of gamma-rays from this reaction are emitted at the instant of fission or a very short time thereafter. This means that more gamma-rays are obtained which are coincident (or nearly so) with fission than gamma-rays associated with a period of as much as several seconds. No accurate conclusions can be reached regarding the periods of the delayed gamma-rays from this experiment, although these delayed gamma-rays may very well be associated with the periods reported by Roberts

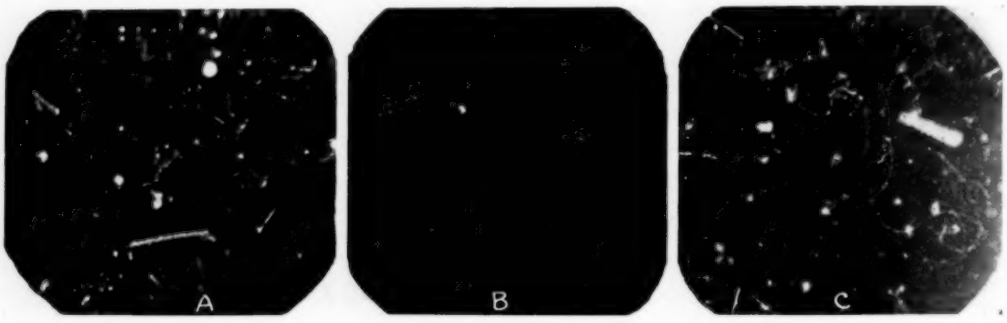

FIG. 5. Regenerative fission (?) (See photograph (A)). Three successive cloud-chamber photographs separated by 30 sec. B is delayed ½ sec. after 11 sec. of neutron bombardment of the uranium.

et al.[2] On the other hand, these measurements do not show any definite difference in the general energy distribution of the gamma-rays emitted during bombardment and after a delay of ½ second after bombardment. One delayed track (photographed in the first delay experiment discussed) had an energy of the order of 9 or 10 Mev, and the trend of curve B of Fig. 4 indicates that there might very well be high energy delayed gamma-rays.

We should like to call attention to an interesting photograph obtained during this work, Fig. 5(A). Fig. 5 shows a series of three successive photographs with 30-second intervals between them. (A) and (C) are taken during the bombardment of the uranium while (B) is the delayed picture. Picture (C) shows more than the average number of electron tracks on it, none of which have energies as great as 2 Mev. In picture (A) are seen many fairly high energy tracks, most of which show definite curvature, and most of which are about the same age. In only one other picture that we have taken have there been as many as two electrons of energies greater than 2 Mev. This is, therefore, a very exceptional photograph. The magnetic field was only 990 gauss which means that the energies are under 10 Mev. Because of the very large number of tracks it is difficult to measure many of them. (Four of these tracks were measured to have energies less than 8 Mev.) The occurrence of such a large burst of electrons might be attributed at once as being due to a cosmic-ray shower. If so, the shower did not occur near the cloud chamber because the directions of the tracks seem to be random. Also the energies involved are lower than is usual in cosmic-ray showers, although it is believed that such low energy showers have been photographed with a vertical cloud chamber. Another more interesting interpretation of this photograph would be that it shows a case of multiple fission, perhaps due to a regenerative or chain process.

Although the cloud chamber with air and alcohol was not very sensitive to neutrons, we do have evidence for delayed neutrons[2] in our delayed photographs. However, they are not numerous enough to warrant a systematic study.

In conclusion, we wish to acknowledge the aid of the Duke University Research Council in this work, and also the valuable criticisms of associates in the Physics Department.

On the Total Scattering of X-Rays from Crystals

G. G. HARVEY
Eastman Laboratory, Massachusetts Institute of Technology, Cambridge, Massachusetts
(Received May 19, 1939)

A general formula is derived for the total intensity of x-radiation scattered by a general crystal in any direction. In those directions satisfying the Laue equations the formula gives the usual result, while in other directions there is obtained a formula for the total intensity of the diffuse scattering. The derivation is based on classical electromagnetic theory. The form of the result is independent of any assumptions as to spherical symmetry of the scattering atoms or isotropy of thermal vibrations, these factors merely affecting the numerical values of scattering factors and temperature factors and their dependence on angle. Absorption, and the effects of the interaction of incident and scattered radiation are neglected.

THE problem of the scattering of x-rays by crystals has been treated by numerous writers from many points of view. Debye[1, 2] in his original papers on the subject was concerned with the problem of the effect of temperature on the intensity of the reflected radiation. He showed[1] that a crystal consisting of atoms vibrating about lattice points would give rise to two kinds of scattering: first, the regularly reflected rays in certain directions satisfying the Laue equations, due to the periodic arrangement of the scattering centers; and second, a diffusely scattered radiation in all directions, due to the thermal vibrations of the atoms. Since a crystal does not consist of atoms bound by elastic forces to lattice points about which they vibrate, but rather of atoms bound to each other and forming a vibrating system, it is satisfactory to find that essentially the same result[2] was obtained on taking account of the normal vibrations of the lattice. In fact, von Laue has shown the equivalence of the two methods in a comprehensive paper.[3] Other treatments of the same problem have been given by Darwin,[4] Waller,[5] Faxén,[6] and v. Laue[3, 7] the results in all cases being essentially the same. Most of these papers have been rather formidable. Their main object has been an investigation of the effect of temperature on the intensity of the reflected radiation and they have been concerned with the problem of calculating the temperature factor in terms of known atomic constants and crystalline properties. The diffusely scattered radiation has usually been an incidental feature; in none of these cases has a quantitative formula been given for the intensity of the diffuse scattering in a form which can be directly compared with experiment. The scattering elements have usually been taken as atoms, considered as points. This defect can be partially remedied by introducing a scattering factor for each atom[3, 7] but such a procedure necessarily omits the incoherent portion of the scattering from each atom, since point atoms do not give rise to such scattering. The usual procedure has been to add on the Compton scattering.[8] Although this can be justified it seems rather artificial. From the point of view of one interested in the diffuse scattering the Compton radiation is just as much a part of the process as is the radiation scattered as a result of the thermal vibrations.

On the other hand, when considering the theory of diffuse scattering it has been usual to avoid reflected radiation.[8–10] This has been done by assuming throughout the calculation that the direction of scattering is well away from a direction of reflection.

If one is not concerned with a detailed calcu-

[1] P. Debye, Verh. d. Deutsch. Phys. Ges. **15**, 678, 738 and 857 (1913).
[2] P. Debye, Ann. d. Physik **43**, 49 (1914).
[3] M. v. Laue, Ann. d. Physik **81**, 877 (1926).
[4] C. G. Darwin, Phil. Mag. **27**, 315 (1914).
[5] I. Waller, Zeits. f. Physik **17**, 398 (1923); Ann d. Physik **79**, 261 (1926); **83**, 154 (1927); Zeits. f. Physik **51**, 213 (1928); Diss. Upsala (1925).
[6] H. Faxén, Ann. d. Physik **54**, 615 (1917); Zeits. f. Physik **17**, 266 (1923).
[7] M. v. Laue, Ann. d. Physik **42**, 1561 (1913).
[8] E.g., Y. H. Woo, Phys. Rev. **38**, 6 (1931), and other papers.
[9] G. E. M. Jauncey and G. G. Harvey, Phys. Rev. **37**, 1193 and 1203 (1931).
[10] G. E. M. Jauncey, Phys. Rev. **42**, 453 (1932).

lation of the temperature factor in terms of known constants but merely with its existence, then it is an easy matter to derive a formula for the total intensity of the radiation scattered in any direction by a general crystal.[11] It is the purpose of the present note to do this from the point of view of classical electromagnetic theory. It is well known that such a procedure leads to the same results as a quantum-mechanical calculation except for effects of electron exchange and relativity. Strictly speaking, a rigorous calculation of the scattering from a crystal is a problem in dispersion theory and has been treated very fully from this point of view, especially by Waller.[5] We shall here be concerned with those cases in which dispersion may be neglected.

Theory

Consider a general triclinic crystal having n atoms, of any number of kinds, in a unit cell determined by the three translation vectors $\mathbf{a}_1$, $\mathbf{a}_2$ and $\mathbf{a}_3$. Let $\mathbf{r}_j$ be a vector from the origin of any unit cell to the equilibrium position of the center of the jth atom in that cell. Let the direction of an incident beam of x-rays be specified by a unit vector $\mathbf{s}_0$ in the direction of the beam; it is desired to compute the intensity of the radiation scattered in a direction determined by a unit vector $\mathbf{s}$. We may consider an incident beam of plane-polarized radiation with its electron vector $\mathcal{E}$ perpendicular to the plane of scattering determined by $\mathbf{s}$ and $\mathbf{s}_0$. Then the electric intensity of the incident beam at any point will be given by

$$\mathcal{E}=\Re\mathcal{E}_0 \exp\left[2\pi\nu i(t-\mathbf{s}_0\cdot\mathbf{r}/c)\right], \qquad (1)$$

where ν is the frequency of the incident radiation, $\mathbf{r}$ a vector from any convenient origin O to the point in question and $t=0$ is chosen so that $\mathcal{E}_0$ is real. $\Re$ denotes the real part of the expression following it. Then at a distance R from the crystal, large compared with the crystal dimensions, the instantaneous wave scattered by a fixed configuration of the N electrons contained in the crystal will be given by $\Re A$ where

$$A=\frac{e^2}{mc^2R}\sum_{\alpha=1}^{N}\mathcal{E}_\alpha \qquad (2)$$

and

$$\begin{aligned}\mathcal{E}_\alpha&=\mathcal{E}_0\exp\left[2\pi\nu i\{t-R/c+\mathbf{R}_\alpha\cdot(\mathbf{s}-\mathbf{s}_0)/c\}\right]\\&=\mathcal{E}_0\exp\left[(2\pi i/\lambda)(ct-R)\right]\\&\quad\times\exp\left[(2\pi i/\lambda)(\mathbf{s}-\mathbf{s}_0)\cdot\mathbf{R}_\alpha\right]. \qquad (3)\end{aligned}$$

$\mathbf{R}_\alpha$ is a vector from O to the αth electron in the crystal. The square of the amplitude of this wave is

$$|A|^2=AA^*=\frac{e^4}{R^2m^2c^4}\sum_{\alpha=1}^{N}\sum_{\beta=1}^{N}\mathcal{E}_\alpha\mathcal{E}_\beta^*, \qquad (4)$$

where X^* is the complex conjugate of X. The solution to the problem now consists in evaluating Eq. (4) and then obtaining an average value of the intensity.

With this end in view we express the vector $\mathbf{R}_\alpha$ in more explicit form. Using $\mathbf{a}_1$, $\mathbf{a}_2$, $\mathbf{a}_3$ and $\mathbf{r}_j$ as previously defined we introduce a vector $\boldsymbol{\zeta}_j$ measured from the end of $\mathbf{r}_j$ to the instantaneous position of the center of the jth atom in any unit cell (this displacement being due to thermal motion) and a vector $\boldsymbol{\varrho}_{jk}$ from the instantaneous center of atom j to the kth electron in that atom. Without any loss of generality we may take the crystal to be a parallelepiped M_1-1 units along $\mathbf{a}_1$, M_2-1 units along $\mathbf{a}_2$ and M_3-1 units along $\mathbf{a}_3$. We may conveniently take the origin O to be at the origin of the crystal. Then the vector $\mathbf{R}$ from O to the kth electron in the jth atom in the unit cell m_1, m_2, m_3 units along $\mathbf{a}_1$, $\mathbf{a}_2$, $\mathbf{a}_3$, respectively, will be given by

$$\mathbf{R}_{m,\,jk}=m_1\mathbf{a}_1+m_2\mathbf{a}_2+m_3\mathbf{a}_3+\mathbf{r}_j+\boldsymbol{\zeta}_j+\boldsymbol{\varrho}_{jk}. \qquad (5)$$

For abbreviation we shall write

$$\mathbf{A}_m=m_1\mathbf{a}_1+m_2\mathbf{a}_2+m_3\mathbf{a}_3 \qquad (6)$$

and by a subscript m shall always mean three quantities m_1, m_2, m_3. Eq. (5) then becomes

$$\mathbf{R}_{m,\,jk}=\mathbf{A}_m+\mathbf{r}_j+\boldsymbol{\zeta}_j+\boldsymbol{\varrho}_{jk}. \qquad (7)$$

[11] Ewald (*Handbuch der Physik*, Vol. 23, Pt. 2 (1933)) has given a simple derivation for crystals of one kind of atom, obtaining essentially Debye's result (reference 2), but he, too, uses atoms rather than electrons as scattering units. He states also that the diffuse scattering increases monotonically with scattering angle, whereas this is actually not the case on taking account of the electron distribution in the atom.

Substituting this value for $\mathbf{R}$ in Eqs. (3) and (4) gives

$$AA^*=\frac{e^4\mathcal{E}_0^2}{R^2m^2c^4}\sum_{m,\,j,\,k}\exp\left[\frac{2\pi i}{\lambda}(ct-R)\right]\times\exp\left[\frac{2\pi i}{\lambda}(\mathbf{s}-\mathbf{s}_0)\cdot\mathbf{R}_{m,\,j,\,k}\right]\times\sum_{m',\,j',\,k'}\exp\left[\frac{-2\pi i}{\lambda}(ct-R)\right]\times\exp\left[\frac{-2\pi i}{\lambda}(\mathbf{s}-\mathbf{s}_0)\cdot\mathbf{R}_{m',\,j',\,k'}\right], \quad (8)$$

where the summations are taken so as to include all possible pairs of electrons in the crystal. If for abbreviation we write

$$\boldsymbol{\kappa}=\frac{2\pi}{\lambda}(\mathbf{s}-\mathbf{s}_0) \quad (9)$$

and use Eq. (7), expressing the summations more explicitly, Eq. (8) becomes

$$AA^*=\frac{e^4\mathcal{E}_0^2}{R^2m^2c^4}\sum_{m,\,m'}\exp\left[i\boldsymbol{\kappa}\cdot(\mathbf{A}_m-\mathbf{A}_{m'})\right]\times\sum_{j,\,j'}\{\exp\left[i\boldsymbol{\kappa}\cdot(\mathbf{r}_j+\boldsymbol{\zeta}_j-\mathbf{r}_{j'}-\boldsymbol{\zeta}_{j'})\right]\times\sum_{k,\,k'}\exp\left[i\boldsymbol{\kappa}\cdot(\boldsymbol{\varrho}_{jk}-\boldsymbol{\varrho}_{j'k'})\right]\}. \quad (10)$$

The expression given by Eq. (10) is proportional to the intensity scattered by a given configuration of electrons instantaneously at rest, the quantities $\boldsymbol{\zeta}$ and $\boldsymbol{\varrho}$ depending on the time. The observed intensity will be obtained by averaging over all values of $\boldsymbol{\zeta}$ and $\boldsymbol{\varrho}$. $\boldsymbol{\zeta}$ varies due to thermal vibrations of the atoms while $\boldsymbol{\varrho}$ varies due to the "orbital" motion of the electrons. The greatest frequency of thermal vibration will be of the order of magnitude of ν_m where $h\nu_m/k=\Theta$, the characteristic temperature of the crystal. The "frequency" of the orbital motion will be of the order of magnitude of the orbital frequency in an hydrogenic Bohr atom:

$$\omega=2RcZ^2/n^3 \quad (11)$$

in the nth quantum state, R being the Rydberg constant. $\omega\sim10^{15}Z^2/n^3$ while all $\nu_m\sim10^{12}$ sec.$^{-1}$; for radiation of wave-length $\lambda\sim1A$, $\nu\sim10^{18}$ sec.$^{-1}$. Hence for not too high atomic numbers and not too long a wave-length of incident radiation we may assume that the electrons remain essentially at rest while the electric vector of the incident wave goes through a complete cycle. For this reason we may disregard the phase of the radiation given by Eq. (10). In the same way we may assume the atomic centers to be essentially at rest while the electrons perform several complete excursions about their respective nuclei.[12]

To take account of the orbital motion of the electrons let $p_{jk}(\boldsymbol{\varrho})dv_{jk}$ be the probability that electron k in atom j is in a volume element dv_{jk} at a vector distance $\boldsymbol{\varrho}$ from the instantaneous center of atom j. Eq. (10) is to be multiplied by $p_{jk}(\boldsymbol{\varrho})p_{j'k'}(\boldsymbol{\varrho}')dv_{jk}dv_{j'k'}$ and integrated over all space. By definition

$$\int p_{jk}(\boldsymbol{\varrho})dv_{jk}=1, \quad (12)$$

since it is certain that each electron must be somewhere. Thus, for those terms in Eq. (10) for which $m=m'$, $j=j'$ and $k=k'$ we shall get a contribution

$$M_1M_2M_3\sum_{j=1}^{n}Z_j, \quad (13)$$

where Z_j is the atomic number of the jth atom and n the number of atoms in the unit cell. Those terms in Eq. (10) for which $m=m'$, $j=j'$ but $k\neq k'$ refer to two different electrons in the same atom. These terms will contribute

$$M_1M_2M_3\sum_{j=1}^{n}\int\int\sum_{k,\,k'-1}^{Z_j}{}'\exp\left[i\boldsymbol{\kappa}\cdot(\boldsymbol{\varrho}_{jk}-\boldsymbol{\varrho}_{jk'})\right]\times p_{jk}(\boldsymbol{\varrho})p_{jk'}(\boldsymbol{\varrho})dv_{jk}dv_{jk'}, \quad (14)$$

the accent denoting the omission of those terms for which $k=k'$. For the purposes of the present discussion we are not interested in the form of $p_{jk}(\boldsymbol{\varrho})$ but merely recall that

$$\int\exp\left[i\boldsymbol{\kappa}\cdot\boldsymbol{\varrho}_{jk}\right]p_{jk}(\boldsymbol{\varrho})dv_{jk}=f_{(kk)j}, \quad (15)$$

where $f_{(kk)j}$ is the amplitude scattered coherently

[12] We shall neglect the Doppler effect due to these motions. See v. Laue (reference 3).

by an electron of type k in an atom of type j. Now

$$\sum_{k,\,k'}' f_{(kk)j} f^*_{(k'k')j} = \sum_{k,\,k'} f_{(kk)j} f^*_{(k'k')j} - \sum_k f_{(kk)j} f^*_{(kk)j} \quad (16)$$

and

$$\sum_{k,\,k'} f_{(kk)j} f^*_{(k'k')j} = f_j f_j^*, \quad (17)$$

where

$$f_j = \sum_k f_{(kk)j} \quad (18)$$

and $|f_j|$ is the usual atomic scattering factor for an atom of type j. Hence expression (14) becomes

$$M_1 M_2 M_3 \sum_{j=1}^{n} \{ f_j f_j^* - \sum_{k=1}^{Z_j} f_{(kk)j} f^*_{(kk)j} \}. \quad (19)$$

Next consider the terms for which $m = m'$ but $j \neq j'$. For such terms the ϱ_{jk} are completely independent of each other so that as far as summation with respect to k is concerned we shall merely have $f_j f_{j'}^*$ and shall be left with

$$M_1 M_2 M_3 \sum_{j,\,j'}' f_j f_{j'}^* \exp [i\boldsymbol{\kappa} \cdot (\mathbf{r}_j + \boldsymbol{\zeta}_j - \mathbf{r}_{j'} - \boldsymbol{\zeta}_{j'})] \quad (20)$$

and this expression is to be averaged over all values of $\boldsymbol{\zeta}$. Suppose the probability that the center of atom j is in dv_j at a vector distance $\boldsymbol{\zeta}_j$ from its equilibrium position to be $q_j(\boldsymbol{\zeta}) dv_j$; then the expression (20) is to be multiplied by $q_j(\boldsymbol{\zeta}) q_{j'}(\boldsymbol{\zeta}') dv_j dv_{j'}$ and integrated over all configurations, i.e., we require the value of

$$M_1 M_2 M_3 \sum_{j,\,j'}' f_j f_{j'}^* \exp [i\boldsymbol{\kappa} \cdot (\mathbf{r}_j - \mathbf{r}_{j'})] \times \int\int \exp [i\boldsymbol{\kappa} \cdot (\boldsymbol{\zeta}_j - \boldsymbol{\zeta}_{j'})] q_j(\boldsymbol{\zeta}) q_{j'}(\boldsymbol{\zeta}') dv_j dv_{j'} \quad (21)$$

with the requirement

$$\int q_j(\boldsymbol{\zeta}) dv_j = 1.$$

Again, we are not concerned with the form of the probability functions $q_j(\boldsymbol{\zeta})$ but merely remark that the expression

$$\left| \int \exp [i\boldsymbol{\kappa} \cdot \boldsymbol{\zeta}_j] q_j(\boldsymbol{\zeta}) dv_j \right| \equiv \exp [-M_j] \quad (22)$$

is the temperature factor for an atom of type j in the crystal in question; it is convenient to denote this in the usual Debye-Waller form $\exp [-M_j]$ where M_j is defined by Eq. (22). If we denote the atomic scattering factor for an atom in the crystal at temperature T by f_j^T then

$$f_j^T = f_j \exp [-M_j] \quad (23)$$

and expression (21) becomes

$$M_1 M_2 M_3 \sum_{j,\,j'}' f_j^T f_{j'}^{T*} \exp [i\boldsymbol{\kappa} \cdot (\mathbf{r}_j - \mathbf{r}_{j'})]. \quad (24)$$

Now

$$\sum_j f_j^T \exp [i\boldsymbol{\kappa} \cdot \mathbf{r}_j] = F, \quad (25)$$

where F is the structure factor of the unit cell. Thus the summation in (24) can be written

$$\sum_{j,\,j'}' f_j^T f_{j'}^{T*} \exp [i\boldsymbol{\kappa} \cdot (\mathbf{r}_j - \mathbf{r}_{j'})] = FF^* - \sum_j f_j^T f_j^{T*}. \quad (26)$$

Finally, those terms for which $m \neq m'$ contribute

$$\sum_{m,\,m'}' \exp [i\boldsymbol{\kappa} \cdot (\mathbf{A}_m - \mathbf{A}_{m'})] \times \sum_{j,\,j'} \exp [i\boldsymbol{\kappa} \cdot (\mathbf{r}_j - \mathbf{r}_{j'})] f_j^T f_{j'}^{T*}$$

$$= FF^* \sum_{m,\,m'}' \exp [i\boldsymbol{\kappa} \cdot (\mathbf{A}_m - \mathbf{A}_{m'})]$$

$$= FF^* \{ \sum_{m,\,m'} \exp [i\boldsymbol{\kappa} \cdot (\mathbf{A}_m - \mathbf{A}_{m'})] - M_1 M_2 M_3 \}. \quad (27)$$

But

$$\sum_{m,\,m'} \exp [i\boldsymbol{\kappa} \cdot (\mathbf{A}_m - \mathbf{A}_{m'})]$$

is the usual interference function for a parallelepipedal lattice and may easily be shown[13] to have the value

$$\prod_{l=1}^{3} \frac{\sin^2 \frac{1}{2} M_l \boldsymbol{\kappa} \cdot \mathbf{a}_l}{\sin^2 \frac{1}{2} \boldsymbol{\kappa} \cdot \mathbf{a}_l}. \quad (28)$$

Thus the average value of Eq. (10), obtained by

---

[13] E.g. $\sum_{m=0}^{M-1} e^{imx} \sum_{m'=0}^{M-1} e^{-im'x}$

$= [1 + e^{ix} + e^{2ix} + \cdots e^{i(M-1)x}] \times [1 + e^{-ix} + e^{-2ix} + \cdots + e^{-i(M-1)x}]$

$= \frac{e^{iMx} - 1}{e^{ix} - 1} \times \frac{e^{-iMx} - 1}{e^{-ix} - 1}$

$= \frac{(e^{\frac{1}{2}iMx} - e^{-\frac{1}{2}iMx})^2}{(e^{\frac{1}{2}ix} - e^{-\frac{1}{2}ix})^2} = \frac{\sin^2 \frac{1}{2} Mx}{\sin^2 \frac{1}{2} x}$, etc.

combining the terms in expressions (13), (19), (26), (27) and (28), is given by

$$\overline{AA^*}=\frac{e^4\mathcal{E}_0^2}{R^2m^2c^4}\Big\{FF^*\prod_{l=1}^{3}\frac{\sin^2\frac{1}{2}M_l\boldsymbol{\kappa}\cdot\mathbf{a}_l}{\sin^2\frac{1}{2}\boldsymbol{\kappa}\cdot\mathbf{a}_l}$$
$$+M_1M_2M_3\sum_{j=1}^{n}\Big[Z_j-\sum_{k=1}^{Z_j}f_{(kk)j}f^*_{(kk)j}$$
$$+f_jf_j^*-f_j^Tf_j^{T*}\Big]\Big\}. \quad (29)$$

Eq. (29) gives the average square of the electric vector of the radiation scattered from an incident beam polarized with its electric vector $\mathcal{E}_0$ perpendicular to the plane of scattering. If the incident beam is unpolarized then we shall obtain the actual scattered intensity by replacing the expression $e^4\mathcal{E}_0^2/R^2m^2c^4$ in Eq. (29) by I_e, the Thomson scattering from a single electron for unpolarized radiation

$$I_e=I_0\frac{e^4}{R^2m^2c^4}\left(\frac{1+\cos^2 2\theta}{2}\right), \quad (30)$$

where I_0 is the intensity of the incident beam and 2θ is the angle of scattering. The scattered intensity is thus

$$I=I_eF^2\prod_{l=1}^{3}\frac{\sin^2\frac{1}{2}M_l\boldsymbol{\kappa}\cdot\mathbf{a}_l}{\sin^2\frac{1}{2}\boldsymbol{\kappa}\cdot\mathbf{a}_l}$$
$$+I_eM_1M_2M_3\sum_{j=1}^{n}\Big[Z_j-\sum_{k=1}^{Z_j}f^2_{(kk)j}+f_j^2-f_j^{T2}\Big], \quad (30)$$

where we have replaced ff^* by f^2 and understand by f the usual tabulated scattering factor, i.e. $|f|$, and have done the same for f_{kk} and F. Eq. (30) is the solution to the problem and gives the total intensity of the scattered radiation in any direction. However, for those directions for which the Laue equations

$$\boldsymbol{\kappa}\cdot\mathbf{a}_l=2\pi h_l \quad (h_l=0, 1, 2, \cdots) \quad (31)$$

or in their more usual form

$$\begin{aligned}(\mathbf{s}-\mathbf{s}_o)\cdot\mathbf{a}_1&=h\lambda,\\ (\mathbf{s}-\mathbf{s}_o)\cdot\mathbf{a}_2&=k\lambda, \quad (h, k, l=0, 1, 2, \cdots)\\ (\mathbf{s}-\mathbf{s}_o)\cdot\mathbf{a}_3&=l\lambda,\end{aligned} \quad (32)$$

are satisfied, the first term of Eq. (30) becomes

$$I_1=I_eM_1^2M_2^2M_3^2F^2 \quad (33)$$

and is thus the only one of importance since each of the M's is a very large number except for exceedingly fine particles. Eq. (33) is the usual expression for the intensity of reflection from a crystal. On the other hand, since the maxima of $\sin^2 nx/\sin^2 x$ are extremely sharp for large n (having widths at half-maximum $\sim 1/n$) we may completely disregard this first term if we stay sufficiently far away from the directions of reflection.[14]

Thus the intensity of the diffuse scattering, which must always be measured in regions in which no regular reflection is present, will be given by

$$I_2=M_1M_2M_3I_e\sum_{j=1}^{n}\{Z_j-\sum_{k=1}^{Z_j}f^2_{(kk)j}+f_j^2-f_j^{T2}\}. \quad (34)$$

The first two terms of Eq. (34) are obtained by adding intensities and correspond to incoherent Compton scattering; if the atoms were points instead of having finite size the sum of these terms would vanish. The last two terms correspond to radiation scattered as a consequence of the thermal vibrations of the atoms in the crystal lattice. If the atoms were at rest the sum of these terms would vanish. It is to be noticed that no assumption was made as to the isotropy of such vibrations. If the vibrations are not isotropic then the temperature factor Eq. (22) will depend not only on $(\sin\theta)/\lambda$ but also on the orientation of the crystal with respect to the x-ray beam.[15] Eq. (34), however, remains formally the same. The same is true in regard to the electronic distributions in the atoms. Whether or not they are spherically symmetrical does not affect the form of the result but only the values of the f's.[16]

Equation (34) is as far as classical theory can take us under the assumptions made. But recog-

[14] Just what is meant by "sufficiently far" is a question into which we do not enter here.

[15] In this connection see, for example, C. Zener, Phys. Rev. **49**, 122 (1936); G. W. Brindley, Phil. Mag. **21**, 790 (1936). Also G. E. M. Jauncey and W. A. Bruce, Phys. Rev. **50**, 408 and 413 (1936); E. O. Wollan and G. G. Harvey, Phys. Rev. **51**, 1054 (1937).

[16] A formula similar to Eq. (34) has been given by Jauncey (reference 10) for the diffuse part of the scattering from a complex crystal. In his derivation, however, Jauncey made the (unnecessary) assumption that the thermal vibrations and electronic distributions had spherical symmetry.

nizing that the first two terms of this equation are due to Compton scattering we may see what modifications would be brought about in a quantum-mechanical treatment of the problem. First, the Pauli exclusion principle would restrict the number of possible transitions giving rise to incoherent scattering. This means that an amount

$$\sum_{k\neq l} f^2_{(kl)j}, \tag{35}$$

the summation being taken over all pairs of electrons with the same spin and $k\neq l$, is to be subtracted from the expression in { } in Eq. (34).[17] The quantities f_{kl} are defined by

$$f_{kl}=\int \psi_k \exp\left[i\boldsymbol{\kappa}\cdot\mathbf{r}\right]\psi_l^* dv \tag{36}$$

and for $k=l$ reduce to the expressions in Eq. (15) since $|\psi|^2 dv = p(\varrho)dv$. The expression (35) represents a small correction term.[18] In addition, all those terms corresponding to Compton scattering must be divided by $(1+\alpha \text{ vers } 2\theta)^3$, where $\alpha=h/mc\lambda$, in order to take account of the fact that the scattered quanta have lost some of their energy in the scattering process. Thus the intensity of the diffuse scattering is given by

$$I_{\text{e.u.}}=\frac{1}{N_o}\sum_{j=1}^{n}\left\{\frac{Z_j-\sum_{k=1}^{Z_j} f^2_{(kk)j}-\sum_{k\neq l} f^2_{(kl)j}}{(1+\alpha \text{ vers } 2\theta)^3} + f_j^2 - f_j^{T2}\right\}, \tag{37}$$

where the intensity is now expressed in *electron units* per molecule of scattering substance; N_o is the number of molecules per unit cell of the crystal.

[17] I. Waller and D. R. Hartree, Proc. Roy. Soc. **119**, 124 (1929).

[18] For the relative importance of this term in the diffuse scattering from crystals see G. G. Harvey, P. S. Williams and G. E. M. Jauncey, Phys. Rev. **46**, 365 (1934).

AUGUST 1, 1939 PHYSICAL REVIEW VOLUME 56

On Alleged Discontinuities in the Diffuse Scattering of X-Rays from Crystals at Small Angles

G. G. HARVEY
Eastman Laboratory, Massachusetts Institute of Technology, Cambridge, Massachusetts

(Received June 10, 1939)

It is pointed out that the positions of discontinuities in the diffuse scattering from crystals, reported by Laval, all occur at places corresponding to reflections of radiation of one-half, one-third, etc. the wave-length of the main beam. For the case of aluminum, microphotometer traces of films exposed in such a way as to accentuate the expected effect, are reproduced. They show no discontinuities of the kind reported by Laval, but do show peaks corresponding to the reflection of radiation of half the primary wave-length. It is concluded that the effect reported by Laval most probably does not exist.

IN a short note Laval[1] claims to have found that the diffuse scattering from a large number of crystals varies in a discontinuous manner at small angles of scattering. Taking the case of Cu $K\alpha$ radiation diffracted by powdered aluminum, he reports a total of nine discontinuities, six of which occur at values of $(\sin\theta)/\lambda$ less than that corresponding to the first Debye-Scherrer-Hull line (111) for this wave-length. He states that the diffuse scattering increases smoothly with increasing scattering angle until a discontinuity is reached; the scattered intensity then suddenly drops to a smaller value and then increases again until the next edge is reached, and so on. A decrease of 40 percent in intensity is reported for one edge at $(\sin\theta)/\lambda=0.072$. The magnitude of the discontinuity is not given

[1] J. Laval, Comptes rendus **201**, 889 (1935).

for any other crystal or edge. Two laws are stated governing the positions of these edges: (1) For various wave-lengths the position of any given edge occurs at the same value of $(\sin\theta)/\lambda$; (2) for a given wave-length radiation but different scattering materials the position of a given edge is a linear function of the atomic number of the scatterer. As evidence for this second law a large number of edges is reported for a number of crystals. These data have been plotted, in the form given by Laval, and are shown in Fig. 1. It is seen that the points do fall very closely on straight lines. From this it was concluded that the edges were an atomic property and not dependent on the crystalline structure. It is asserted, though no numerical data are given, that the edges for powdered rocksalt occur at the positions characteristic of both sodium and chlorine.

On the usual ideas of scattering and atomic structure it is difficult to see what such edges could be due to. In fact, before trying to explain the effect, it seems worth while to examine the experimental evidence in some detail. To be specific let us confine ourselves to the case of powdered aluminum. If one computes the $(\sin\theta)/\lambda$ values corresponding to reflections from aluminum crystals one is struck by the fact that every one of Laval's reported edges coincides very closely with some submultiple of these. This immediately suggests an explanation of the effect. Laval obtained "monochromatic" radiation (Cu $K\alpha$) by reflection from a rocksalt crystal. Of course at the same time the crystal would reflect any radiation present having one-half, one-third, etc. the wave-length of Cu $K\alpha$

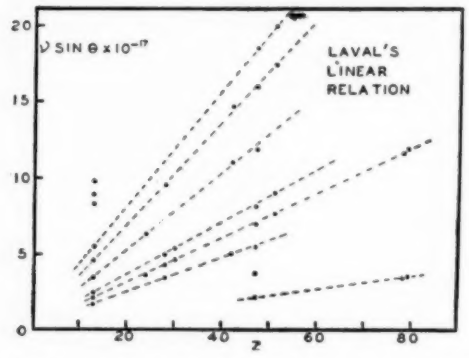

FIG. 1. Values of $\nu \sin\theta \times 10^{-17}$ as a function of atomic number.

and these wave-lengths would be diffracted by the scattering substance. If one measured the positions of these diffracted lines and computed the $(\sin\theta)/\lambda$ values, assuming the wave-length to be Cu $K\alpha$, then the calculated values of $(\sin\theta)/\lambda$ would be submultiples of the true values. Now the excitation potential for Cu $K\alpha$ radiation is about 9 kv and any voltage above about $8000n$ will give rise to some radiation of wave-length one nth that of Cu $K\alpha$. Laval does not give any experimental details, but a potential of 35 kv would not be an unusual value to use. The diffuse scattering is weak at best and one would want to use as much power as possible.

With the above facts in mind a copper target tube was run at about 38 kv and a beam of Cu $K\alpha$ radiation was reflected from a rocksalt crystal and then scattered from a sample of powdered aluminum, in the form of a pressed slab, at the center of an evacuated camera. The film was exposed for 200 hours, roughly 1000 times that necessary to bring out the diffraction due to Cu $K\alpha$. In addition to this and the diffuse background there appeared on the film very weak lines corresponding to the diffraction of radiation of one-half the wave-length of Cu $K\alpha$ from the (111), (200) and (220) planes of aluminum. A microphotometer trace of such a film is shown in the lower curve of Fig. 2. From the relative intensities of the lines it is concluded that the beam of radiation striking the sample contained a few percent of wave-length one-half that of Cu $K\alpha$. The absorption coefficient of this radiation was measured in aluminum and the logarithmic curve of intensity *versus* thickness of absorber was a straight line within experimental error and agreed quite closely with that to be expected for Cu $K\alpha$. Laval states that he had determined by absorption that his beam did not contain any parasitic radiation but it would require a rather precise determination to detect a small amount of radiation of a different wave-length.

The question then arises as to how such peaks might be mistaken for discontinuities. All of Laval's measurements were made with an ionization chamber and electrometer, i.e., at a finite number of angular positions; thus it would be possible, though not very probable, to take measurements in such a way as to think one had

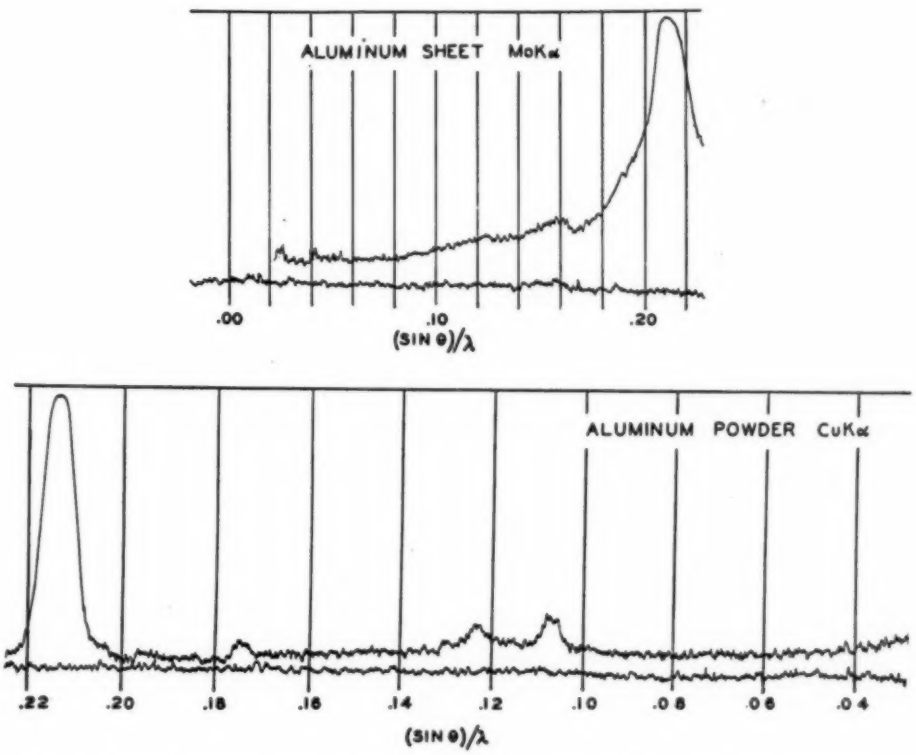

FIG. 2. Microphotometer trace of Cu $K\alpha$ radiation scattered from powdered aluminum.

passed a discontinuity. The shape of these weak peaks depends to a considerable extent on the exact geometry of the experimental arrangement. For example, the upper curve in Fig. 2 shows the result of one run with Mo $K\alpha$ radiation on a sheet of aluminum. Here the peaks do resemble discontinuities to some extent. The large discontinuity of 40 percent reported by Laval in the case of aluminum at $(\sin\theta)/\lambda = 0.72$ clearly is not evident in either of the curves in Fig. 2. It corresponds to the (111) line for a wave-length of one-third that of the primary.

It is possible to account very closely for every one of the 36 edges reported by Laval, and assembled in Fig. 1, as due to reflections of wave-lengths of one-half, one-third and one-fourth that of Cu $K\alpha$ and we are forced to conclude that the effect reported by Laval most probably does not exist. The fact that the points in Fig. 1 fall so closely on straight lines is purely fortuitous, perhaps unfortunately so as it would naturally lead one to suspect that the effect was purely atomic, rather than due to the crystalline structure of the materials.

The Nuclear Five-Body Problem*

WARREN A. TYRRELL, JR.†
Sloane Physics Laboratory, Yale University, New Haven, Connecticut

(Received April 26, 1939)

Perturbational and variational calculations with single-particle Legendre functions have been made for the nuclear five-body problem of He^5. The symmetric Hamiltonian is employed; the values of the nuclear parameters chosen favor high binding. With a symmetric interaction, Li^5 and He^5 differ only in the Coulomb energy, states of the former lying about one Mev above those of the latter. The calculations show that there is no state of He^5 which is stable against dissociation into an alpha-particle and a neutron. There are two low-lying virtual levels, one of ^2P, the other of ^2S symmetry; according to the Hartree model, the energies of these states are -11.7 and -6.5 Mev, respectively. Second-order perturbation calculations diminish the interval $^2S-^2P$ radically and locate both the states in the neighborhood of -19.0 Mev. The last two results are roughly confirmed by variational calculations with two variation parameters (alpha-particle model), and -20 Mev may be set as a probable lower bound to the position of either state. These estimated values fall some seven Mev short of the experimental energy.

I. INTRODUCTION

ALTHOUGH much attention has been devoted to the theory of the light nuclei, little consideration has been given to the nuclear five-body problems. This is due partially to the fact that He^5 and Li^5 are of only minor experimental importance, and partially to the fact that Li^6 and higher nuclei offer more challenging problems and more stringent tests of theory.

There are reasons, however, why the five-body problem is of interest. There are now available from several investigations data which lead to an experimental energy of He^5. Moreover, for He^4, the first-order (Hartree) approximation is good, and convergence of higher terms is rapid. For Li^6, the Hartree model is poor, and higher terms converge slowly. This makes He^5 mathematically interesting as an intermediate case.[1]

II. ASSUMPTIONS AND PRELIMINARIES

The analysis is based upon the work of Margenau and Carroll on Li^6. Care has been taken to use the same notation as far as possible, and the reader is referred to their paper[2] for an explanation of points which are omitted here.

The symmetric Hamiltonian is assumed; the potential between pairs of nuclear particles is taken to be

$$V_{ij}=-A\exp(-r^2_{ij}/a^2)\times(w+mP_{ij}+bQ_{ij}+hP_{ij}Q_{ij}). \quad (1)$$

For the parameters, the following values are employed:

$$w=-2/15;\quad m=14/15;\quad b=7/15;\quad h=-4/15;$$
$$A=35.60\text{ Mev};\quad a=2.25\times10^{-13}\text{ cm}.^3$$

The values of w, m, b, h are derived from the Breit-Feenberg and Kemmer inequalities[4] with equality signs taken, a choice corresponding to maximum binding in the Hartree approximation for light nuclei.

Since individual particle coordinates are used, the Hamiltonian for the five-body problem is[5]

$$H=-\frac{4}{5}\frac{\hbar^2}{2M}\Sigma_k\nabla_k^2+\frac{2}{5}\frac{\hbar^2}{2M}\Sigma_{k>l}\nabla_k\cdot\nabla_l+\Sigma_{k>l}V_{kl}$$
$$+\text{Coulomb interaction}.$$

The $\nabla_k\cdot\nabla_l$ terms and the numerical factors in the kinetic energy operators arise from the transformation to the center of mass of the system.

The single-particle functions employed are

* Part of a dissertation presented to the Faculty of the Graduate School of Yale University in candidacy for the degree of Doctor of Philosophy.

† Now with the Bell Telephone Laboratories, Red Bank, New Jersey.

[1] Preliminary results for the ^2P state of He^5 have been presented at the New York meeting of the American Physical Society. Cf. Phys. Rev. **55**, 678 (1939).

[2] H. Margenau and K. G. Carroll, Phys. Rev. **54**, 705 (1938).

[3] It has recently been suggested that an interaction of shorter range and greater depth is needed to agree with proton-proton scattering data. Cf. G. Breit, H. M. Thaxton and L. Eisenbud, Phys. Rev. **55**, 603 (1939).

[4] G. Breit and E. Feenberg, Phys. Rev. **50**, 850 (1936); N. Kemmer, Nature **140**, 192 (1937).

[5] H. Margenau and D. T. Warren, Phys. Rev. **52**, 790 (1937).

solutions of the Schrödinger equation for the isotropic three-dimensional harmonic oscillator. Thus, they are products of a radial Gaussian exponential, an associated Legendre function, and an azimuthal exponential, and they can be designated by the usual spectroscopic notation. The functions contain a common parameter q (q or k, for the two-parameter scheme), to be adjusted later for minimum energy. All functions are symmetrized by writing them in determinantal form. Generalized spin functions are used:

$\eta_1 \sim$ proton, $s_z=-\frac{1}{2}$; $\eta_3 \sim$ neutron, $s_z=-\frac{1}{2}$;
$\eta_2 \sim$ proton, $s_z=+\frac{1}{2}$; $\eta_4 \sim$ neutron, $s_z=+\frac{1}{2}$.

For a detailed description of the method for evaluating any matrix element H_{ij}, reference 2 may be consulted.

III. First-Order Calculations for the Two Lowest States

In this section, the Coulomb energy will be omitted. In the Hartree approximation, the lowest state of He^5 and Li^5 has ^2P symmetry and corresponds to the configuration $(1s)^4 2p$. Therefore, for He^5,

$$ {}_p\psi_0=(1/5!)^{\frac{1}{2}}|s\eta_1\cdot s\eta_2\cdot s\eta_3\cdot s\eta_4\cdot 2p_1\eta_4| \qquad (2)$$

can be taken as the lowest state function. The "fifth position" in ${}_p\psi_0$ may be filled equally well by the product of $2p_1$, $2p_0$, or $2p_{-1}$ and either η_3 or η_4; the Hamiltonian is diagonal for these six functions, and each corresponds to the same total spin, total angular momentum, and energy.

For Li^5, the fifth position must contain η_1 or η_2.

In terms of one variation parameter $\sigma=qa^2$, ${}_p\psi_0$ gives the first-order energy

$$ {}_pH_{00}=3.5T\sigma-\frac{36}{15}A\left(2+\frac{1}{\sigma+2}\right)\left(\frac{\sigma}{\sigma+2}\right)^{\frac{1}{2}}, \qquad (3)$$

where $T\equiv\hbar^2/Ma^2$. The expression (3) has a minimum of -12.3 Mev at $\sigma=1.6$.

In the same approximation, the next highest state is of ^2S symmetry, and is represented by the configurations $(1s)^4 2s$ and $(1s)^3(2p)^2$. In the former configuration there is but one function:

$$ {}_s\psi_0=(1/5!)^{\frac{1}{2}}|s\eta_1\cdot s\eta_2\cdot s\eta_3\cdot s\eta_4\cdot 2s\eta_4|. \qquad (4)$$

There are 10 distinct functions in $(1s)^3(2p)^2$; each of these is not alone an acceptable wave function, for the spin and isotopic spin matrices are not properly diagonal. It is necessary to combine all 10 functions linearly into a function, say ${}_s\psi_1$, which is suitably diagonalized. The method of performing the combination is well known from the theory of atomic spectra. ${}_s\psi_0$ and ${}_s\psi_1$ are degenerate and may be combined linearly to give an energy lower than that from either function alone. Solution of the secular equation corresponding to ${}_s\psi_0$ and ${}_s\psi_1$ shows, however, that this lowest energy differs so little from ${}_sH_{00}$ that the configuration $(1s)^3(2p)^2$ may safely be neglected. The excellence of (4) might be expected from the fact that, of the available 11 functions, it alone comprises the alpha-particle group (closed s shell).

In terms of σ, (4) yields the first-order energy

$$ {}_sH_{00}=3.8T\sigma-\frac{36}{15}A\left[2+\frac{2.5}{(\sigma+2)^2}\right]\left(\frac{\sigma}{\sigma+2}\right)^{\frac{1}{2}}. \qquad (5)$$

This has a minimum of -7.1 Mev at $\sigma=1.2$.

The function (2) or (4) represents He^5 as an alpha-particle group and a p neutron or s neutron, respectively. This suggests the use of two variation parameters, one ($\sigma=qa^2$) for the four $1s$ particles, and one ($\kappa=ka^2$) for the $2p$ or $2s$ neutron. The functions (2) and (4) then lead to the first-order energies:[6]

$$\begin{aligned} {}_pH_{00}=&(2.4\sigma+\kappa)T \\ &+3.2T\sigma^{7/2}\kappa^{5/2}\left(\frac{1}{\sigma+\kappa}\right)^5-\frac{72}{15}A\left(\frac{\sigma}{\sigma+2}\right)^{3/2} \\ &-\frac{1152}{15}A\sigma^{3/2}\left(\frac{\kappa}{\sigma+\kappa}\right)^{5/2}\left(\frac{1}{\sigma+\kappa+4}\right)^{5/2}, \qquad (6) \end{aligned}$$

$$\begin{aligned} {}_sH_{00}=&\frac{1}{1-\Delta^2}\left\{\frac{2}{5}T\left[\frac{9}{2}-\sigma\left(\frac{4}{3}-\Delta^2\right)+\frac{7}{2}\kappa\right.\right. \\ &\left.+4\sqrt{3\Delta}(\sigma\kappa)^{7/4}\frac{7\sigma-3\kappa}{(\sigma+\kappa)^{7/2}}\right] \\ &-\frac{36}{15}A\left[\left(\frac{\sigma}{\sigma+2}\right)^{3/2}(2-\Delta^2)\right. \\ &-\sqrt{6\Delta}\sigma^{9/4}\kappa^{3/4}\frac{\frac{1}{2}(\sigma+1)(\kappa-\sigma)-\sigma}{\{(\sigma+1)[\frac{1}{2}(\sigma+\kappa)+1]-1\}^{5/2}} \\ &\left.\left.+\tfrac{1}{2}(\sigma\beta)^{3/2}(5\beta^2-3\beta\sigma-6\beta+3)\right]\right\}, \qquad (7) \end{aligned}$$

[6] Cf. Section VI of this paper in regard to the calculation of $\nabla_i\cdot\nabla_j$ integrals with two parameter functions.

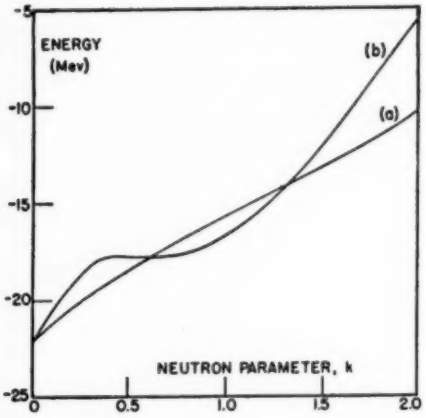

FIG. 1. First-order energies in two parameters. Variation with κ for $\sigma=2.6$. (a) ${}_pH_{00}$, Eq. (6). (b) ${}_sH_{00}$, Eq. (7).

where

$$\beta\equiv\frac{\kappa}{[\frac{1}{2}(\sigma+\kappa)+1]^2-1},$$

$$\Delta\equiv\int(1s)_\sigma(2s)_\kappa d\tau=2\sqrt{3}(\sigma\kappa)^{3/4}(\kappa-\sigma)\left(\frac{1}{\sigma+\kappa}\right)^{5/2}.$$

Δ is a nonorthogonality integral. The similar integral for the P state vanishes identically on account of a difference in orbital angular momentum.

For the alpha-particle, the ground state function

$$\phi_0=(1/4!)^{\frac{1}{2}}|s\eta_1\cdot s\eta_2\cdot s\eta_3\cdot s\eta_4|$$

gives $\mathcal{H}_{00}=2.25T\sigma-(72/15)A(\sigma/(\sigma+2))^{\frac{1}{2}}$, which has a minimum of -25.2 Mev at $\sigma=2.6$. The quantity $1/\sigma^{\frac{1}{2}}$ measures the separation of the particles within the alpha-particle.

In the plane $\kappa=0$, the energies (6) and (7) have shallow minima at $\sigma=2.4$. Each expression differs little in the two planes $\sigma=2.4$ and 2.6. If the value 2.6 is adopted for σ, ${}_pH_{00}$ and ${}_sH_{00}$ are evaluated quite close to their minima, and, in addition, ${}_p\psi_0$ or ${}_s\psi_0$ represents exactly an alpha-particle in its normal state and a p or s neutron, respectively.

Figure 1 shows the variation of (6) and (7) with κ for the fixed value $\sigma=2.6$. The S state curve has a very shallow minimum at about $\kappa=0.6$; the P state curve has no minimum at all.

The quantity $1/\kappa^{\frac{1}{2}}$ measures the separation between the alpha-particle and the neutron. The point $\kappa=0$ corresponds to the removal of the neutron to infinity. For any value of σ,

$$(H_{00})_{\kappa=0}-\mathcal{H}_{00}=0.15T\sigma.$$

This difference arises because H_{00} and $\mathcal{H}_{00}$ are referred to different centers of mass (c.m.). Analysis shows that, with respect to the c.m. of He^5, the alpha-particle has $0.03T\sigma$ translational energy, and the neutron at infinity has the remaining $0.12T\sigma$. This "spurious" kinetic energy accounts for the shift in the minimum of H_{00} for $\kappa=0$.

IV. THE COULOMB ENERGY

The Coulomb energy (C.E.) of the lowest states of He^5 is due to the single interaction of the two protons in the s shell; for both one- and two-parameter functions, the C.E. of He^5 is given approximately by previous calculations[7] with one parameter for He^4. Since, in first-order approximation, the excited proton of both Li^5 and Li^6 is in a $2p$ state, the Coulomb energies of these two nuclei are approximately equal. From previous work, however, only the C.E. of Li^6 for one-parameter functions is known.

The expressions for the Coulomb term in the first-order energy are

He^5: $E_c=0.51\sigma^{\frac{1}{2}}$ Mev (1 or 2 parameters)
Li^5: $E_c=1.43\sigma^{\frac{1}{2}}$ Mev (1 parameter only).

The inclusion of the C.E. raises the curves of Fig. 1 by $0.51(2.6)^{\frac{1}{2}}=0.8$ Mev. For Li^5 with two-parameter functions, in the region of physical

TABLE I. *List of excited configurations for the ²P and ²S states of* He^5.

P STATE				*S* STATE	
DOUBLY EXCITED		QUADRUPLY EXCITED		DOUBLY EXCITED	
CONFIGURATION	NO. OF FUNCTIONS	CONFIGURATION	NO. OF FUNCTIONS	CONFIGURATION	NO. OF FUNCTIONS
$(1s)^4 3p$	1	$(1s)^4 4p$	1	$(1s)^4 3s$	1
$(1s)^3 2p 2s$	7	$(1s)^3 2p 3s$	7	$(1s)^3 2p 3p$	21
$(1s)^3 2p 3d$	21	$(1s)^3 2p 4d$	21	$(1s)^3 (2s)^2$	3
$(1s)^2 (2p)^3$	15	$(1s)^3 2s 3p$	7	$(1s)^3 (3d)^2$	17
	—	$(1s)^3 3d 3p$	21	$(1s)^2 (2p)^2 2s$	18
	44	$(1s)^3 3d 4f$	35		—
		$(1s)^2 (2p)^2 3p$	33		60
		$(1s)^2 (2s)^2 2p$	6		
		$(1s)^2 (3d)^2 2p$	30		
			—		
			161		

[7] W. Heisenberg, Zeits. f. Physik **96**, 473 (1935).

interest ($\kappa<\sigma$), the C.E. will raise the He^5 energy surface less than $(1.43-0.51)(2.6)^{\frac{1}{2}}\leqq 1.5$ Mev. Since the lowest states of Li^5 and He^5 differ only in the Coulomb term and hence by about 1 Mev, the remainder of this paper will be devoted to He^5 alone. Higher order Coulomb corrections will be neglected.

V. Perturbation Calculations with One Parameter

Schrödinger perturbation theory gives the energy

$$E=H_{00}+\sum_i{}'\frac{|H_{0i}|^2}{E_0-E_i}=H_{00}+E^{(2)}.$$

The sum is to be taken over all excited states ψ_i. The denominator is the difference of unperturbed energies:

$$E_0-E_i=-nT\sigma,$$

where n is the degree of excitation of ψ_i relative to ψ_0.

Table I is a list of doubly and quadruply excited configurations for the ^2P state and a list of doubly excited configurations for the ^2S state; all configurations are included whose functions combine with ψ_0. The number of different functions subsumed by each configuration is also given.

Table II gives numerical results for both states. The Coulomb energy, the first-order energy, and the second-order energy (corresponding to the pertinent functions of Table I) are listed for significant values of σ.

It is desirable to find the convergence limit of the second-order energy:

$$E^{(2)}=\sum_i{}'\frac{|H_{0i}|^2}{E_0-E_i}=E_D{}^{(2)}+G_Q.$$

G_Q is the second-order energy due to all states higher than doubly excited; the smallest denominator in $-G_Q$ is $4T\sigma$. No kinetic energy terms appear in G_Q on account of selection rules. From matrix algebra

$$-G_Q<(1/4T\sigma)\{(V^2)_{00}-V_{00}{}^2-\Sigma_D V_{0i}{}^2\}.$$

On the right-hand side, the only unknown is $(V^2)_{00}$. The calculation of this quantity with the general potential (1) is straightforward though lengthy; the only new feature is the necessity of investigating all double spin products $Q_{ij}Q_{jk}$ and $Q_{ij}Q_{kl}$.

Values of G_Q and of the sum $H_{00}+E_C+E_D{}^{(2)}+G_Q$ are listed in Table II for both states. Since the second-order energy $E_Q{}^{(2)}$ due to quadruply excited states has been explicitly computed for the P state, better bounds G_S may be calculated for this state:

Table II. *Second-order perturbational calculations for the ^2P and ^2S states of He^5. Summary of numerical results.*

	^2P State					^2S State			
σ	1.0	1.2	1.4	1.6	1.8	0.8	1.0	1.2	1.4
H_{00}	−10.0	−11.4	−12.1	−12.3	−12.0	−5.7	−6.7	−7.1	−6.9
E_C	+0.5	+0.6	+0.6	+0.6	+0.7	+0.5	+0.5	+0.6	+0.6
$E_D{}^{(2)}$	−4.0	−3.9	−3.8	−3.8	−3.8	−6.2	−6.9	−7.4	
G_Q	−6.0	−4.6	−3.9			−9.7	−8.6	−7.6	
Total	−19.5	−19.3	−19.2			−21.1	−21.7	−21.5	
$E_Q{}^{(2)}$	−3.0	−2.7	−2.4	−2.1	−1.9				
G_S	−2.0	−1.3	−1.0						
$H_{00}+\cdots+G_S$	−18.5	−18.7	−18.7						

$$-G_S<(1/6T\sigma)\{(V^2)_{00}-V_{00}{}^2-\Sigma_D V_{0i}{}^2-\Sigma_Q V_{0i}{}^2\}.$$

Values of G_S and of the sum $H_{00}+E_C+E_D{}^{(2)}+E_Q{}^{(2)}+G_S$ are given in Table II for the P state.

VI. Further Variational Calculations with Two Parameters

In an effort to improve the first-order energy (6) for the P state, the function

$$\psi={}_p\psi_0+\mu V_p\psi_0 \tag{8}$$

has been used. Here ${}_p\psi_0$ is the P state function (2) in two parameters, μ is another parameter, and $V=\sum_{i>j}J_{ij}$. The function (8) iterates the ordinary potential. From test work on H^3, it appears that such iteration may be almost as effective as iteration of the total Hamiltonian.

With (8), the variational energy is

$$E=\frac{H_{00}+2\mu(HV)_{00}+\mu^2(HV^2)_{00}}{1+2\mu V_{00}+\mu^2(V^2)_{00}}. \tag{9}$$

The parameter μ is to be eliminated by setting $\partial E/\partial\mu=0$ and solving for μ.[8] The calculation of the denominator of (9) is simple. In connection with the numerator, it is to be noted that the

[8] Since ${}_p\psi_0$ is complex, in general μ will also be complex. In the present work, however, μ is real.

$\nabla_i \cdot \nabla_j$ terms cannot be evaluated by the scheme[2] used for one-parameter work. The fundamental relation between coordinate and momentum matrices, upon which the scheme depends, is not valid for a set of functions in which some functions have one parameter and the rest have a different parameter. Hence, the $\nabla_i \cdot \nabla_j$ integrals must here be computed in a straightforward fashion. On this account, the numerator of (9), especially $(HV^2)_{00}$, involves considerable integration.

For $\sigma = 2.6$, and with μ given its minimizing value, (9) yields energies almost uniformly lower than (6). The lowering is slight: between 0.3 and 0.4 Mev for $0 < \kappa < 2$.

It is worthy of mention that for $\kappa = 0$ (alpha-particle referred to c.m. of He^5), ${}_pH_{00}$ is lowered 0.37 Mev. A four-particle function similar to (8), where ${}_p\psi_0$ is replaced by ϕ_0, lowers $\mathfrak{IC}_{00}$ exactly the same amount. Thus, the difference in the kinetic energy terms due to change of center of mass has no effect upon the more refined calculation of this section; the lowering given by (9) at $\kappa = 0$ is a true lowering of the alpha-particle energy. It is interesting that iteration of the potential is not nearly so effective as a linear variation function scheme.[9]

VII. Discussion

The order and the spacing of the S and P states will be discussed first. The Hartree model gives about 5 Mev. for the difference $^2S - {}^2P$. Table II shows that the second-order calculations diminish the interval so radically that, with the inclusion of the bounds G_Q, the S state apparently may lie below the P state. Examination of Table II shows, however, that as second-order energies from functions of higher excitation are gradually included, the minimizing value of σ becomes progressively smaller. At the smaller values of σ, convergence is slower, and the bounds G are larger. This is true for both states. In addition, the convergence of the second-order energies is slower for the S than for the P state; the bounds G_Q are poorer for the former than for the latter. In view of these facts, it may be expected that further second-order approximation would locate the S state slightly above the P state.

For the S state, some matrix elements H_{0i} involve only s functions. Such integrals are large, because, for oscillator functions, the strongest combination occurs between functions of the same symmetry. On the other hand, for the P state, most H_{0i} contain $1s$ and various p functions, and these integrals are small because of the difference in the orbital (angular momentum) part. For He^5, the Hartree model appears to give correctly the *order* of the low-lying levels but it does not give the *spacing* between levels accurately, *because second-order effects depend critically upon the orbital symmetry of the level concerned.* There are other instances of this symmetry effect. For Li^6, Margenau and Carroll[2] found that the interval $^3D - {}^3S$, which is 2 Mev according to the Hartree model, becomes 6 Mev upon higher approximation. Margenau[10] observes no appreciable change in the interval ^1S (He^6) $- {}^3S$ (Li^6) upon the inclusion of second-order terms, because both levels possess the same orbital symmetry.

The two-parameter variational calculations of Sections III and VI constitute a partial check upon the reliability of the perturbational work with one parameter. A $2p$ or $2s$ function with a parameter κ is equivalent to an expansion of p or s functions, respectively, with the parameter σ. For $\sigma = 2.6$ and $0 < \kappa < 2$, calculation shows that several coefficients in each expansion are large. The curves of Fig. 1 show, therefore, the variational energy corresponding to several important functions. Further variational refinement may change the shape of the curves, especially the curve for the P state, but marked lowering is not to be expected.

It is to be emphasized that the general potential (1) has been used throughout. In regard to more extended variational calculations, one may anticipate that, since there is a considerable correlation[2, 10] between variational and second-order perturbational results, many one-parameter functions would be needed for a close approximation to the convergence limit. Likewise, in an iteration scheme, many powers of V or H would be required.[11]

[9] H. Margenau and W. A. Tyrrell, Jr., Phys. Rev. **54**, 422 (1938).

[10] To be published soon.

[11] G. Horvay, Phys. Rev. **55**, 70 (1939).

As to the results of experimental investigations involving He^5, Williams, Shepherd and Haxby,[12] from a study of the reaction Li^7 (d, α), concluded that He^5 is unstable by 0.84 Mev against dissociation into an alpha-particle and a neutron. The work of Rumbaugh, Roberts and Hafstad[13] seems in agreement with this. Staub and Stephens,[14] from experiments on the scatterin of neutrons by alpha-particles, support this energy value and conclude that this unstable state of He^5 has a ^2P symmetry. In marked contrast to these harmonious results, Joliot and Zlotowski[15] claim that He^5 has a stable state, located 2.2 Mev below dissociation. Bethe[16] has indicated reasons for rejection of the Joliot result. It appears, then, that the lowest energy of He^5 is $-27.6+0.8=-26.8$ Mev.

In the scattering of neutrons by He^4, only one resonance was observed.[14] The present calculations suggest that both s and p waves of the incident neutron participate in this resonance. Staub and Stephens have concluded that the scattering of p waves must predominate in order to account for the height of the resonance peak. The present suggestion in no way vitiates their analysis, for, from the figures they give, a considerable amount of s scattering would give only a small contribution to the total resonance.

VIII. Conclusions*

From a study of Table II and Fig. 1, it is concluded that the ^2P and ^2S levels of He^5 lie close together, with the ^2P probably lower. With a symmetric Hamiltonian, the value -20 Mev may be set as a probable lower bound to the position of these states. From the work of Carroll[17] on Li^7, it is inferred that the set of parameters recently proposed by Breit[3] will give levels for He^5 which are even higher. The estimate given above falls some 7 Mev short of the experimental value. The discrepancy between theory and experiment has the same direction and about the same magnitude as for Li^6 and Li^7. The general conclusions which may be drawn from the present results have already been given.[18]

The writer is indebted to Professor Henry Margenau for suggesting this problem and for advice and supervision throughout the course of the work.

[12] J. H. Williams, W. G. Shepherd and R. O. Haxby, Phys. Rev. **51**, 888 (1937); **52**, 390 (1937). Cf. also M. S. Livingston and H. A. Bethe, Rev. Mod. Phys. **9**, 318–319 (1937).

[13] L. H. Rumbaugh, R. B. Roberts and L. R. Hafstad, Phys. Rev. **54**, 657 (1938).

[14] H. Staub and W. E. Stephens, Phys. Rev. **55**, 131 (1939).

[15] F. Joliot and I. Zlotowski, Comptes rendus **206**, 1256 (1938).

[16] H. A. Bethe, Phys. Rev. **55**, 434 (1939).

* *Note added in proof:*—Since this manuscript was submitted for publication, there has appeared an article by S. Watenabe, Zeits. f. Physik **112**, 159 (1939), in which the nuclear five-body problem is also treated. Watenabe's analysis differs in some detail from the present work; his general results, however, are in substantial agreement with the author's conclusions.

[17] K. G. Carroll, Phys. Rev. **55**, 1128(A) (1939).

[18] W. A. Tyrrell, Jr., K. G. Carroll and H. Margenau, Phys. Rev. **55**, 790 (1939).

Dissociation of Propane, Propylene and Allene by Electron Impact

J. DELFOSSE* AND WALKER BLEAKNEY
Palmer Physical Laboratory, Princeton University, Princeton, New Jersey

(Received June 5, 1939)

The appearance potentials of all the ions from $C_3H_8^+$ to $C_3H_2^+$ and $C_2H_5^+$ to $C_2H_2^+$ that result from the bombardment of propane, propylene and allene have been measured. Although little is known concerning the energies of the various free radicals formed, it is still possible to specify uniquely most of the reactions which lead to the observed ions. This knowledge in turn allows upper limits to be placed on the ionization potentials of the free radicals themselves. These limits range from about 9 to 12 volts, showing that the ionization potentials of these radicals do not differ greatly from one another.

IN recent years the mass spectrograph has been used with some success in the study of the dissociation of molecules when subjected to bombardment by charged particles. In the case of the simple hydrocarbons such as methane,[1] acetylene,[2] ethylene,[3] and ethane[4] measurements of the appearance potentials and the probabilities of ionization have thrown some light on the manner in which these molecules may be broken up into many fragments. It is the purpose of this communication to describe an extension of these investigations to a few of the hydrocarbons containing three carbon atoms, in particular propane C_3H_8, propylene C_3H_6, and allene C_3H_4. Propane has already been investigated by Stewart and Olson[5] and they found that this compound dissociated to give many types of ions, but they gave no indication of the energies involved.

The mass spectrograph used in the present investigation has been described by Bleakney and Hipple[6] in a recent communication. The magnetic field available for this instrument was rather small (1000 gauss), and consequently the velocities of the heavier ions were not high. This means that intense ion beams cannot be used because of space charge limitations. As a result the ionization potentials were not determined with high accuracy, but on the other hand for such interpretation as can be made high accuracy is not needed. Some of the gases studied in this research were prepared by our colleagues in the Chemistry Department, and we are much indebted to them for their courtesy. The results indicate that contaminations were extremely small.

The procedure need not be repeated here in detail since it has often been given in previous papers of this character. It will merely be recalled that the observations are carried out at very low pressure as the gas flows through the apparatus so that all the products occur as the result of single electron impacts on the normal molecule of the gas in question. In Fig. 1 is shown a "mass-spectrum" of the upper mass region for propylene. This is an actual reproduction of a run traced out by an automatic recorder obtained by varying the analyzing field (abscissa) while the detector system measures the current or intensity (ordinate). The mass 44 peak in this picture is an impurity, probably propane and CO_2. Mass 43 contains some impurity but is largely accounted for by the C^{13} isotope. The appearance potential for the formation of each of these ions is obtained by setting the analyzer on a particular peak and recording its intensity as a function of the electron energy. The minimum electron energy necessary to form the ion is compared with that of a gas which is well known, such as argon, and in this way only differences need be measured.

A summary of the types of ions observed and their relative abundances for the three gases propane, propylene, and allene is given in Table I. In each gas the complete molecular ion is

* C.R.B. Fellow.

[1] L. G. Smith, Phys. Rev. **51**, 263 (1937).
[2] Tate, Smith and Vaughn, Phys. Rev. **48**, 523 (1935).
[3] Kusch, Hustrulid and Tate, Phys. Rev. **52**, 843 (1937).
[4] J. A. Hipple, Phys. Rev. **53**, 530 (1938).
[5] H. R. Stewart and A. R. Olson, J. Am. Chem. Soc. **53**, 1236 (1931).
[6] W. Bleakney and J. A. Hipple, Phys. Rev. **53**, 521 (1938).

assigned the arbitrary intensity value 100, and the others are given on this scale. These are actually observed values for electrons of 100 volts energy, and no attempt has been made to correct them for the overlapping of the carbon isotopes. Hydrogen ions are also formed in these gases, but their relative abundance was not measured. No search was made for negative ions. Appearance potential measurements were not made for the complete mass-spectrum first because of lack of time and second because of the difficulty of attaching any meaning to many of them.

The relative probabilities of formation of ions in these compounds present some interesting and peculiar features. Chemical evidence indicates the following structures: allene $CH_2 : C : CH_2$; propylene $CH_2 : CH \cdot CH_3$; propane $CH_3 \cdot CH_2 \cdot CH_3$. It will be noticed from Table I that in propylene mass 27 is about thirteen times as strong as 28. This observation is probably to be correlated with the relative energy necessary to break a single C−C bond as compared to the double C=C bond. An unexpected peculiarity is found in the occurrence of $C_2H_3^+$ and CH_3^+ in allene. One possible, though improbable, explanation for such ions is the presence as an impurity of methylacetylene, an isomer of allene with a CH_3 radical on one end. Another peculiar distribution of intensities is the small yield of the propylene and allene ions $C_3H_6^+$ and $C_3H_4^+$ coming from propane and $C_3H_4^+$ from propylene. Since these ions correspond to stable compounds, it might be supposed that they should be among the most abundant. No explanation of this behavior is known. Perhaps the ions with an even number of electrons are more stable than those with an odd number.

TABLE I. *The ions observed and their relative intensities as measured by the heights of the peaks.*

Ion	Propane (C_3H_8)	Propylene (C_3H_6)	Allene (C_3H_4)
$C_3H_8^+$	100		
$C_3H_7^+$	67		
$C_3H_6^+$	12.4	100	
$C_3H_5^+$	36	148	
$C_3H_4^+$	6.2	50	100
$C_3H_3^+$	85	85	94
$C_3H_2^+$	14	18.5	40
C_3H^+	8.7	12.7	30
C_3^+	1.2	2.7	9
$C_2H_5^+$	340	0	
$C_2H_4^+$	290	5	0
$C_2H_3^+$	152	65	5.2
$C_2H_2^+$	24.5	20	5.8
C_2H^+	5.4	4.6	4.2
C_2^+	0.5	1.5	2.2
$C_3H_8^{++}$	0.1		
$C_3H_7^{++}$	0		
$C_3H_6^{++}$	0.1	0	
$C_3H_5^{++}$	0.4	1.1	
$C_3H_4^{++}$	3.2	4.3	2.7
$C_3H_3^{++}$	3.2	3.2	2.7
$C_3H_2^{++}$	3.6	6.5	2.5
C_2H^{++}	0	0	0
CH_3^+	12.6	1.4	0.9
CH_2^+	6.2	7.1	3.8
CH^+	2	3.8	2.7
C^+	0.8	4.1	2.7

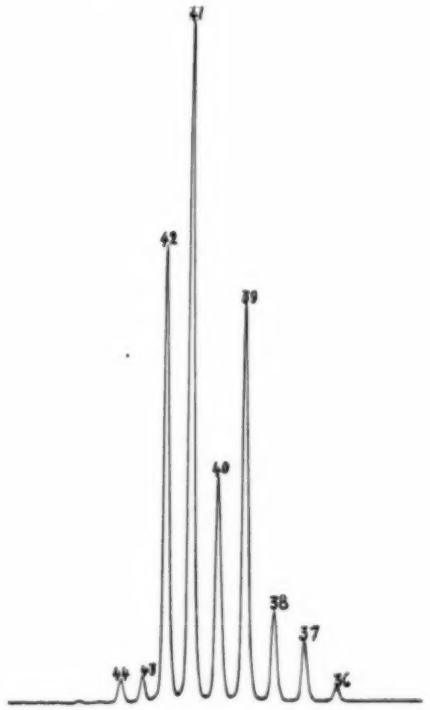

FIG. 1. Mass spectrum in the C_3 region of propylene. Energy of the bombarding electrons about 100 volts.

Before one can make comparisons of the ionization potentials with thermochemical data it is necessary to estimate the various heats of dissociation involved. The energies of the possible states in which three carbons and eight, six, and four hydrogens can exist are shown in Table II. Only the states c_1, e_1, and e_2 are known with any accuracy, the others being correct only in first approximation. The energies are measured from the normal state of the complete molecule in each case. States c_1, e_1, and e_2 have been deduced from the heat of hydrogenation of

TABLE II. *Energies of dissociation of propane, propylene and allene into their various constituents.*

PROPANE		PROPYLENE		ALLENE	
CONFIGURATION	ENERGY	CONFIGURATION	ENERGY	CONFIGURATION	ENERGY
(a_1) C_3H_8	0				
(b_1) C_3H_7+H	2.85				
(c_1) C_3H_6+2H	5.7	(c_2) C_3H_6	0		
(d_1) C_3H_5+3H	8.8	(d_2) C_3H_5+H	3.15		
(e_1) C_3H_4+4H	12.0	(e_2) C_3H_4+2H	6.3	(e_3) C_3H_4	0
(f_1) C_3H_3+5H	15.7	(f_2) C_3H_3+3H	10.0	(f_3) C_3H_3+H	3.75
(g_1) C_3H_2+6H	19.5	(g_2) C_3H_2+4H	13.8	(g_3) C_3H_2+2H	7.5
(h_1) $C_2H_3+CH_3$	2.5	(h_2)			
(i_1) $C_2H_4+CH_4$	0.9	(i_2)			
(j_1) $C_2H_3+CH_4+H$	4.0	(j_2) $C_2H_3+CH_3$	2.8		
(j_1) $C_2H_3+CH_3+H_2$	4.0				
(k_1) $C_2H_2+CH_4+H_2$	2.8	(k_2) $C_2H_2+CH_4$	1.6		
(l_1) 3C+4H	35.2	(l_2) 3C+6H	29.5	(l_3) 3C+4H	23.2

propylene and allene[7] and l_1 and l_2 from the heat of combustion[8] of propane and propylene. States b_1 and d_2 were simply estimated by interpolation and d_1 was deduced from them. A comparison between the states b_1, c_1, d_1, e_1 in propane and the following ones in ethane[4] C_2H_5+H, C_2H_4+2H, C_2H_3+3H, C_2H_2+4H, shows that the removal of one, two, three or four hydrogens requires approximately the same energy in both cases. It will be assumed that the removal of five and six hydrogens require the same energy as in ethane and so the states f_1 and g_1 are determined and f_2, g_2, f_3 and g_3 are easily calculated from them. The states h_1, i_1, j_1, k_1, j_2 and k_2 are independent of these assumptions and are deduced only from l_1, l_2, l_3 and those of ethane,[4] ethylene,[3] acetylene and methane.[1]

The observations on the appearance potentials and the conclusions which may be drawn from them are summarized in Table III. The following notation has been used: X = a molecule or free radical, $A(X^+)$ = appearance potential or minimum energy required to produce the ion X^+ from the parent molecule, $I(X)$ = ionization potential of X, $W(X)$ = excess energy (excitation + kinetic).

In column 1 of Table III are listed some of the important ions observed in the gases studied. The observed appearance potentials in the three gases are given in columns 2, 3 and 4. The processes which best account for these ions are listed in columns 5, 6 and 7. On the basis of the assignment given for each process one may calculate a value for $W(X)+I(X)$ for the free radical X. Only an upper limit can be specified for $I(X)$ because the amount of energy $W(X)$ which goes into excitation of the products or into kinetic energy of translation is unknown. This unknown energy is usually quite small, however, as shown by the agreement in $I(X)$ obtained from the different molecules. The procedure, therefore, is to assume a process of dissociation consistent with the $A(X^+)$ and the energies listed in Table II. In spite of the uncertainties involved in the data this choice is very often unique. The values of $I(X)+W(X)$ are then easily obtained by subtracting from $A(X^+)$ the energy required for dissociation as given in Table II. The data in the last three columns were taken from other papers.[2-4]

A discussion will now be given of some particular cases.

$C_3H_7^+$

There is only one possible choice of reaction leading to this ion.

$$C_3H_8 \rightarrow C_3H_7^+ + H + e.$$

The conclusion is that $I(C_3H_7) \leq 9$ volts, but of course b_1 of Table II is not well known.

[7] Kistiakowsky, Ruhoff, Smith and Vaughan, J. Am. Chem. Soc. **57**, 876 (1935); **58**, 146 (1936).

[8] *International Critical Tables* (McGraw-Hill), and F. R. Bichowsky and F. D. Rossini, *Thermochemistry of Chemical Substances* (Reinhold, 1936).

TABLE III. *Summary of the appearance potentials and the interpretations which may be made.*

X^+	$A(X^+)$ (VOLTS) PROPANE	PROPYLENE	ALLENE	REACTION $C_3H_8\rightarrow$	$C_3H_6\rightarrow$	$C_3H_4\rightarrow$	$I(X)+W(X)$ = UPPER LIMIT OF $I(X)$ C_3H_8	C_3H_6	C_3H_4	C_2H_6	C_2H_4	C_2H_2
$C_3H_8^+$	11.3±0.3						11.3					
$C_3H_7^+$	11.9±0.2			$C_3H_7^+ + H$			9.0					
$C_3H_6^+$	12.3±0.3	10.0±0.2		$C_3H_6^+ + H_2$			11.1	10.0				
$C_3H_5^+$	14.0±0.3	11.8±0.2		$C_3H_5^+ + H_2 + H$	$C_3H_5^+ + H$		9.7	8.7				
$C_3H_4^+$	14.7±1.0	12.4±0.3	9.9±0.2	$C_3H_4^+ + 2H_2$	$C_3H_4^+ + H_2$		11.7	10.6	9.9			
$C_3H_3^+$	15.7±0.5	14.1±0.2	12.5±0.2	$C_3H_3^+ + 2H_2 + H$	$C_3H_3^+ + H_2 + H$	$C_3H_3^+ + H$	9.0	8.7	8.8			
$C_3H_2^+$		15.0±1.0	14.1±0.2		$C_3H_2^+ + 2H_2$	$C_3H_2^+ + H_2$		10.2	11.2			
$C_2H_5^+$	12.3±0.2			$C_2H_5^+ + CH_3$			9.8			9.8		
$C_2H_4^+$	12.2±0.2			$C_2H_4^+ + CH_4$			11.3			10.8	10.8	
$C_2H_3^+$	15.2±0.3	14.5±0.3		$C_2H_3^+ + CH_4 + H$	$C_2H_3^+ + CH_3$		11.2	11.7		10.8	11.0	
				$C_2H_3^+ + CH_3 + H_2$								
$C_2H_2^+$	14.4±0.5	14.0±0.5		$C_2H_2^+ + CH_4 + H_2$	$C_2H_2^+ + CH_4$		11.6	12.4		11.7	11.9	11.2

$C_3H_6^+$

The observed $I(C_3H_6)$ in propylene is 10 volts. Hence from c_1 $C_3H_8 \rightarrow C_3H_6^+ + 2H + e$ will require at least 15.7 volts. The observed $A(C_3H_6^+)$ in propane is below this value and the only possible reaction is therefore

$$C_3H_8 \rightarrow C_3H_6^+ + H_2 + e.$$

Allowing 4.5 volts for the heat of dissociation of hydrogen $I(C_3H_6) \leq 11.1$ volts. This indicates that in this case the total excess energy is about one volt.

$C_3H_5^+$

The way in which this ion is obtained in propylene is unambiguous, giving an upper limit for $I(C_3H_5)$ of 8.7 volts. Once this limit is established, only one possible process can be written for $A(C_3H_5^+)$ in propane requiring less energy than that observed. The results are given in Table II.

$C_3H_4^+$

The ionization potential of this molecule is measured directly in allene and with this knowledge energy considerations determine uniquely the processes responsible for its formation in propylene and propane. It is seen that the hydrogens must come off in molecular form.

$C_3H_3^+$

There are two possible choices for the explanation of this ion in allene. One yields 2H and the other H_2. The second is believed to be the correct one because the other indicates an unusually high value for $I(C_3H_3)$. The same reasoning holds for the assignment in propylene.

$C_3H_2^+$

The process responsible for this ion is unique in allene and the others follow on arguments similar to those given in previous cases.

$C_2H_5^+$

In the formation of this ion and those that follow in the table bonds between carbon atoms must be broken. One would guess from the structure of propane that the easiest way to produce $C_2H_5^+$ would be to ionize the molecule and knock a CH_3 off one end. Energy considerations from Table II indicate that this is the only possible process without ascribing an abnormally low value to $I(C_2H_5)$. Moreover the upper limit deduced on this hypothesis for $I(C_2H_5)$ agrees very nicely with a similar value found in ethane[4] and with the result given by Fraser and Jewitt.[9]

$C_2H_4^+$

In the study of ethylene Kusch, Hustrulid and Tate[3] found a value of 10.8 volts for the ionization potential of this molecule. There is then only one possible explanation of the appearance potential of this ion in propane and that is the formation of $C_2H_4^+ + CH_4$. All other conceivable reactions require too much energy. It may seem a little surprising that this can happen as a result of a single electron impact, but there seems to be no escape from this conclusion. This point will be referred to again in the discussion at the end of this paper.

$C_2H_3^+$

In propylene the simplest way to produce this ion is to remove the CH_3 radical from one end and ionize the remainder. Energetically this turns out to be a unique solution. From state j_1 of Table II it will be seen, however, that in propane there are two possibilities so nearly the same in energy that the experiments are unable to distinguish between them. Both are listed in Table III. It will be noticed that the $I(C_2H_3)$ deduced in propane and propylene agree very well with the earlier results in ethane and ethylene.

$C_2H_2^+$

The ionization potential of acetylene[2] is 11.2 volts. The processes of formation of $C_2H_2^+$ in propane and propylene are given in Table III and they are unique. It will be noticed that all the data on $I(C_2H_2)$ from various gases are in excellent agreement.

In this investigation it appears that all the ions listed in Table III are produced by that reaction which requires the least energy. This has not been true of the simpler hydrocarbons. In fact quite the opposite was true in methane[1] where the highest degree of dissociation seemed

[9] R. G. J. Fraser and T. N. Jewitt, Phys. Rev. **50**, 1091 (1936).

to be preferred. In the two-carbon molecules[3, 4] some hydrogen molecules were formed but not the maximum number possible. However, in propane, propylene and allene the appearance potentials correspond to the formation of the maximum number of molecules in the hydrogen which is removed. It is reasonable to suppose, however, that a molecule of hydrogen is always formed of two atoms which were originally attached to the same carbon. This hypothesis has been verified in the case of ethylene by Delfosse and Hipple.[10] It will also be observed that propylene is much like ethylene except that one hydrogen has been replaced by a CH_3 radical. One might expect, therefore, that CH_4 would be formed in propylene as H_2 is formed in ethylene and the experiments amply verify this hypothesis. Another example of this behavior occurs in propane where CH_4 appears in the formation of $C_2H_4^+$.

The construction of the apparatus was made possible through the work of Dr. J. A. Hipple, Jr., and it is a pleasure to acknowledge this assistance as well as his help with the initial work on propane. We are greatly indebted to the Research Corporation for financial aid which has helped materially in the perfection of our apparatus.

[10] J. Delfosse and J. A. Hipple, Phys. Rev. **54**, 1060 (1938).

AUGUST 1, 1939 PHYSICAL REVIEW VOLUME 56

Collision Cross Sections for D−D Neutrons*

W. H. ZINN, S. SEELY
College of the City of New York, New York

AND

V. W. COHEN
Columbia University, New York, New York

The nuclear collision cross sections of 22 elements for the neutrons from a deuteron-deuteron source have been measured. The geometrical arrangement of the experiment was such that only small corrections to the measured transmission were necessary. The neutron energy was 2.88±0.04 Mev. The cross sections are found to vary irregularly with the atomic weight. The proton cross section determined for both paraffin and water scatterers is found to be 2.36×10^{-24} cm², which is smaller than the value predicted by theory. In addition, the cross sections of a number of elements for neutrons of 2.46 Mev energy have been measured. For some elements the cross section is found to increase with an increase in neutron energy, for others it decreases.

THE total collision cross section of the fast neutrons from radon plus beryllium sources for the nuclei of many of the elements of the periodic table have been measured by Dunning.[1] These cross sections when plotted as a function of the atomic weight show a slow and regular increase with atomic weight. Since, however, the neutrons from Rn+Be are highly inhomogeneous in energy, the total cross sections found with them are only averages for a considerable energy interval.

The importance in nuclear theories of neutron-proton scattering and nuclear scattering in general makes it highly desirable to measure cross sections with neutrons of a single known energy. It is well established that the neutrons from the deuteron-deuteron reaction are, in the main, monoenergetic and hence this source has been used in a number of investigations in which such neutrons were required. Scattering cross sections for deuteron-deuteron neutrons have been measured by Booth and Hurst,[2] Ladenburg and Kanner,[3] and recently by Kikuchi and Aoki.[4]

* Publication assisted by the Ernest Kempton Adams Fund for Physical Research of Columbia University.

[1] J. R. Dunning, Phys. Rev. **45**, 586 (1934).

[2] E. T. Booth and C. Hurst, Proc. Roy. Soc. **161**, 248 (1937).

[3] R. Ladenburg and M. H. Kanner, Phys. Rev. **52**, 911 (1937).

[4] Seishi Kikuchi and Hiroo Aoki, Proc. Phys.-Math. Soc. Japan **21**, 75 (1939); Phys. Rev. **55**, 108 (1939).

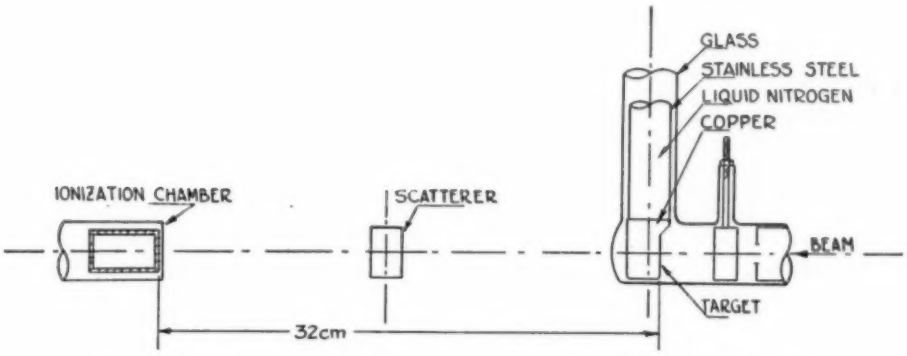

FIG. 1. Arrangement of neutron source, scatterer, and ionization chamber.

In this paper the results of the measurements of the cross sections of 22 elements for neutrons of 2.88 Mev energy are given, as well as the cross sections of some of these elements for neutrons of 2.46 Mev energy. Most of the values given here have been reported as preliminary measurements;[5] in a few instances further investigation has resulted in small changes in the values given previously.

APPARATUS AND TECHNIQUE

The total collision cross section (capture plus scattering) may be determined by measuring the transmission through a sample of material placed in the path of a neutron beam. The ideal arrangement for such an experiment would be to use a point source of neutrons, a point detector, a scatterer of infinitesimal width, and no scattering material in the vicinity of either source or detector. A neutron on suffering either capture or scattering through a finite angle will then fail to be detected. In the present experiment the geometrical arrangement of the source, scatterer and detector is shown schematically in Fig. 1. The scattering samples all had diameters of 3.2 cm and were supported on a thin fiber structure midway between the target and the ionization chamber, the front face of which was 32 cm from the target. The ionization chamber had a diameter of 2.2 cm and a length of 4 cm, and was filled with helium at ten atmospheres pressure. The recoils of the helium nuclei were recorded by a linear amplifier and a scale of two counting circuit. The gain of the amplifier was set so that only the largest recoils, that is, those which had received a considerable portion of the energy of the neutron, were counted. This precaution is necessary since there is some evidence[6] that a deuteron-deuteron source emits neutrons of about 1.0 Mev energy in addition to the main group. Furthermore an anomalous and large value for the helium cross section for 1.0 Mev neutrons has been discovered by Staub and Stephens,[7] from which it follows that the effect of even a small component of low energy neutrons would be unduly large.

The following checks show that the results given here are not influenced by the presence of a group of low energy neutrons. As has been pointed out by Staub and Stephens, the number of recoils recorded when monoenergetic neutrons impinge on a gas-filled ionization chamber should vary linearly with the bias of the pulse selecting Thyratron in the recording circuit. Such a plot produced a straight line for a considerable variation of Thyratron grid voltage on either side of the voltage used in these measurements. Also visual observations of the pulses on a cathode-ray screen established the fact that recoils from 1.0 Mev neutrons could not be counted. As a further check some of the cross sections were measured with a hydrogen-filled chamber and gave values identical, within the limits of error, with those found with the helium-filled chamber.

The neutron generator used in this work has

[5] W. H. Zinn, S. Seely and V. W. Cohen, Phys. Rev. **53**, 921 (1938). S. Seely, W. H. Zinn and V. W. Cohen, Phys. Rev. **55**, 679 (1939).

[6] T. W. Bonner, Phys. Rev. **53**, 711 (1938).

[7] H. Staub and W. E. Stephens, Phys. Rev. **55**, 131 (1939).

been described[8] and is so designed that the amount of scattering material in the neighborhood of the target is reduced in a minimum. The target was heavy water ice frozen on a thin-walled copper cup cooled by liquid nitrogen. From the thickness of the copper and nitrogen, and a knowledge of the mean free path of neutrons in these substances, it is estimated that a negligibly small number of neutrons were scattered into the beam by the target support. The deuterons were magnetically separated from the molecular ion beam and were focused into a spot approximately 5 mm in diameter. Under these conditions the source of neutrons was a sufficient approximation to a point source.

In measurements of this kind it is desirable to have the background due to neutrons from points other than the target as small as possible. The correction due to room scattering was determined by placing a paraffin cylinder 28 cm long and of the same diameter as the scattering samples between the target and the ionization chamber. The neutron intensity under these conditions was 3 percent of the intensity when the paraffin was removed. This low background intensity is due to the fact that neutrons which have lost energy by scattering are not recorded because the counting circuit was set to discriminate against low energy recoils. The background was also shown to be small by means of an "inverse square" measurement.

In order to eliminate any error due to fluctuations of the deuteron current to the target, a current integrator was used. The accelerating voltage was maintained constant to better than one percent by manual manipulation of a resistance in the primary of the transformer of the high tension apparatus. However, errors due to fluctuations in intensity of the neutron beam are possible with constant voltage and a current integrator, because the condition of the target and the composition of the deuteron beam may vary with time. The effect of these was minimized by making observations cyclically, that is, first a count for the direct beam was made, second, a count with the scatterer in place, third, a background count, etc. The time of counting in each case was so adjusted that the total number of neutrons counted with the scatterer in place was the same as the total number without.

The accelerating potential used in these measurements was 121 kv. Bonner's[6] latest Q value of 3.29 Mev for the ${}_1H^2+{}_1H^2$ reaction gives, for the energy of the neutrons which are emitted in the forward direction, a value of 2.88 ± 0.04 Mev. Those emitted at right angles to the deuteron beam have an energy of 2.46 ± 0.04 Mev. The width of 80 kv for the neutron energy spectrum results from the use of a thick target and is also due to the finite angle subtended by the ionization chamber at the target.

TABLE I. *Total collision cross sections. Neutron energy—2.88±0.04 Mev.*

ELEMENT	COMPOUND USED	G/CM²	CORRECTED TRANSMISSION	$\sigma\times10^{24}$ CM^{-2}
${}_1H$	$C_{22}H_{46}$	1.976	0.571	2.32±0.09
${}_1H$	H_2O	3.00	.543	2.40± .09
${}_1D$	D_2O	3.32	.574	2.17± .08
${}_5B$	B_4C	4.34	.626	1.98± .07
${}_6C$		6.14	.547	1.97± .07
${}_7N$		7.05	.658	1.38± .06
${}_8O$		9.92	.633	1.25± .05
${}_{11}Na$		6.31	.676	2.37± .09
${}_{12}Mg$		10.88	.545	2.25± .07
${}_{13}Al$		9.92	.599	2.34± .07
${}_{14}Si$		4.31	.774	2.77± .08
${}_{16}S$		8.25	.623	3.12± .15
${}_{17}Cl$	CCl_4	4.77	.541	3.42± .16
${}_{19}K$		6.22	.741	3.13± .15
${}_{25}Mn$		11.76	.611	3.82± .12
${}_{26}Fe$		15.68	.588	3.15± .10
${}_{29}Cu$		22.86	.549	2.82± .10
${}_{30}Zn$		18.24	.576	3.28± .10
${}_{34}Se$		12.75	.675	4.05± .16
${}_{42}Mo$		12.14	.733	4.06± .14
${}_{50}Sn$		22.38	.608	4.39± .16
${}_{80}Hg$		33.45	.585	5.34± .20
${}_{82}Pb$		33.44	.520	6.74± .24

RESULTS AND DISCUSSION

The results of this investigation for neutrons of 2.88 Mev energy are summarized in Table I. In the first column are given the elements and the atomic numbers; in the second column are listed the compounds which were used in those cases in which the pure elements were not available; the third column gives the mass per cm²; the fourth column contains the corrected transmissions, the last column gives the scattering cross sections calculated from these transmissions. Two corrections were applied to the measured transmissions. (1) Room scattering: this is a substantially constant term which is

[8] W. H. Zinn and S. Seely, Phys. Rev. **52**, 919 (1937).

subtracted from the intensities observed with and without the scatterer in place. It decreases the measured transmission in most cases by about 1.2 percent. (2) Scattering of neutrons into the ionization chamber by the scatterer: for isotropic scattering this correction amounts to a decrease of 0.7 percent in the measured transmission. For hydrogen and deuterium where the scattering in the room system is nonisotropic, the corrections are 3 percent and 1.3 percent, respectively. Since all the scatterers were approximately one-half mean free path long the correction for multiple scattering is negligible.

Reasonable care was exercised with regard to the purity of the materials used, compounds, in general, being avoided because of the difficulty of insuring their freedom from moisture contamination. Materials obtainable only in powder or liquid form were placed in thin-walled brass or glass cells. A similar empty cell was used in obtaining the count for the unfiltered beam so that no correction for the effect of the cell was necessary. The liquid oxygen and liquid nitrogen were placed in glass Dewar flasks. The purity of the oxygen was verified by measuring the boiling point with a platinum resistance thermometer.

Neutron-Proton Cross Section

In Table I two values for the neutron-proton cross section are given, one obtained with a paraffin scatterer and the other with water as the scattering material. Repeated measurements, under varying conditions, were made on these substances; for paraffin in particular the dimensions of the samples were varied as well as the source of the paraffin. The chemical composition of the paraffin was estimated by measuring the melting point. The cross sections determined from water and paraffin agree within the limits of error assigned to the measurements and since the cross sections of oxygen and carbon which enter into the proton determination were measured with comparable precision, neither measurement is to be preferred to the other. In view of the great importance of the neutron-proton interaction in nuclear theory it seems quite urgent to make a more precise study of the neutron-proton scattering cross section. The chief limitation in accuracy attainable with the present apparatus is due to slight fluctuations in the emitted neutron intensity associated with changing conditions of the ice target, and with fluctuations in the accelerating voltage. This difficulty may be overcome by using a monitor detector system for checking the neutron emission during readings. Such a system is now under construction in this laboratory.

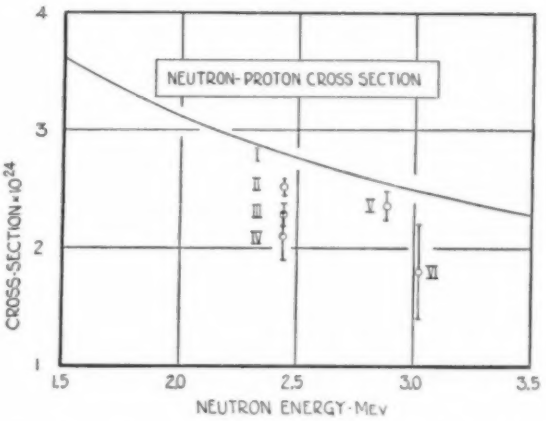

FIG. 2. I. Theoretical curve. II. Aoki. III. Kikuchi and Aoki. IV. Ladenburg and Kanner. V. This paper. VI. Booth and Hurst.

In Fig. 2 the neutron-proton cross sections as measured by various experimenters using deuteron-deuteron neutrons are plotted as a function of the energy of the neutrons. The energy of the neutrons in each case has been computed with $Q=3.29$ Mev. The average of our water and paraffin measurements, namely, $2.36\pm0.12\times10^{-24}$ cm^2, is plotted as representing best the results of this investigation. The solid curve is obtained from the following equation[9] for the scattering cross section.

$$\sigma=\frac{4\pi^2\hbar}{M}\left(\frac{3}{4}\,\frac{1+\alpha_0 r_0}{|E_0|+\frac{1}{2}E}+\frac{1}{4}\,\frac{1+\alpha_1 r_0}{|E_1|+\frac{1}{2}E}\right),$$

where $E_0=2.17$ Mev is the binding energy of the deuteron; $r_0=2.8\times10^{-13}$ cm is the value of the range of the nuclear forces obtained from experiments on proton-proton scattering.[10] $E_1=0.066$ Mev is the energy of the singlet state of the deuteron. This value is chosen so that the slow neutron cross section is in agreement with the

[9] J. Schwinger and E. Teller, Phys. Rev. **52**, 286 (1937).
[10] G. Breit, H. M. Thaxton and L. Eisenbud, Phys. Rev. **55**, 1018 (1939).

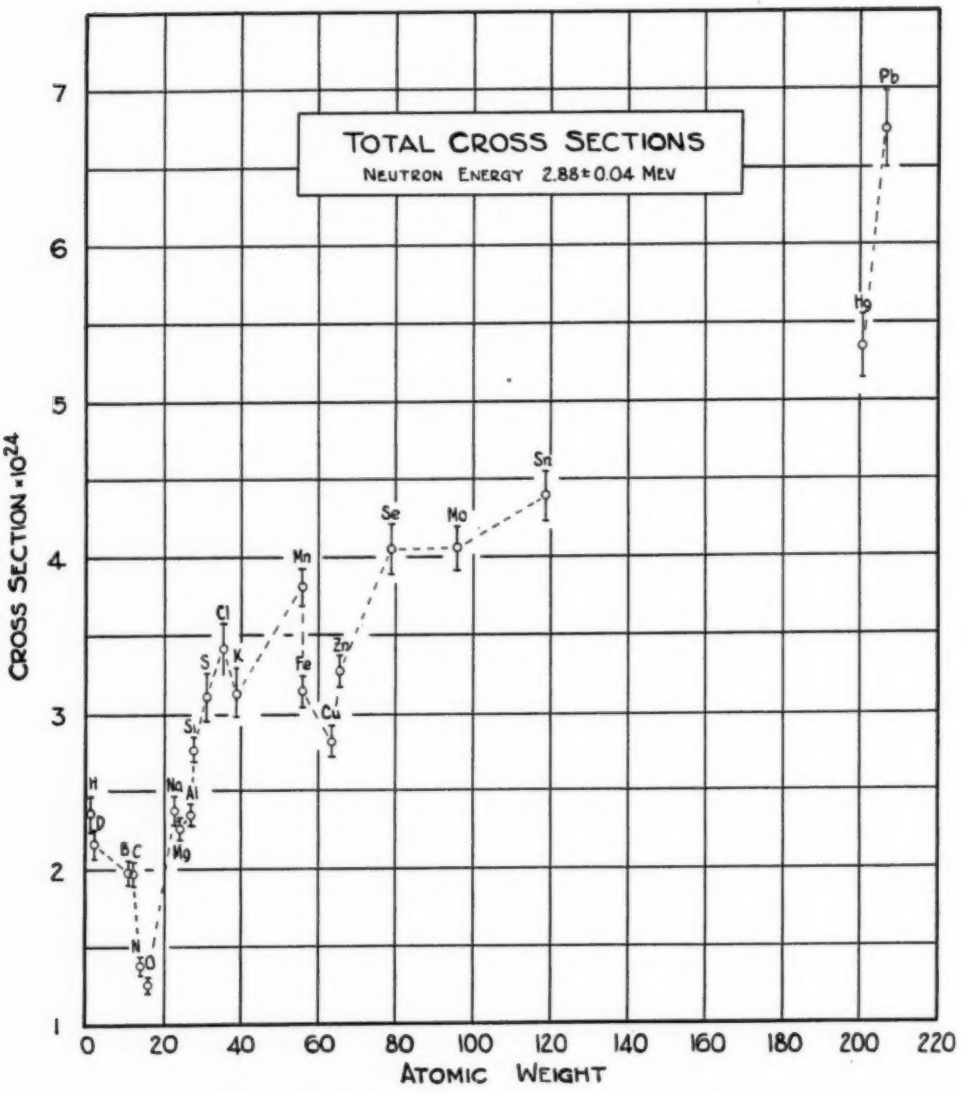

FIG. 3. Cross sections as a function of atomic weight.

value of 20×10^{-24} cm² given by Cohen, Goldsmith and Schwinger.[11]

Ladenburg and Kanner[12] first pointed out that a small discrepancy exists between theory and experiment if one assumes a reasonable value for the range of the nuclear forces. An examination of Fig. 2 shows that all measurements made so far definitely lie below the theoretical curve. No reasonable value for the slow neutron cross section will allow a sufficient change in the binding energy of the singlet state of the deuteron to bring the theoretical and experimental values into agreement. Theory gives a cross section in agreement with our value of 2.36×10^{-24} cm² if the range is assumed to be 1.88×10^{-23} cm². A revision of the theory in order to remove this difficulty, among others, has been proposed by Schwinger.[13] This revised theory does give values for the neutron-proton cross sections which are lower than those calculated from the above formula without requiring a value for the range of the nuclear forces in disagreement with the range found in proton-proton scattering experiments.

[11] V. W. Cohen, H. H. Goldsmith and J. Schwinger, Phys. Rev. **55**, 106 (1939).

[12] R. Ladenburg and M. H. Kanner, Phys. Rev. **52**, 1255 (1937).

[13] J. Schwinger, Phys. Rev. **55**, 235 (1939).

Cross Sections as a Function of Atomic Weight

In Fig. 3 the cross sections are plotted against the atomic weight. It is clearly evident that there is no smooth and regular increase with atomic weight as found by Dunning[1] with the Rn+Be neutrons or a periodic variation as has been suggested by Kikuchi and Aoki.[4] These results are not directly comparable with those of Ladenburg and Kanner[3] who measured the cross sections for some of the lighter elements or with those of Kikuchi and Aoki because of the different neutron energies used. Staub and Stephens[7] have determined the ratio of the helium cross section to that of hydrogen for these energies from which it follows that the He cross section is 3.3×10^{-24} cm^2. It is to be noted that in going from helium to oxygen the cross section decreases to almost one-third. On the basis of a simplified potential model, Fay[14] has made calculations for the variation of nuclear cross section with atomic number and finds, for certain neutron energies, very sharp resonances. Insufficient elements of higher atomic number have been measured in this work to permit a quantitative comparison. However, in view of the inhomogeneity of the neutron energy, one would expect a smoothing out of extremely sharp resonances into the kind of variation actually observed.

Cross Sections as a Function of Neutron Energy

The considerable difference between our value of the oxygen cross section for 2.88-Mev neutrons and that of Ladenburg and Kanner[3] for 2.4-Mev neutrons and the rather large differences between our values and those of Kikuchi and Aoki[4] for such elements as sodium and potassium suggest that the cross sections are quite sensitive to the energy of the neutrons. Accordingly, we have measured the cross section of some elements for two different neutron energies under identical experimental conditions; these are given in Table II.

Table II. *Cross sections for different energies.*

Element	Atomic Number	Neutron Energy	
		2.46 Mev	2.88 Mev
C	6	1.37±0.05	1.97±0.05
N	7	1.40± .06	1.38± .06
O	8	1.05± .03	1.25± .05
Na	11	2.70± .16	2.37± .09
Al	13	2.99± .07	2.34± .06
S	16	2.77± .14	3.12± .15
K	19	3.44± .18	3.13± .15

For each element measured, with the exception of nitrogen, the change in cross section is greater than the error of the measurement. In some cases, notably carbon and aluminum, the percentage change in cross section is considerably greater than the percentage change in neutron energy. It is also to be noted that for about one-half of the elements measured the cross section increases with an increase in neutron energy while for the remainder it decreases. These facts indicate strongly that here we are dealing with a resonance scattering of the neutrons. That this is indeed the case is shown by the recent results of Aoki.[15]

The following should be noted for the elements of Table II: in each case where a real difference exists between our value of a cross section of 2.88 Mev and the measurements of other observers for a lower energy of neutrons, the change in cross section is in such a direction as to bring the values into agreement.

The writers wish to express their indebtedness to the Department of Physics of Columbia University for the laboratory facilities placed at their disposal, to Professor John R. Dunning for the loan of an amplifier and ionization chamber, to Professor S. L. Quimby for measuring the boiling point of the liquid oxygen and to Dr. Julian Schwinger for helpful discussions concerning the neutron-proton cross section.

[14] C. A. Fay, Phys. Rev. **50**, 560 (1936).

[15] Hiroo Aoki, Phys. Rev. **55**, 795 (1939).

The Concentration of Isotopes by the Evaporative Centrifuge Method

J. W. BEAMS AND C. SKARSTROM
Rouss Physical Laboratory, University of Virginia, Charlottesville, Virginia
(Received May 31, 1939)

The air-driven vacuum-type tubular centrifuge has been used for the concentration of the isotopes of chlorine by the "evaporative" centrifuge method. The separations obtained were about the same as predicted by the theory provided the experimental conditions approximately conformed to the assumptions of the theory. With a steel tube 11″ long and 3″ inside diameter, containing baffles to prevent remixing, and spinning at 1060 r.p.s., carbon tetrachloride vapor could be withdrawn from the axis at the rate of 3.2 grams per minute without decreasing the separation factor. This separation factor for chlorine, which at any instant is the ratio of the concentrations of the light to heavy isotopes at the axis, divided by the same ratio at the periphery, was 1.025 in the above case. It is believed that the method is practical in the case of the heavier elements.

ALTHOUGH the general theory for the separation of isotopes by centrifuging has not been completely worked out, the theory for the separation obtained in an ideal gas and in an incompressible liquid after equilibrium is established was given by Lindemann and Aston in 1919.[1, 2] Since that time it has been further discussed and extended, especially by Mulliken,[3] Chapman[4] and Harkins,[5] and several attempts have been made to obtain a separation experimentally.[3, 6, 7] In every case the experiments proved to be unsuccessful and the method was generally considered as impractical. However, the high rotational speed, as well as the convection-free sedimentation, attained by the self-balancing vacuum-type ultracentrifuge[8, 9] has encouraged us to give the method another trial. This seemed worth while because, according to the theory, the separation factor should depend principally upon the differences in the masses of the isotopes rather than their absolute values so that, if successful, the method could separate the isotopes of the heavier elements as well as the lighter. The preliminary results[10–13] indicated that a separation in very rough accord with theory could be obtained provided the process was carried out slowly enough for equilibrium to be established. In the present paper a continuation of this work is described, in which the theory has been more accurately verified, and in which improvements in the experimental technique have greatly increased the rate of separation.

The general procedure principally used in this work is similar to the "evaporative centrifuge" method suggested by Mulliken.[3] It consists in drawing out vapor from the axis of a hollow spinning rotor containing liquid near its periphery. If this process takes place slowly enough for an equilibrium to be established between sedimentation and diffusion, and if the vapor approximately obeys the ideal gas laws, then the separation factor

$$S=\exp\frac{(M_2-M_1)\omega^2r^2}{2RT} \qquad (1)$$

for a mixture of two isotopes, where S is defined as the ratio of the concentrations of light to heavy isotopes at the axis divided by the same ratio at the periphery of the rotor. M_2 and M_1 are the atomic weights of the heavy and light

[1] F. A. Lindemann and F. W. Aston, Phil. Mag. (6) **37**, 523 (1919).
[2] F. W. Aston, *Mass Spectra and Isotopes* (Arnold, 1933).
[3] R. S. Mulliken, J. Am. Chem. Soc. **44**, 1033 (1922); **44**, 1729 (1922); **45**, 1592 (1923).
[4] S. Chapman, Phil. Mag. (6) **38**, 182 (1919); Phil. Trans. **A217**, 115 (1918).
[5] W. D. Harkins, J. Frank. Inst. **194**, 783 (1922).
[6] J. Joly and J. H. J. Poole, Phil. Mag. (6) **39**, 372 (1920).
[7] J. H. J. Poole, Phil. Mag. (6) **41**, 818 (1921).
[8] J. W. Beams and E. G. Pickels, Rev. Sci. Inst. **6**, 299 (1935).
[9] J. W. Beams, J. App. Phys. **8**, 795 (1937); Rev. Mod. Phys. **10**, 245 (1938).
[10] J. W. Beams and F. B. Haynes, Phys. Rev. **50**, 491(L) (1936).
[11] J. W. Beams and A. V. Masket, Phys. Rev. **51**, 384(A) (1937).
[12] Skarstrom, Carr and Beams, Phys. Rev. **55**, 591(A) (1939).
[13] Somewhat similar results have been reported recently on the separation of bromine by R. F. Humphreys, Phys. Rev. **55**, 674(A) (1939).

isotopes, respectively. ω is the angular velocity of the centrifuge; r is the radial distance from the liquid surface to the axis; T the absolute temperature; and R the gas constant. The change in average atomic weight $\Delta\bar{A}$ of the element in the residue from that in the original material, according to Mulliken,[3] is, for a mixture of two isotopes:

$$\Delta\bar{A}=\frac{(M_2-M_1)^2X_1X_2\omega^2r^2}{2RT}$$

$$\times\log_e C \text{ approximately,} \quad (2)$$

where X_1 and X_2 represent the mole fractions of the light and heavy isotopes in the material and C is the so-called cut which is the ratio of the volume of the material present initially to the volume of residue remaining in the centrifuge. Mulliken has further shown that the above formulas for the separation are independent of the state of combination of the element.

Since the separation to be expected should be the same for any compound of the element, it was decided to carry out the development work with carbon tetrachloride because of its availability, noninflammability, suitable vapor pressure at room temperature, and easy condensability at dry-ice temperature. Furthermore, the isotopic analysis was simplified because it is suitable for density measurements, and chlorine could be conveniently used in the mass spectrograph available. Since the concentration of C^{13} is small, there are five principal molecular species, namely $C^{12}(Cl^{35})_4$; $C^{12}(Cl^{35})_3Cl^{37}$; $C^{12}(Cl^{35})_2(Cl^{37})_2$; $C^{12}Cl^{35}(Cl^{37})_3$; and $C^{12}(Cl^{37})_4$. In ordinary CCl_4, if each molecular species is built up from the atoms according to chance, then the concentrations of the various species are given by the terms of the binomial expansion of $(X_1+X_2)^4$.

In some of the preliminary experiments a rotor having a hollow flat cylindrical chamber 8.9 cm diameter and 0.64 cm high was spun in a vacuum[9-11] at 1550 r.p.s. The CCl_4 vapor was drawn out of the center at the rate of 2 cc of liquid per hour. Under these conditions the observed separation was only about 40 percent of that to be expected from the equilibrium theory. If the rate of drawing out vapor was decreased, the separation was increased, so it was concluded that the rate of withdrawal of vapor was too rapid for approximate equilibrium to be established without stirring. In order to correct this, an apparatus was developed for spinning long hollow tubes in a vacuum. Fig. 1 shows a vertical section of the apparatus. The rotating members consist of the tubular centrifuge C which spins inside the vacuum chamber V, an air-supported air-driven turbine T situated above V, and the flexible shafts A and L which lie in their vertical axis of rotation. The shaft A

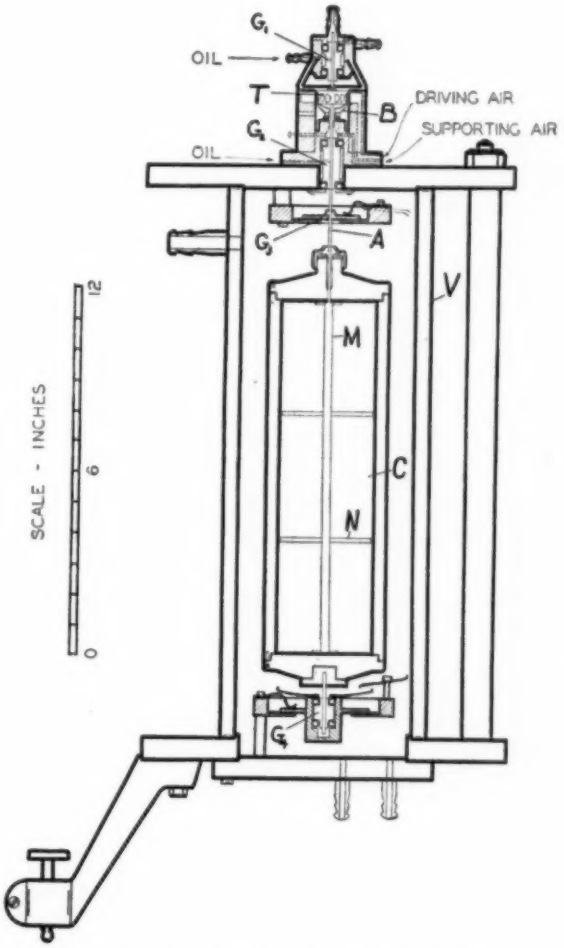

FIG. 1. Schematic vertical section of the centrifuge.

is a hollow stainless steel tube (hypodermic needle tubing gauge 14). It passes through the vacuum tight oil glands G_1 and G_2, which have been described in detail previously.[9] The shaft A was fastened to the air turbine by a chuck and to the tubular rotor C by a pinchuck which both clamps the shaft and imbeds itself into a lead

gasket, forming a vacuum-tight seal. Consequently the tubular rotor can be evacuated through the hollow shaft A. The pillbox-shaped Duralumin turbine T (1″ diameter × $\frac{3}{8}$″) is supported by an air cushion formed between its undersurface and the Bakelite collar B. This air cushion supports all of the rotating members, which weigh about 25 lb. If this free air space directly beneath the turbine is made small and care is taken to make sure that the rubber or Duprene ring upon which B rests is uniformly flexible, rotors weighing at least 75 lb. can be supported. The turbine is driven by air jets impinging upon flutings milled into its periphery.[14] The auxiliary bearings G_3 and G_4 inside the vacuum chamber were added to reduce precessional motions, especially during the period of acceleration. Each of these bearings, which were made of hard babbitt, was mounted in a loose plate that was kept in contact with a fixed plate by leaf springs. This construction supplied sufficient radial friction to inhibit the precession. These bearings were supplied with oil by the drippings from the oil gland G_2, the lower one receiving the overflow from the upper. This vacuum pump oil is finally collected, filtered, and used over again. The tubular rotor C was made of chrome molybdenum steel alloy[15] 11″ long × 4″ O.D. × $\frac{1}{2}$″ wall, with a yield point of 159,000 lb./in.^{2}. This tube has already had 700 hours of rotation at from 1000 to 1100 r.p.s. On one occasion the speed was increased to 1200 r.p.s. At this speed the rotor stretched radially, causing the gaskets between the tube and the Duralumin ST14 end caps to leak. Upon examination the internal diameter of the rotor was found to have increased 0.02″. The tube was boiled in water for 30 minutes and has since been in use 400 hours at about 1060 r.p.s. Care was taken to machine carefully both the inner and outer walls of the tube and to see that it was dynamically balanced. The small steel tube M is uniformly perforated with a large number of fine holes so that the vapor is drawn out at a uniform rate along the axis of the spinning tube. N are circular Duralumin ST14 disks perforated with holes, which served to brace the tube M. The vacuum chamber V consisted of an 18″ length of cold-rolled steel tubing 7″ O.D. × $\frac{1}{2}$″ wall, which was closed at both ends by steel disks that had been lapped to fit. Vacuum wax was used to give a vacuum-tight seal. Three tie rods were used to bolt the chamber together. As a precaution against explosion, the apparatus was enclosed by a barricade consisting of a 10″ thickness of soft wood. The vacuum chamber was evacuated through dry-ice traps by a mercury diffusion pump backed by a Cenco Hyvac pump.

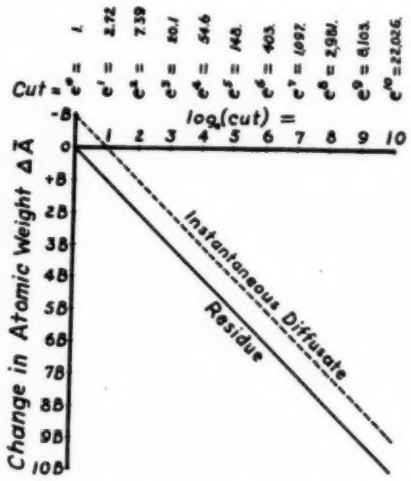

FIG. 2. Relation between the change in average atomic weight $\Delta\bar{A}$ and $\log_e C$. For chlorine under the experimental conditions $B = \frac{(Cl^{37} - Cl^{35})^2\omega^2r^2}{2RT} X_1X_2 = 9\times10^{-3}$ app. For CCl_4 the change in average molecular weight $\Delta M = 36$. $\times10^{-3}$ log C.

To operate the machine 105 cc of CCl_4 were either injected into the rotor through A by a long small hypodermic needle or were distilled in while the rotor was running. The former method was usually used when the rotor was started from rest, and the latter when the material had to be put in with the rotor at full speed, i.e., when several different "batches" were centrifuged the same day. Since the pressure of the CCl_4 vapor at the center was only about one-seventh that at the periphery, the rotor acts as a pump and pulls the CCl_4 in very rapidly, especially when the air is removed from the system. The condensation

[14] For a more detailed description of this type of driving and supporting mechanism, reference should be made to J. App. Phys. **8**, 795 (1937); Rev. Mod. Phys. **10**, 245 (1938); Rev. Sci. Inst. **9**, 413 (1938).

[15] Obtained from the Summerill Tubing Company, Bridgeport, Pennsylvania. Recently we have used tubes from the same source of chrome molybdenum steel 4130 X SAE 24″ long × 4″ O.D. × $\frac{1}{2}$″ wall, with tensile strength of 200,000 lb./in.^{2}.

of the CCl_4, of course, at first heats the rotor since it is in a vacuum, but is not enough to give serious trouble because of the rotor's size. Vacuum pump oil is forced into G_2 at a pressure about 15 lb./in.^{2} greater than the supporting air pressure. The vacuum pump oil pressure in G_1 was about 10 lb./in.^{2}. The supporting air pressure could be varied over as much as 20 lb./in.^{2} without causing instability in the air cushion, but it was usually set at 45 lb./in.^{2}. The driving pressure was set at 100 lb./in.^{2} until the desired speed was attained, then reduced to the proper value to keep the centrifuge at constant speed. The speed was measured by beating the note given off by the turbine against a known frequency. The air pressure was held constant by a pressure regulator which, when properly set, kept the rotational speed sufficiently constant. The variations in the rotational speed were very slow because of the large moment of inertia of the rotor, so that the air valves could be adjusted manually. The total amount of air required to accelerate the centrifuge was 20 cu. ft./min. and to keep it at constant speed at 1060 r.p.s. was 11 cu.ft./min. each, reduced to standard conditions.

After reaching the desired speed the air was quickly pumped out of the rotor C. The CCl_4 vapor was allowed to flow out through A at the desired speed and was condensed in dry-ice traps in a number of successive fractions. The first fractions collected showed a concentration of the light isotope, while the last fractions and the residue showed a concentration of the heavy isotope. The changes in the isotopic ratio were determined by differential density measurements and by the mass spectrometer. In the density measurement considerable quantities of material were necessary and it was essential to purify it carefully. Baker's C. P. CCl_4 was distilled several times to remove as many impurities as possible before centrifuging. Since in the process of centrifuging the material might become contaminated by oil or other impurities in the machine, each fraction measured was again purified by shaking with P_2O_5 followed by several vacuum distillations until the density remained unchanged with further distillation. The CCl_4 was then placed in a special Pyrex glass pyknometer with long uniform capillaries closed with glass stoppers. This pyknometer was placed in a temperature bath which was constant to at least 0.01°C as measured by a Beckmann thermometer. The heights of the menisci in the capillaries were determined by a cathetometer. Weighings were made on a chemical balance. The pyknometer held about 3.60 grams of CCl_4 and the density changes could be determined to 0.006 percent. The mass spectrometer was modeled after one described by Blewett.[16] A change in the isotopic ratio of about two percent could be determined and only a few drops of the material were required. The mass-spectrometer determinations also are independent of possible impurities. The two methods were in good agreement in almost every determination.

In Fig. 2 the solid curve shows the change in the average atomic weight $\Delta\bar{A}$ of the residue remaining in the rotor as a function of the amount of residue, while the dashed curve shows the $\Delta\bar{A}$ in a very small amount of the material drawn off at any instant (instantaneous diffusate). The curves are computed from Mulliken's theory[3, 5] assuming equilibrium is established when the vapor was drawn out slowly enough to insure that stirring was absent and equilibrium was approximately established. The experimental results obtained were in good accord with the curves. Because of the small changes obtained with small cuts, the measurements were carried out on samples which were residues with cuts from 6 to 330. The circles in

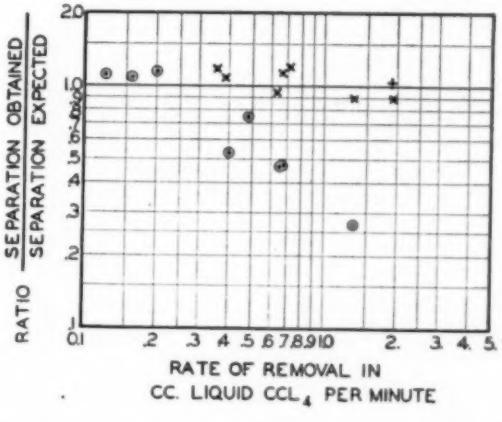

FIG. 3. The circles give the results obtained with the hollow tube shown in Fig. 1. The crosses give the results obtained with the "spider" baffles shown in Fig. 4.

[16] J. P. Blewett, Phys. Rev. **49**, 900 (1936).

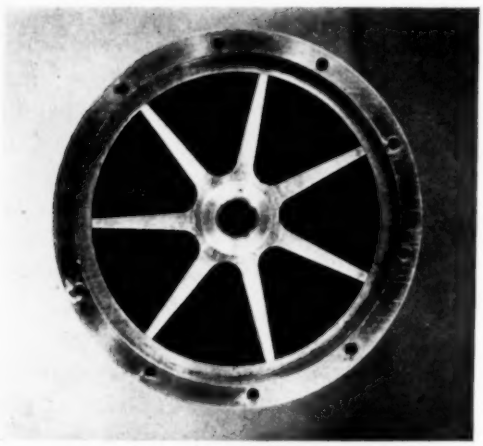

FIG. 4. Photograph of tubular rotor with end cap removed, showing the "spider" baffle in place. The vapor enters the axial channel through a large number of uniformly spaced small holes (not shown) connecting the sector-shaped compartments with the axial channel.

Fig. 3 give the ratio of the separation obtained experimentally, divided by the separation computed from the theory (Eq. (2)), plotted against the rate of removal of the material from the hollow tube of Fig. 1. It will be observed that when the rate of removal exceeds about $\frac{1}{5}$ cc/min., the efficiency of separation begins to fall off. In the absence of a complete theory of the separation, it was of course impossible to compute the time required for equilibrium to be established, although rough estimations indicated that it might be more rapid than indicated by the experiments. The possibility that the isotopic composition at the surface of the liquid was changed to an enrichment of the heavy isotope, which would cause the efficiency of separation to decrease at high withdrawal speeds, also could be ruled out. When the evaporation takes place from the liquid surface, it is cooled. This increases the density of the surface layer and causes violent stirring in the liquid[9] so that it automatically is kept uniformly mixed during the centrifuging. The possibility of stirring in the vapor due to thermal gradients also was eliminated by theoretical calculations and experimentally by introducing hydrogen at a few mm pressure into the rotor to minimize temperature gradients. The introduction of the hydrogen produced no appreciable change. It was decided finally that the decrease in efficiency was caused by stirring or remixing in the vapor. Since the angular momentum of the vapor is conserved as it moves from the liquid surface near the periphery toward the center, it rotates at a higher angular velocity than the centrifuge. This "whirlwind" apparently became large enough to stir or remix the vapor at withdrawal speeds above one-fifth of a cc per min. In order to reduce this type of stirring, a star-shaped spider made of Duralumin ST14 was introduced into the rotor, as shown in Fig. 4. This formed long sector-shaped cells for the diffusion to take place and should reduce circulation. With this arrangement it was found that no decrease in efficiency was observed with a rate of withdrawal of 2 cc of liquid CCl_4 per minute (represented by the crosses in Fig. 3), which was the highest rate we could obtain through the gauge 14 shaft A at room temperature.

The above experimental results show that the separation attained is roughly that predicted by the theory, provided equilibrium exists. Hence the assumption of the theory that the vapor obeys the ideal gas laws apparently does not introduce large errors.

In these experiments the value of the separation factor S was 1.025 for chlorine.* The value of $\Delta\bar{A}$, of course, changed as the isotopic ratio changes, since the mole fractions X_1 and X_2 change. Unfortunately, a tube is not a very strong mechanical construction for a centrifuge and the peripheral velocity was only about 2.5×10^4 cm/sec. In the smaller centrifuges we obtained a separation factor for carbon tetrachloride of 1.1 with a peripheral velocity of 5×10^4 cm/sec. However, the very high speed with which the vapor can be withdrawn from the long tubular rotor gives it a great advantage. Starting with 105 cc of CCl_4 in the tubular rotor, one obtains about 40 cc of liquid CCl_4 with the isotopic ratio changed by 2.5 percent in 32.5 min., or 14 cc of liquid CCl_4 with the isotopic ratio changed by five percent in 46 min., or 1 g

* The separation factor S for carbon would, of course, be 1.012, since the mass difference of the isotopes is one. Hence the carbon 13 is concentrated in the residue in the centrifuging of CCl_4. One advantage of using compounds is that isotopes of all of the different elements in a compound are separated simultaneously.

with the ratio changed by 12.8 percent in 52.3 min. In addition to these, one also simultaneously collects a series of intermediate fractions with the enrichments given by the dashed curve in Fig. 2. By recentrifuging these intermediate fractions the rate of isotopic enrichment is much increased.

Conclusions

It will be observed from the above results that in order to get large changes in the isotopic ratio, very large "cuts" must be made. This means that one must start with large volumes of material and recentrifuge many times. The intermediate fractions must also be collected and recentrifuged. Such a procedure is rather slow and tedious unless several machines are available that may be run simultaneously. On the other hand, if large quantities of material are desired, with, say, 15 percent or 20 percent or less change in the isotopic ratio, the method in its present state is comparatively fast. Apparently, from experiment, equilibrium is established very quickly when stirring is eliminated by baffles, so that even in the case of compounds of the heaviest elements, it should be possible to pass the material through the machine rapidly. Since the separation factor depends only upon the differences in the masses, the results obtained with chlorine should be practically duplicated in any element whose isotopes have a mass difference of two. If they have a greater mass difference or spread, as in the case of many of the heavier elements, the separation factor is increased by this difference in the exponent of e. The evaporative centrifuge method can only be used for substances which may be liquefied at the periphery of the rotor which, at the same time, have a considerable vapor pressure. Fortunately this limitation is not as serious as might be thought at first, because many of the compounds of the elements (including the metal organic compounds) may be used. Furthermore, the vacuum-type centrifuges have been operated successfully in our laboratory with the rotor temperatures varying from 100°C to liquid-air temperatures. Incidentally, it should be noted that the absolute temperature enters into the equation for the separation factor in the denominator of the exponent of e. Consequently the separation increases with decreasing temperatures.

In the above experiments, when stirring was prevented by baffles, it was not possible to draw out the vapor fast enough to obtain a measurable decrease in separation due to absence of equilibrium. However, it is possible to more than double the diameter of the tubular shaft so that the rate at which equilibrium is established will undoubtedly set the final limit to the speed with which the material can be centrifuged.

The amount of material that can be passed through a single machine and still have equilibrium practically established should be proportional to the length of the tube. As yet we have found no upper limit to the length of tube that can be spun, and there is little doubt that tubes several feet long can be spun successfully. The equilibrium probably would be established faster in smaller diameter tubes. The separation factor can be increased considerably over the values obtained in the above experiments with somewhat stronger rotor material available. Even a small increase in rotor strength, and hence greater permissible peripheral velocity, should make possible considerable increase in the separation factor, since the peripheral velocity is squared in the exponent of e, Eq. (1).

For large concentrations of the isotopes in smaller quantities of material, it is probable that the evaporative centrifuge method is inferior to other possible centrifuge methods. The continuous-flow vacuum-type tubular centrifuge,[17] which at present is being used, possesses several points of superiority over the evaporative method. Furthermore, Professor Urey has suggested to us that if an apparatus somewhat analogous to his fractionating columns could be mounted in a long tubular centrifuge in such a way that the separation would result from the effective diffusions of the material through the centrifugal field many times (i.e., the material would diffuse from periphery to center, then be thrown back out without diffusion. This process would take place over and over again), then the separation could be greatly increased. If such an arrangement proves to be feasible experimentally, it should be a relatively fast method of separation

[17] J. W. Beams, Rev. Sci. Inst. **9**, 413 (1938).

—first, because of the large values for the separation factor; and second, because of the high speed with which equilibrium between diffusion and sedimentation is apparently established. It is hoped that a test of this method can soon be made.

The writers are greatly indebted to Mr. H. E. Carr, who did many of the mass-spectrometer measurements; to Messrs. Fritz Linke and Philipp Sommer, instrument makers, who constructed the centrifuges; and to the Research Corporation for a grant in support of the work.

AUGUST 1, 1939 PHYSICAL REVIEW VOLUME 56

Regularities in the Third Spectrum of Thorium

R. J. LANG
Department of Physics, University of Alberta, Edmonton, Canada
(Received May 24, 1939)

The thorium spectrum is very rich in lines and extends into the far ultraviolet beyond 200A. The lines have been classified into II, III and IV as far as 1500A by means of the pole effect. A condensed spark in air and in nitrogen between metallic electrodes was used. The Th III spectrum lies on the short side of 3500A with most of its strong lines between 3000 and 2200A. Twenty-four energy levels are given.

A CONDENSED spark in air or nitrogen between electrodes of metallic thorium connected to a 30,000-volt transformer was employed to separate the lines of the thorium spectrum into the three spectra II, III and IV. In a previous report[1] the main lines of Th IV were classified into the usual single-electron doublet system with the very large ^2P interval of 12,818 cm^{-1}. (See note at end.) These Th IV lines are scattered throughout the spectrum from 2694 to 847A and are easily distinguished by the pole effect, in the region down to 1500A where it can be applied, by the fact that while the lines are very intense they are completely broken, while Th II lines are not affected at all, or very slightly, and those of Th III are intermediate, i.e., they are markedly constricted but not entirely broken. Of course there are gradations in any one spectrum and in the region between 3500 and 3000A, where there is complete overlapping of II and III, it is not always possible to distinguish them. The most of the main lines of Th III appear to lie between 3000 and 2200A but it seems likely that some of the several thousand lines in the vacuum spark below 1000A will belong to this spectrum. There are many strong lines in the region between 600 and 400A.

Owing to the structure of the IV spectrum, in which the deepest term is a doublet D arising from a single (d) electron, it is to be expected that the III spectrum will have a structure similar to Zr III[2] and not to Ce III.[3] The intervals of the (dp) terms are hopelessly irregular already in Zr III and the intensity rules in the $(ds)^3D-(dp)^3P^3D^3F$ multiplets in Zr III and Cb IV[4] are so badly obeyed that sometimes the satellites have greater intensity than the main diagonal lines. Consequently an attempt was made to find intervals which might be suitable for the $(ds)^3D$ and the (deepest) $(d^2)^3F$ terms.

Table I shows twelve even and twelve odd energy values and the lines upon which these are based. Many of these lines are the strongest in the spectrum.

During the progress of this work two reports on thorium spectra appeared.[5, 6] Through the

[1] R. J. Lang, Can. J. Research **A14**, 43 (1936).

[2] C. C. Kiess and R. J. Lang, Nat. Bur. Stand. J. Res. **5**, 305 (1930).

[3] H. N. Russell, R. B. King, and R. J. Lang, Phys. Rev. **52**, 456 (1937).

[4] R. J. Lang, *Zeeman Verhandelingen* (Martinus Nijhoff, Hague, 1935), p. 44.

[5] Mark Fred, Astrophys. J. **87**, 176 (1938).

[6] T. L. de Bruin and J. N. Lier, Proc. K. Akad. Amsterdam **41**, 956 (1938).

TABLE I. *Energy levels in the spectrum of* Th III.

	0.00	620.39	1,467.79	3,119.97	4.691.19	4.748.69	4,947.58	5,897.34	6,137.31	6,778.92	6,828.09	10,018.70
47,934.14					65 2,311.51 43,248.48				120 2,391.50 41,801.95	15 2,428.80 41,160.05	160 2,431.69 41,111.10	
46,108.18						3 2,417.08 41,359.74	15 2,428.80 41,160.05		120 2,501.07 39,970.87	50 2,541.86 39,329.42	110 2,545.07 39,279.92	
45,923.68	10 2,176.83 45,923.82	110 2,206.63 45,303.79		130 2,335.51 42,804.13	40 2,424.57 41,231.94	160 2,427.95 41,174.51		60 2,497.56 40,027.01	100 2,512.69 39,786.01			40 2,784.34 35,904.62
45,269.16					160 2,463.65 40,577.88				90 2,554.70 39,131.75	110 2,597.28 38,490.29	90 2,600.60 38,441.20	
43,623.50	120 2,291.63 43,623.64	40 2,324.69 43,003.26	140 2,371.43 42,155.80		100 2,567.81 38,932.11	120 2,571.61 38,874.57			50 2,666.84 37,486.41			50 2,974.92 33,604.61
41,007.62		100 2,475.29 40,387.07	40 2,528.33 39,539.99	60 2,638.60 37,887.64								
40,949.90					40 2,757.15 36,258.68	30 2,761.52 36,201.32	10 2,776.79 36,002.30		40 2,871.70 34,812.38	50 2,925.61 34,170.99		60 3,232.07 30,931.31
40,409.12	160 2,473.94 40,409.12	50 2,512.52 39,788.78		100 2,680.95 37,289.18				90 2,896.72 34,511.69				
40,032.42	60 2,497.21 40,032.59	100 2,536.54 39,411.94		70 2,708.31 36,912.51				70 2,928.70 34,134.95				
37,217.41	125 2,686.13 37,217.32	20 2,731.66 36,597.02				40 3,078.98 32,468.90	100 3,097.97 32,269.82		70 3,216.58 31,080.03			
37,068.46							40 3,112.35 32,120.80		60 3,232.07 30,931.31	70 3,300.53 30,289.45		
33,224.20		40 3,066.24 32,603.87	70 3,148.05 31,756.51	8 3,320.86 30,104.07								

kindness of the author of the first paper and the Ryerson Laboratory a set of plates of thorium spectra was made available as well as a long list of measurements in the spark spectrum made by Mr. Ference. The author's appreciation is hereby expressed.

NOTE ON THE SPECTRUM Th IV

In the report on this spectrum a term designated as X was given. It now seems clear that this is part of the $7P-7D$ multiplet as follows:

$7P_2-7D_2$	2146.93	(20)	46,563.4	
				1806.1
$7P_2-7D_3$	2066.77	(100)	48,369.5	
				12,817.2
$7P_1-7D_2$	1684.05	(50)	59,380.6	

The multiplet given tentatively as $5F-5G$ has not been confirmed and probably has no reality.

The thorium metal was supplied by the Westinghouse Lamp Company through the courtesy of Dr. R. E. Meyers.

The 7.4μ Fundamental Vibration of Methyl Chloride

ALVIN H. NIELSEN* AND HARALD H. NIELSEN
Mendenhall Laboratory, Ohio State University, Columbus, Ohio

(Received June 10, 1939)

A new and fairly successful attempt has been made to resolve the fundamental vibration-rotation band ν_3 of methyl chloride with the aid of a prism-grating spectrometer. The rotational line spacing averaged over the P and R branches was found to be 1.15 cm^{-1}. From this value the moment of inertia A was calculated as 48.0×10^{-40} g cm^2. The Q branch of this band has a satellite at a separation of about 1.0 cm^{-1} toward lower frequencies. This line is taken to be the Q branch for ν_3 in CH_3Cl^{37} since it agrees very well with the calculated position of this band when valence forces are assumed.

I. INTRODUCTION

BENNETT and Meyer[1] in 1928 first applied the methods of high resolution in the infrared to the spectra of the methyl halides. They succeeded in resolving the doubly degenerate perpendicular vibrations ν_2, ν_4, and ν_6 for all the halides. They did not, however, succeed in resolving any of the parallel vibrations ν_1, ν_3, or ν_5 except ν_5 for CH_3F at 9.55μ. Somewhat later Nielsen and Barker[2] attempted to resolve ν_3 for CH_3Cl at 7.4μ with a little better success and estimated the line spacing to be 1.3 cm^{-1}. Barker and Plyler[3] remeasured ν_5 for CH_3Cl at 13.7μ and were able to resolve the P branch, but not the R branch. From their work they give the line spacing of the parallel band as 1.1 cm^{-1}. They also found the Q branch of the CH_3Cl^{37} isotope band distant from the CH_3Cl^{35} band by 6.0 cm^{-1}. Since the resolution in the parallel bands has in no case been good the writers felt that another attempt at ν_3 would not be amiss and a report of this investigation follows.

II. EXPERIMENTAL

A prism-grating spectrometer, described in previous papers in this journal, equipped with a rocksalt monochromator and an echellete grating ruled with 2000 lines per inch by R. W. Wood at Johns Hopkins University was used in this experiment. The slits of the instrument were adjusted to include a spectral interval of 0.6 cm^{-1} and galvanometer deflections were noted at intervals of 0.2 cm^{-1} with the cell in the beam and out of the beam. After experimenting with various cell lengths it was finally found that a 2.0 cm cell at $\frac{1}{2}$ atmosphere pressure showed the lines to best advantage. Since the 6.26μ water vapor band has some very intense lines in this region which caused difficulty in the earlier investigation an effort was made to dry the spectrometer. The spectrometer has had built

* Department of Physics, University of Tennessee.

[1] W. H. Bennett and C. F. Meyer, Phys. Rev. **32**, 888 (1928).

[2] A. H. Nielsen and E. F. Barker, Phys. Rev. **46**, 970 (1934).

[3] E. F. Barker and E. K. Plyler, J. Chem. Phys. **3**, 367 (1935).

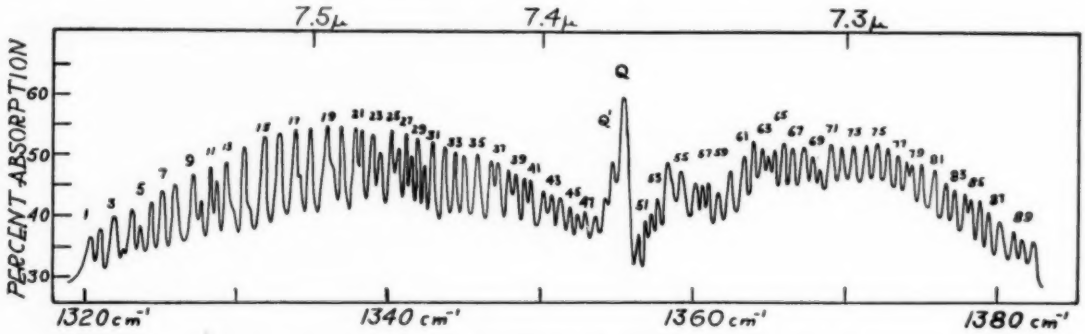

FIG. 1. The curve shows the rotational structure of ν_3 for CH_3Cl.

around it a box which can be sealed and made airtight when measurements are to be made in this region. The air is then dried by quantities of P_2O_5 distributed in photographic trays placed inside the box. When percent absorption for all points of the region was computed even the most intense water vapor lines were not found troublesome.

III. Discussion

Figure 1 shows the result of the new attempt to resolve ν_3 plotted with ordinates in percent absorption against abscissae of frequency in cm^{-1} and wave-length in μ. The frequencies of the lines, numbered in sequence beginning on the low frequency side of the band, are given in column three of Table I. It will be observed from the figure that the lines in the P branch are resolved much more completely than the lines in the R branch and that some of the lines appear double. This is, no doubt, because the CH_3Cl^{37} isotope band which overlaps the CH_3Cl^{35} band is intense enough to be observed. Since the two bands are not exactly coincident the effect would be to double the lines in some cases and destroy the regularity in others. In column two of the table an effort has been made to identify the lines with their ordinal numbers counting outwardly from the Q branch. The unprimed numbers in column two refer to the lines assumed to belong to the CH_3Cl^{35} band, and the primed ones refer to the CH_3Cl^{37} band. Taking an average spacing of the rotation lines attributed to CH_3Cl^{35} over both P and R branches a value of about 1.15 cm^{-1} is obtained. This value of $\Delta\nu$ gives a moment of inertia A for the molecule of about 48.0×10^{-40} g cm^2 in good agreement with the value 50×10^{-40} g cm^2 obtained by Barker and Plyler from their work on ν_5.

In each set of observations made the Q branch appeared to have a satellite (Q' in Fig. 1) located at a distance of between 0.8 cm^{-1} and 1.0 cm^{-1} toward lower frequencies. This line is assumed to be the Q branch of the CH_3Cl^{37} band which overlaps with the principal absorption in this region. Since this vibration is one in which the carbon and chlorine atoms vibrate essentially as a bound pair against the hydrogen triangle causing only a change in the CH_3 angle the effect of a change in mass of the chlorine atom should be less observable than for ν_5, in which the chlorine atom vibrates against the CH_3 pyramid and the measured separation is 6.0 cm^{-1}. When the above assumptions are made the isotope shift may be calculated and is found to be about 1.0 cm^{-1} which agrees with the observed displacement.

The writers express their gratitude to the National Research Council for a grant-in-aid which provided part of the equipment used in the above investigation.

Table I. *Frequencies of the lines in ν_3 of CH_3Cl in cm^{-1}.*

Line	Ident.	ν	Line	Ident.	ν
1		1320.4	48	− 1′	1353.6
2		1320.9	49	− 1	1354.2
3		1322.0	Q' branch (CH_3Cl^{37})		1354.5
4	−27	1323.1	Q branch (CH_3Cl^{35})		1355.3
5	−27′	1323.7	50		1356.4
6	−26	1324.4	51	+ 2′	1356.8
7	−26′	1325.2	52	+ 2	1357.2
8	−25′, −25	1325.9	53	+ 3′	1357.6
9	−24	1327.3	54	+ 3	1358.2
10	−24′	1327.7	55	+ 4′	1359.2
11	−23	1328.3	56	+ 4	1360.1
12	−23′	1328.7	57	+ 5′	1360.6
13	−22′, −22	1329.4	58	+ 5	1360.9
14	−21′, −21	1330.6	59	+ 6′	1361.6
15	−20′, −20	1331.8	60	+ 6, +7′	1362.4
16	−19′, −19	1332.7	61	+ 7	1363.2
17	−18′, −18	1333.8	62	+ 8′	1363.8
18		1334.8	63	+ 8	1364.4
19	−17′, −17	1335.0	64	+ 9′	1364.8
20	−16′, −16	1336.8	65	+ 9	1365.3
21	−15′	1337.9	66	+10′	1365.9
22	−15	1338.2	67	+11	1366.5
23	−14′	1339.0	68	+11′	1367.2
24	−14	1339.4	69	+12	1367.8
25	−13′	1340.1	69′	+12′	1368.2
26	−13	1340.6	70	+13	1369.1
27	−12′	1341.0	71	+13′	1369.7
28	−12	1341.4	72	+14	1370.6
29	−11′	1341.8	73	+14′	1371.3
30	−11	1342.3	74	+15	1372.1
31	−10′	1342.9	75	+15′	1372.8
32	−10	1343.7	76	+16	1373.4
33	− 9′	1344.2	77	+16′	1374.0
34	− 9	1344.9	78	+17	1374.2
35	− 8′, −8	1345.9	79	+17′	1375.1
36	− 7′	1346.7	80	+18′, +18	1375.9
37	− 7	1347.2	81	+19	1376.6
38	− 6′	1347.9	82	+19′	1377.2
39	− 6	1348.2	83	+20	1378.0
40	− 5′	1348.9	84	+20′	1378.3
41	− 5	1349.3	85	+21	1379.0
42	− 4′	1350.2	86	+21′	1379.6
43	− 4	1350.7	87	+22	1380.4
44	− 3′	1351.2	88	+22′	1381.1
45	− 3	1351.9	89	+23	1381.9
46	− 2′	1352.4	90	+23′	1382.8
47	− 2	1352.8			

Space Charge and Field Waves in an Electron Beam

SIMON RAMO
General Engineering Laboratory, General Electric Company, Schenectady, New York
(Received May 8, 1939)

W. C. Hahn has shown that the basic characteristics of a new type of vacuum tube using a velocity modulated electron beam may be explained by means of waves propagating along the beam. For an "ideal" tube in which the beam was assumed to be of uniform density throughout its length he described the small amplitude, slow "space charge" waves which have axial symmetry. In the following paper a study is made first of the more general slow space charge waves which do not necessarily possess symmetry about the axis. Two cases are considered. First, a very high magnetic focusing field is assumed, so that the motion of electrons in any but the axial direction may be neglected. Then the magnetic focusing field is assumed to be completely absent, and waves having components of velocity of electrons in all directions are treated. Also in the following, attention is given to the fast "field waves" which may exist in the idealized tube under certain conditions. The waves have been termed "space charge" waves and "field waves" because, for the former type, the phase velocities are close to beam velocity and the wave energy is mainly in the electrons. In the case of the field waves, the phase velocities are large compared to beam velocity and the energy is mainly in the electromagnetic field.

INTRODUCTION

THE problem of electromagnetic waves in an electron beam has recently become important because such waves are excited and utilized in a new type of electron tube[1,2] which may be used to generate, amplify, or detect ultra-high frequency signals. W. C. Hahn[1] has shown that the basic characteristics of this so-called velocity modulation type of vacuum tube may be explained by means of waves propagating along the electron beam of the tube. In his analysis an idealized tube was assumed in which the electron beam and its coaxial perfectly conducting shield were assumed to be infinitely long, the beam consisting of a uniform density of electrons, ρ_0, all traveling at the same constant velocity, v_0, in the absence of waves. This condition was made a possible one by certain additional assumptions: Sufficient positive ions were supposed to be contained in the beam to nullify the average current and average space charge due to the electrons. The heavy positive ions were assumed not to depart, as did the very much lighter electrons, from their drift velocity in the event of passage of a wave. Hence, with these assumptions the positive ions did not enter into the wave motion but simply aided in establishing convenient steady (zero signal) conditions.

For this ideal tube Hahn described the small signal, slow "space charge" waves which have axial symmetry and pointed out that faster waves would be expected. In the following paragraphs a study is made of the more general* slow space charge waves which do not necessarily possess symmetry about the axis.

Also in the following, attention is given to the fast "field waves" which may exist in the idealized tube if conditions are proper. The waves have been termed "space charge waves" and "field waves" because, for the former type, the phase velocities are close to beam velocity and the wave energy is mainly in the electrons. In the case of the "field waves" the phase velocities are large compared to beam velocity and the energy is mainly in the electromagnetic field.

The space charge and the field waves will be studied for two cases, the theory being limited to small wave amplitudes, or signals, in each case: (1) For a very high magnetic focusing field. The focusing field will be assumed so large that motion of electrons in any but the axial direction may be neglected. (2) For no magnetic focusing field. In this case wave components of velocity of electrons may exist in all directions. It is found possible to divide both space charge

[1] W. C. Hahn, "Small Signal Theory of Velocity Modulated Electron Beams," Gen. Elec. Rev. **42**, 258 (1939).
[2] W. C. Hahn and G. F. Metcalf, "Velocity Modulation Tubes," Proc. I. R. E., February, 1939.

* The importance of the asymmetrical waves lies in the fact that a starting and utilizing mechanism may be designed for almost any conceivable wave. To determine which type of wave should be started and utilized requires a comparison of their characteristics, especially as regards the potential transconductance of the tube and the optimum drift tube length (reference 1). It is therefore of considerable importance to consider the asymmetrical waves.

and field waves into two classes which can exist independently and which exhibit differences in their characteristics.

High Magnetic Focusing Field

If the magnetic focusing field is sufficiently high the theory need only consider motion of electrons in the axial direction. This suggests that the equations may be most easily set up in terms of the retarded scalar electric and magnetic vector potentials because only the axial component of the vector potential will be required. If the potential functions be substituted into Maxwell's equations by use of the relations:[3]

$$\begin{aligned} \bar{E} &= -\nabla\Phi - \frac{1}{c}\frac{\partial \bar{A}}{\partial t} \\ \bar{H} &= \nabla \times \bar{A}, \end{aligned} \tag{1}$$

in which $\bar{E}$ is the electric field vector, $\bar{H}$ is the magnetic field vector, Φ is the scalar electric potential and $\bar{A}$ is the vector magnetic potential, then the equations reduce to the well-known wave equations for Φ and $\bar{A}$:

$$\begin{aligned} \left[\nabla^2 - \frac{1}{c^2}\frac{\partial^2}{\partial t^2}\right]\Phi &= -\rho \\ \left[\nabla^2 - \frac{1}{c^2}\frac{\partial^2}{\partial t^2}\right]\bar{A} &= -\frac{\rho\bar{v}}{c}, \end{aligned} \tag{2}$$

in which c is the velocity of light, ρ and $\bar{v}$ are charge density and velocity, respectively, and Heaviside-Lorentz or rational units are used throughout. Eqs. (2) imply that the divergence of $\bar{A}$ has been determined by[3]

$$\nabla \cdot \bar{A} = -\frac{1}{c}\frac{\partial \Phi}{\partial t}. \tag{3}$$

Since only the wave part of the solution is desired, it will be convenient to denote the scalar electric potential, the charge density and the velocity by

$$\Phi_1 \epsilon^{i(\omega t - \gamma z)}, \quad \rho_1 \epsilon^{i(\omega t - \gamma z)}, \quad \text{and} \quad v_z \epsilon^{i(\omega t - \gamma z)},$$

respectively. Then using cylindrical coordinates, Eq. (2) becomes

$$\frac{\partial^2 \Phi_1}{\partial r^2} + \frac{1}{r}\frac{\partial \Phi_1}{\partial r} + \frac{1}{r^2}\frac{\partial^2 \Phi_1}{\partial \theta^2} + (k^2 - \gamma^2)\Phi_1 = -\rho_1, \tag{4}$$

in which $k = \omega/c$.

It is easy to express ρ_1 in terms of Φ_1. From Appendix A, we obtain

$$\rho_1 = \frac{e\rho_0}{m}\frac{\gamma^2 - k^2}{(\omega - \gamma v_0)^2}\Phi_1, \tag{6A}$$

so that Eq. (4) now becomes

$$\frac{\partial^2 \Phi_1}{\partial r^2} + \frac{1}{r}\frac{\partial \Phi_1}{\partial r} + \frac{1}{r^2}\frac{\partial^2 \Phi_1}{\partial \theta^2} + (k^2 - \gamma^2)\left[1 - \frac{e\rho_0}{m(\omega - \gamma v_0)^2}\right]\Phi_1 = 0, \tag{5}$$

whose solution appropriate about the origin, is[4]

$$\Phi_1 = B_n J_n(Tr)\epsilon^{in\theta}, \tag{6}$$

where B_n is an arbitrary constant and

$$T = \left\{(k^2 - \gamma^2)\left[1 - \frac{e\rho_0}{m(\omega - \gamma v_0)^2}\right]\right\}^{\frac{1}{2}}. \tag{7}$$

In the space between the beam and the conducting boundary the charge density is zero so that we may write directly for the electric scalar potential in this region*

$$\Phi_2 = C_n[I_n(\tau r) + D_n K_n(\tau r)], \tag{8}$$

in which I_n and K_n are modified Bessel functions of the first and second kind, respectively,[5] and

$$\tau = (\gamma^2 - k^2)^{\frac{1}{2}}. \tag{9}$$

The constant D_n is determined by writing that the tangential electric field must equal zero at the surface of the perfectly conducting cylinder where $r = bR$. This requirement is satisfied by equating Φ_2 to zero at this radius.

[3] See for instance *Introduction to Theoretical Physics*, a text by J. C. Slater and N. H. Frank (McGraw-Hill Book Co., 1933), Chap. XXI

[4] See for instance, *Electrical and Optical Wave Motion*, a text by H. Bateman (Cambridge, 1915), Chapter III.

* The modified Bessel functions are appropriate here for the slow space charge waves because for these waves γ is very nearly equal to $\omega/v_0 = \gamma_0$, the propagation constant of the beam. For $\gamma \approx \gamma_0$, τ will be appropriately real.

[5] See for instance, *Theory of Bessel Functions*, a text by G. N. Watson (Cambridge, 1922).

Thus

$$D_n = -\frac{I_n(\tau Rb)}{K_n(\tau Rb)}. \tag{10}$$

Two more conditions remain to be applied at the edge of the beam, where $r=b$. These two conditions will serve to determine the ratio C_n/B_n and also the value of γ in terms of the given parameters. Continuity of the tangential electric field is obtained by continuity of the potentials. This gives

$$\frac{C_n}{B_n} = \frac{I_n(\tau b)+D_nK_n(\tau b)}{J_n(Tb)}. \tag{11}$$

For continuity of tangential magnetic fields Eq. (1) discloses that since only z components of $\bar{A}$ exist then the only component of $\bar{H}$ is the azimuthal component, H_θ. Continuity of this component requires continuity of $\partial A_z/\partial r$ which by Eq. (3) leads to continuity of $\partial\Phi/\partial r$. Hence

$$\frac{C_n}{B_n} = -\frac{(\tau b)}{(Tb)}\frac{I'(\tau b)+D_nK_n'(\tau b)}{J_n'(Tb)}, \tag{12}$$

in which the primes indicate derivatives of the Bessel functions with respect to their arguments.

A comparison of (11) and (12) yields

$$(Tb)\frac{J_n'(Tb)}{J_n(Tb)} = (\tau b)\frac{I_n'(\tau b)+D_nK_n'(\tau b)}{I_n(\tau b)+D_nK_n(\tau b)}, \tag{13}$$

which for $n=0$ is the same as the equation for the determination of γ derived by Hahn[1] for the case of an infinite magnetic focusing field (except for an easily recognizable difference in notation).

With sufficient time and a complete set of tables, it is possible to determine the values of γ for the various order of waves and then compare the $n=0$, 1, 2, etc. waves for transconductances, optimum drift tube length and distribution over the cross section. Some idea of the relative usefulness of the various waves may be obtained more quickly if the tube parameters are specialized somewhat by making $R=1$. With this selection of parameters the solution (6) holds over the entire tube cross section. Eq. (8) is no longer significant and the boundary condition at the conductor yields simply

$$J_n(Tb)=0. \tag{14}$$

For each value of n there will be a series of roots to this equation; the mth root of the nth order wave will be designated as (p_{nm}). Eq. (7) then yields

$$\frac{p_{nm}^2}{b^2} = (k^2-\gamma^2)\left[1-\frac{e\rho_0}{m(\omega-\gamma v_0)^2}\right]. \tag{15}$$

Space charge waves

For the slow space charge waves γ is very nearly equal to $\gamma_0=\omega/v_0$ and if this be substituted in (15) there results

$$[\omega-\gamma v_0]^2 = -e\rho_0 \Big/ m\left[\frac{p_{nm}^2}{b^2(k^2-\gamma_0^2)}-1\right] \tag{16}$$

and finally

$$\gamma=\gamma_0[1\pm\delta], \tag{17}$$

in which

$$\delta = \left\{\frac{e\rho_0(\gamma_0^2-k^2)b^2}{m\omega^2[p_{nm}^2\gamma_0^2-b^2k^2]}\right\}^{\frac{1}{3}} \tag{18}$$

and will usually be found so small compared to unity that the substitution of γ_0 for γ at times in its derivation may be considered justified.

It is now possible to write the ratio of conduction current modulation density $(\rho_0 v_z+v_0\rho_1)$ to the velocity modulation (v_z). If the former is denoted by ξ_z, Eq. (2A) may be altered to*

$$G_w = \xi_z/v_z = -\rho_0/\pm\delta. \tag{19}$$

This shows that the transconductance of the velocity modulation tube, whether due to the symmetrical wave of zero order or waves of higher order will have essentially the same general characteristics. For example, the waves may occur in pairs and if the starting mechanism is such as to introduce velocity modulation into the beam but no conduction current modulation at some point along its length,[1] then there will be another point farther along the beam at which the conduction current modulation present in the beam will be a maximum. The distance between these points will be that for which $\gamma_0\delta l$ is an odd multiple of $\pi/2$ radians, l being the distance between the two points.[1] Since from Eq. (18) the value of δ is seen to decrease as

* This ratio will be termed "wave transconductance" and will be denoted by G_w.

p_{nm} increases, the wave transconductance will increase with p_{nm}, as will also the optimum drift tube length.

An important consideration in comparing the potential practical application of the waves of various n's and m's is their distribution over the cross section. For $n=0$, $m=1$ the wave will vary with the $J_0(Tr)$ function between $r=0$ and $r=b$, $(T=p_{01}/b)$ and so will have maximum amplitude at $r=0$, and will decrease to zero at $r=b$. The (0,2) wave will have one reversal of phase between $r=0$ and $r=b$, advance to a negative maximum then decrease to zero again at $r=b$. The (0,3) wave will have two reversals, the (0,4) wave three reversals, etc. The* waves of $n>0$ will start at zero amplitude at the origin, have m maximum points and $(m-1)$ reversals of phase between $r=0$, and $r=b$ before returning to zero at $r=b$.

Field waves

There are also solutions to Eq. (15) for which the value of γ is far removed from γ_0. If γ is very much less than γ_0^2 then $(\omega-\gamma v_0)^2$ is very nearly equal to ω^2. The quantity $e\rho_0/m$ which we shall call ω_0^2 is recognized as the square of the familiar natural angular frequency of oscillation of a plasma of electron charge density ρ_0. Thus we know that ω_0^2/ω^2 is appreciably less than unity for electron beam tubes, making $[1-\omega_0^2/\omega^2]$ a positive quantity. Eq. (15) is thus seen to have solutions for which γ^2 is smaller than k^2 these values of γ^2 being given approximately by†

$$\gamma^2=k^2-\frac{p_{nm}^2}{b^2[1-\omega_0^2/\omega^2]}. \tag{20}$$

Equation (20) indicates also that there is a cut-off frequency corresponding to each value of p_{nm}^2/b^2 and ω^2 below which the waves will not propagate, since then γ^2 becomes negative and γ becomes imaginary. If it is remembered that $k=\omega/c$, the cut-off frequency, ω_c, is found from (20) to be given by

$$\omega_c^2=\omega_0^2+c^2p_{nm}^2/b^2. \tag{21}$$

At cut-off, $\gamma=0$ and the wave velocity is infinite. As the frequency approaches infinity the wave velocity decreases to c.

Zero Magnetic Focusing Field

Axial waves

When the magnetic focusing field does not restrict the motion to the axial direction the equations must contain additional variables. Before attempting a general solution, however, it seems pertinent to inquire whether the wave just studied may still exist without the restricting action of the magnetic focusing field. It would be of practical value to learn that there is a space charge wave which in the complete absence of focusing field will still possess only the axial components of velocity and conduction current modulation.

To answer this it may first be noted that in the foregoing analysis every equation is still valid. However it is necessary that additional equations be written if the radial and azimuthal velocities are to be zero without the restricting influence of the magnetic focusing field. To meet these added restraints the force on the electron in the azimuthal and radial directions must be zero. Now the force on the electron is

$$\bar{F}=\bar{E}e+e(\bar{v}\times\bar{H})/c. \tag{22}$$

If there are no components of velocity other than in the axial direction, then as before $A_\theta=A_r=0$. From Eq. (3)

$$A_z=(k/\gamma)\Phi_1, \tag{23}$$

so that substitution in Eq. (1) shows the electric and magnetic fields to be

$$\begin{aligned} E_r&=-\frac{\partial\Phi_1}{\partial r}, & H_r&=-\frac{1}{r}\frac{ink}{\gamma}\Phi_1,\\ E_\theta&=-\frac{in}{r}\Phi_1, & H_\theta&=-\frac{k}{\gamma}\frac{\partial\Phi_1}{\partial r}, \\ E_z&=\frac{i(\gamma^2-k^2)}{\gamma}\Phi_1, & H_z&=0. \end{aligned} \tag{24}$$

If these are substituted into Eq. (22) the condi-

* These statements may be verified by a glance at curves or tables of the J_n functions.

† This result makes use of the approximation $(\omega-\gamma v_0)^2=\omega^2$ which amounts to neglecting γ^2/γ_0^2 with respect to unity. This is consistent with the approximation that has been made throughout in neglecting the relativity correction to mass. It is evidently not difficult to omit these approximations and obtain more precise expressions for very high beam velocities if necessary.

tion that the force components in the azimuthal and radial directions be zero results in

$$0=-\frac{ein}{r}\Phi_1+\frac{e}{c}v_0H_r=\frac{ein}{r}\Phi_1\left[-1+\frac{kv_0}{c\gamma}\right],$$
$$0=-e\frac{\partial\Phi_1}{\partial r}-\frac{e}{c}v_0H_\theta=e\frac{\partial\Phi_1}{\partial r}\left[-1+\frac{kv_0}{c\gamma}\right] \tag{25}$$

(if, as usual, cross-product modulation terms are neglected). These equations are both satisfied when

$$\gamma=kv_0/c. \tag{26}$$

Thus this "axial" wave, if it is to exist, must be a very fast wave for the ratio v_0/c is well below unity in all practical cases making γ much less than k.

We have already seen that waves for which γ is less than k may occur above certain cut-off frequencies for any given tube geometry and electron density. There are obviously series of discrete frequencies above the cut-off point for which

$$\gamma=kv_0/c,$$

which frequencies are found by substituting this value of γ in Eq. (20). Since the purely axial wave may exist at discrete frequencies for no magnetic field and at any frequency (above a certain cut-off frequency) for infinite magnetic field, it appears that at some finite magnetic field bands of frequencies will exist for which these waves are possible.

Division of possible waves

Let us turn now to the more general case in which radial and azimuthal velocities are possible. A convenient way to set up the equations so that the various possible waves are disclosed most easily is suggested by the following line of thought. In a region bounded by a cylinder, free of charge and in which the dielectric constant is uniform, it is convenient to express the various components of the electric and magnetic fields in terms of E_z and H_z, which satisfy the equations

$$(\nabla^2+k_1^2)E_z=0,$$
$$(\nabla^2+k_1^2)H_z=0, \tag{27}$$

whose solutions can immediately be written in cylindrical coordinates. It is convenient then to speak of "E type" waves for which H_z is zero and the "H type" waves for which E_z is zero.[6] Now, consider an observer who moves with the average velocity of the beam, v_0. As is shown in Appendix B, this moving observer would set up equations which are identical with those already solved for the case of a cylindrical boundary by Rayleigh[7] and more recently by others.[6] The dielectric constant would be a fictitious one dependent upon electron density and frequency.

The moving observer might accordingly divide the waves which he would predict into the E and H types, all other field, velocity, and current components being expressed in terms of E_z and H_z. Now by use of the Lorentz[8] transformations, all these expressions could be transformed into relations appropriate for a stationary observer, H_z and E_z being invariant under the transformation, and the problem could be considered solved. However, now that we are assured that all the phenomena may be thus expressed in terms of E_z and H_z, it will be well to discard the moving observer and regard him as of only momentary value in indicating a simple line of attack.

In Appendix C it is shown that E_z and H_z obey the equations

$$(\nabla^2+k_E^2)E_z=0,$$
$$(\nabla^2+k_H^2)H_z=0, \tag{28}$$

in which

$$k_E^2=\frac{\omega^2[c^2\omega_b^2-v_0^2\omega_0^2]+c^2\omega_0^2[\omega_0^2-2\omega\omega_b]}{c^4(\omega_b^2-\omega_0^2)} \tag{29}$$

and

$$k_H^2=k^2\left[1-\frac{\omega_0^2}{\omega^2}\right]. \tag{30}$$

These equations have solutions of the form

$$J_n[(k_E^2-\gamma^2)^{\frac{1}{2}}r]\epsilon^{in\theta} \tag{31}$$

and

$$J_n[(k_H^2-\gamma^2)^{\frac{1}{2}}r]\epsilon^{in\theta}.$$

The components of the first two of Eqs. (1B)

[6] See for instance "Hyper-Frequency Wave Guides" by Carson, Mead and Schelkunoff, Bell Sys. Tech. J., **5**, 15 (1936).

[7] Rayleigh, Phil. Mag., Vol. 43 (1897).

[8] See for instance, *Electricity and Magnetism*, a text by J. H. Jeans (Cambridge, 1927), page 604.

may be rearranged to give

$$E_\theta\left[\gamma^2+k^2-\frac{\omega_0^2}{c^2}\right]=-\frac{n}{r}\frac{\omega_0^2 v_0}{\omega_b c^2}E_z-ik\frac{\partial H_z}{\partial r},$$

$$H_r\left[\gamma^2+k^2-\frac{\omega_0^2}{c^2}\right]=\frac{n}{r}\left[\frac{\omega_0^2}{\omega_b c}-k\right]E_z+i\gamma\frac{\partial H_z}{\partial r},$$

$$E_r\left[\gamma^2+k^2-\left(k+\gamma\frac{v_0}{c}\right)\frac{\omega_0^2}{\omega_b c}\right]=\frac{kn}{r}H_z-i\left[\gamma-\alpha\frac{v_0}{c}\right]\frac{\partial E_z}{\partial r}, \tag{32}$$

$$H_\theta\left[\gamma^2+k^2-\left(k+\gamma\frac{v_0}{c}\right)\frac{\omega_0^2}{\omega_b c}\right]=-\frac{\gamma n}{r}H_z+i\left[\frac{\omega_0^2}{\omega_b c}-k\right]\frac{\partial E_z}{\partial r}.$$

These expressions, together with those for the velocities (8C) (9C) (10C), the currents (13C) (14C) (15C), and the charge density (21C) constitute the necessary relations for all the wave quantities in terms of E_z and H_z.

The H type wave

Consider now the wave for which E_z is zero. The single boundary condition requires that E_θ vanish at $r=b$ or that

$$J_n'[(k_H^2-\gamma^2)^{\frac{1}{2}}b]=0. \tag{33}$$

Designating these roots by q_{nm}, we have from (30)

$$\gamma^2=k^2\left[1-\frac{\omega_0^2}{\omega^2}\right]-\frac{q_{nm}^2}{b^2}. \tag{34}$$

Only values of γ which are less than k are evidently possible. Thus the H type of wave is always a fast wave with a velocity of propagation exceeding c and a cut-off frequency given by

$$\omega_0^2=\omega_0^2+c^2q_{nm}^2/b^2. \tag{35}$$

The $n=0$ or symmetrical H waves, which might be designated as the H_{0m} waves will have only the following components: H_z, H_r, E_θ; v_θ and ξ_θ, all other field, velocity, current, and charge density components being zero. The $n>0$ waves will however have H_z, H_r, E_θ, E_r, H_θ, ξ_θ, ξ_r, v_r, and v_θ components in general, only the v_z and ξ_z components being missing.

The E type wave

When $H_z=0$ the boundary condition at $r=b$ requires that

$$J_n[(k_E^2-\gamma^2)^{\frac{1}{2}}b]=0, \tag{36}$$

so that

$$k_E^2-\gamma^2=p_{nm}^2/b^2. \tag{37}$$

For the space charge waves $\omega_b=\omega-\gamma v_0$ is very small compared to ω and approximations based on this fact permit (37) to be solved for γ, and give the approximate relation

$$\gamma=\gamma_0\left\{1+\frac{\omega_0^2b^2}{c^2p_{nm}^2}\pm\frac{b^2\omega_0^2}{c^2p_{nm}^2}\times\left[1+\frac{p_{nm}^2c^2}{b^2}\left(\frac{c^2}{\omega^2\omega_0^2}\frac{p_{nm}^2}{b^2}+\frac{1}{\omega^2}+\frac{1}{\omega_0^2}\right)\right]^{\frac{1}{2}}\right\}. \tag{38}$$

In the case of the fast field waves, ω_b is very nearly equal to ω (unless the beam velocity is very high) and k_E^2 is given approximately by.

$$k_E^2=\frac{\omega^2-\omega_0^2}{c^2}=k^2\left[1-\frac{\omega_0^2}{\omega^2}\right], \tag{39}$$

which substituted in (37) yields

$$\gamma^2=k^2\left[1-\frac{\omega_0^2}{\omega^2}\right]-\frac{p_{nm}^2}{b^2}. \tag{40}$$

The cut-off frequency of these waves is given by

$$\omega_0^2=\omega_0^2+\frac{c^2p_{nm}^2}{b^2}. \tag{41}$$

For both the space charge and the field waves only the following components may be present in the E_{0m} type waves: E_z, E_r, H_θ, v_r, v_z, ξ_r, ξ_z, and ρ_1. The E_{nm} waves in which $n>0$ will in general have all components.

Acknowledgment

The author is indebted to W. C. Hahn for many valuable discussions of both the theory originally worked out by the latter as well as of the present study.

Appendix A

From continuity we have

$$-\frac{\partial \rho_1}{\partial t}=\frac{\partial}{\partial z}(\rho_0 v_z+\dot{v}_0\rho_1) \tag{1A}$$

or

$$\rho_1=\frac{\gamma\rho_0}{\omega-\gamma v_0}v_z. \tag{2A}$$

(This neglects modulation cross-products of ρ and $\bar{v}$ and thus limits the theory to small signals.) But

$$m d\bar{v}/dt=eE_z, \tag{3A}$$

in which E_z is the amplitude of the z modulation component of $\bar{E}$, e is the charge and m is the mass of the electron. Now

$$\frac{dv_z}{dt}=\frac{\partial v_z}{\partial t}+\frac{\partial v_z}{\partial z}\frac{dz}{dt}=i[\omega-\gamma v_0]v_z, \tag{4A}$$

for small signals and from Eqs. (1) and (3), E_z is seen to be given by

$$E_z=i[\gamma\Phi_1-kA_z]=i[\gamma-k^2/\gamma]\Phi_1. \tag{5A}$$

The above equations then yield

$$\rho_1=\frac{e\rho_0}{m}\frac{\gamma^2-k^2}{(\omega-\gamma v_0)^2}\Phi_1. \tag{6A}$$

Appendix B

The moving observer would write, in his own units and system of moving axes,

$$\nabla\times\bar{E}=-\frac{1}{c}\frac{\partial\bar{H}}{\partial t},\qquad \nabla\cdot\bar{E}=\rho_1,$$
$$\nabla\times\bar{H}=\frac{1}{c}\left[\frac{\partial\bar{E}}{\partial t}+\xi\right],\quad \nabla\cdot\bar{H}=0. \tag{1B}$$

Now in the force equation (22), terms of type $\bar{v}x\bar{H}$ will not occur since cross-products of wave components are being discarded. Thus

$$\bar{\xi}=\rho_0\bar{v}=\rho_0 e\bar{E}/i\omega m \tag{2B}$$

or

$$\bar{\xi}=-\frac{e\rho_0}{\omega^2 m}\frac{\partial\bar{E}}{\partial t}. \tag{3B}$$

From continuity,

$$-i\omega\rho_1=\nabla\cdot\bar{\xi}=\rho_0 e\nabla\cdot\bar{E}/i\omega m \tag{4B}$$

or

$$\rho_1=+e\rho_0\nabla\cdot\bar{E}/\omega^2 m. \tag{5B}$$

Thus substitution in (1B) yields

$$\nabla\cdot\bar{E}(1-e\rho_0/m\omega^2)=0,$$
$$\nabla\cdot\bar{H}=0,$$
$$\nabla\times\bar{E}=-\frac{1}{c}\frac{\partial\bar{H}}{\partial t}, \tag{6B}$$
$$\nabla\times\bar{H}=-\frac{1}{c}\frac{\partial E}{\partial t}\left(1-\frac{e\rho_0}{\omega^2 m}\right),$$

which are identical with the equations for a medium of uniform dielectric constant

$$(1-e\rho_0/m\omega^2).$$

Appendix C

Taking the curl of the first of Eqs. (1B) and combining with the second yields

$$\nabla\times\nabla\times\bar{E}=-\frac{1}{c^2}\frac{\partial\bar{\xi}}{\partial t}-\frac{1}{c^2}\frac{\partial^2\bar{E}}{\partial t^2} \tag{1C}$$

or

$$-\nabla^2\bar{E}+\nabla(\nabla\cdot\bar{E})=-\frac{i\omega}{c^2}\bar{\xi}+k^2\bar{E} \tag{2C}$$

and finally,

$$(\nabla^2+k^2)\bar{E}-i\omega\bar{\xi}/c^2-\nabla(\rho_1)=0, \tag{3C}$$

the z component of which is

$$(\nabla^2+k^2)E_z-i\omega\xi_z/c^2+i\gamma\rho_1=0. \tag{4C}$$

In a similar fashion it is found that

$$\nabla\times\nabla\times\bar{H}=\frac{1}{c}\nabla\times\bar{\xi}-\frac{1}{c^2}\frac{\partial^2\bar{H}}{\partial t^2} \tag{5C}$$

and finally

$$(\nabla^2+k^2)H_z+(1/c)(\nabla\times\bar{\xi})_z=0. \tag{6C}$$

ξ_z, ρ_1, and $(\nabla\times\xi)_z$ must now be expressed in terms of E_z and H_z. This may be done as follows:

From the force equation (22)

$$im(\omega-\gamma v_0)v_z=eE_z \tag{7C}$$

or

$$v_z=\omega_0^2E_z/i\rho_0\omega_b \tag{8C}$$

and, similarly

$$v_r=\frac{\omega_0^2}{i\rho_0\omega_b}\left[E_r-\frac{v_0}{c}H_\theta\right], \tag{9C}$$

$$v_\theta=\frac{\omega_0^2}{i\rho_0\omega_b}\left[E_\theta+\frac{v_0}{c}H_r\right], \tag{10C}$$

in which the substitutions,

$$\omega_0^2=e\rho_0/m \tag{11C}$$

and

$$\omega_b=\omega-\gamma v_0, \tag{12C}$$

have been introduced. Now

$$\xi_z=\rho_0v_z+v_0\rho_1=\omega_0^2E_z/i\omega_b+v_0\rho_1, \tag{13C}$$

$$\xi_r=\frac{\omega_0^2}{i\omega_b}\left[E_r-\frac{v_0}{c}H_\theta\right], \tag{14C}$$

$$\xi_\theta=\frac{\omega_0^2}{i\omega_b}\left[E_\theta+\frac{v_0}{c}H_r\right]. \tag{15C}$$

And from the continuity equation

$$-i\omega\rho_1=\nabla\cdot\bar{\xi}=\rho_0\nabla\cdot\bar{v}-i\gamma v_0\rho_1 \tag{16C}$$

or

$$\nabla\cdot\bar{v}=-i\omega_b\rho_1/\rho_0. \tag{17C}$$

But from Eqs. (8C), (9C), and (10C),

$$\nabla\cdot\bar{v}=\frac{\omega_0^2}{i\rho_0\omega_b}\times\left\{\nabla\cdot\bar{E}+\frac{v_0}{c}\left[\frac{1}{r}\frac{\partial H_r}{\partial\theta}-\frac{1}{r}\frac{\partial}{\partial r}(rH_\theta)\right]\right\}. \tag{18C}$$

The binomial in the brackets is recognized as the z component of $(-\text{curl } H)$ and so by the second and third of Eqs. (1B), (18C) becomes

$$\nabla\cdot\bar{v}=\frac{\omega_0^2}{i\rho_0\omega_b}\left[\rho_1-\frac{v_0}{c^2}i\omega E_z-\frac{v_0}{c^2}(\rho_1v_0+\rho_0v_z)\right], \tag{19C}$$

$$=\frac{\omega_0^2}{i\rho_0\omega_b}\left[\rho_1-\frac{v_0}{c^2}i\omega E_z-\frac{v_0}{c^2}\frac{\omega_0^2}{i\omega_b}E_z\right], \tag{20C}$$

$$\rho_1=\frac{iv_0\omega_0^2}{c^2\omega_b}\frac{\omega_0^2-\omega\omega_b}{\omega_b^2-\omega_0^2}E_z. \tag{21C}$$

This result may now be substituted into (13C) to give

$$\xi_z=iE_z\frac{\omega_0^4c^2-v_0^2\omega_0^2\omega\omega_b-c^2\omega_0^2\omega_b^2}{c^2\omega_b(\omega_b^2-\omega_0^2)}, \tag{22C}$$

from which,

$$k_E^2=-i\omega\xi_z/cE_z+i\gamma\rho_1/E_z+k^2, \tag{23C}$$

$$=\frac{\omega^2[c^2\omega_b^2-v_0^2\omega_0^2]+c^2\omega_0^2[\omega_0^2-2\omega\omega_b]}{c^4[\omega_b^2-\omega_0^2]}, \tag{24C}$$

$$(\nabla\times\xi)_z=\frac{1}{r}\frac{\partial}{\partial r}(r\xi_\theta)-\frac{1}{r}\frac{\partial\xi_r}{\partial\theta}=\rho_0(\nabla\times\bar{v})_z, \tag{25C}$$

$$=\frac{\omega_0^2}{i\omega_b}\left[(\nabla\times\bar{E})_z+\frac{v_0}{c}\frac{1}{r}\frac{\partial}{\partial r}(rH_r)+\frac{v_0}{c}\frac{1}{r}\frac{\partial H_\theta}{\partial\theta}\right]. \tag{26C}$$

But

$$(\nabla\times\bar{E})_z=-i\omega H_z/c \tag{27C}$$

and from $\nabla\cdot\bar{H}=0$ it follows that

$$i\gamma H_z=\frac{1}{r}\frac{\partial}{\partial r}(rH_r)+\frac{1}{r}\frac{\partial H_\theta}{\partial\theta}. \tag{28C}$$

Substitution in (26C) results in

$$(\nabla\times\xi)_z=\frac{\omega_0^2}{i\omega_b}\left[-\frac{i\omega}{c}+\frac{iv_0\gamma}{c}\right]H_z=\frac{\omega_0^2}{c}H_z. \tag{29C}$$

Consequently,

$$k_H^2=k^2+\frac{1}{c}(\nabla\times\xi)_z=k^2[1-\omega_0^2/\omega^2]. \tag{30C}$$

Neutron Production and Absorption in Uranium*

H. L. Anderson, E. Fermi and Leo Szilard
Columbia University, New York, New York

(Received July 3, 1939)

It has been found[1–3] that there is an abundant emission of neutrons from uranium under the action of slow neutrons, and it is of interest to ascertain whether and to what extent the number of neutrons emitted exceeds the number absorbed.

This question can be investigated by placing a photo-neutron source in the center of a large water tank and comparing, with and without uranium in the water, the number of thermal neutrons present in the water. In the previous experiments of this type[1, 3] it was attempted to have as closely as possible a spherically symmetrical distribution of neutrons. The number of thermal neutrons present in the water was determined by measuring along one radius the neutron density ρ as a function of the distance r from the center, and then calculating $\int r^2 \rho dr$. A difference in favor of uranium of about five percent was reported by von Halban, Joliot and Kovarski.[4]

Since one has to measure a small difference, slight deviations from a spherically symmetrical distribution might give misleading results. The present experiments which are based on the same general principle do not require such symmetry. In order to measure the number of thermal neutrons in the water we filled the tank with a ten-percent solution of $MnSO_4$. The activity induced in manganese is proportional to the number of thermal neutrons present. A physical averaging was performed by stirring the solution before measuring the activity of a sample with an ionization chamber. To obtain an effect of sufficient magnitude, about 200 kg of U_3O_8 was used.

The experimental arrangement is shown in Fig. 1. A photo-neutron source, consisting of about 2 g of radium and 250 g of beryllium was placed in the center of the tank. The geometry was such that practically all neutrons emitted by the source and by the uranium oxide were slowed down and absorbed within the tank. Each irradiation extended over several half-life periods of radiomanganese and the observed activity of the solution was about four times the background of the ionization chamber. Alternating measurements were taken with the cans filled with uranium oxide, and with empty cans of the same dimensions. The activity proved to be about ten percent higher with uranium oxide than without it. This result shows that in our arrangement more neutrons are emitted by uranium than are absorbed by uranium.

In order to find the average number of fast neutrons emitted by uranium for each thermal neutron absorbed by uranium, we have to determine what fraction of the total number of neutrons emitted by the photo-neutron source is, in our experiment, absorbed in the thermal region by uranium. The number of photo-neutrons

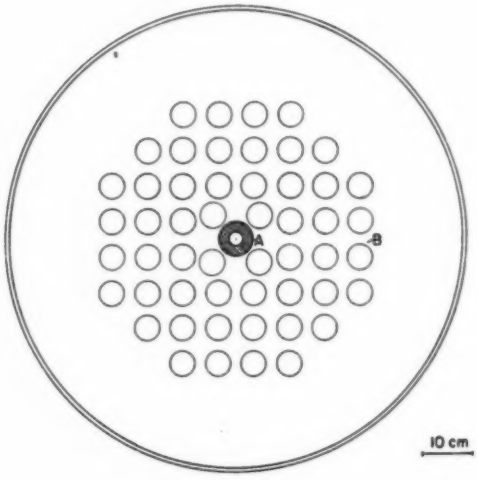

Fig. 1. Horizontal section through center of cylindrical tank which is filled with 540 liters of 10-percent $MnSO_4$ solution. A, Photo-neutron source composed of 2.3 grams of radium and 250 grams of beryllium. B, One of 52 cylindrical cans 5 cm in diameter and 60 cm in height, which are either empty or filled with uranium oxide.

* Publication assisted by the Ernest Kempton Adams Fund for Physical Research of Columbia University.

[1] v. Halban, Joliot and Kovarski, Nature **143**, 470 (1939).

[2] L. Szilard and W. H. Zinn, Phys. Rev. **55**, 799 (1939).

[3] Anderson, Fermi and Hanstein, Phys. Rev. **55**, 797 (1939).

[4] v. Halban, Joliot and Kovarski, Nature **143**, 680 (1939).

emitted by the source is indicated by the activity of the solution in the tank when the irradiation is carried out with empty cans surrounding the source. We obtained a measure of this number by taking into account that in our solution about 20 percent of the neutrons are captured by manganese and the rest by hydrogen. In order to obtain, in the same units, a measure of the number of neutrons absorbed by uranium we proceeded in the following way: A mixture of sand and manganese powder, having the same thermal neutron absorption as uranium oxide replaced the uranium oxide in $\frac{1}{4}$ of the cans which were distributed uniformly among the other uranium oxide-filled cans. After irradiation, all this powder was mixed together, a ten-percent $MnSO_4$ solution was prepared from a sample, and its activity was measured with our ionization chamber.

In this way we found that about 50 percent of the neutrons emitted by the source are absorbed as thermal neutrons by uranium in our arrangement. It follows that, if uranium absorbed only thermal neutrons, the observed ten-percent increase in activity obtained with uranium present would correspond to an average emission of about 1.2 neutrons per thermal neutron absorbed by uranium. This number should be increased, to perhaps 1.5, by taking into account the neutrons which, in our particular arrangement, are absorbed at resonance in the nonthermal region by uranium, without causing neutron emission.

From this result we may conclude that a nuclear chain reaction could be maintained in a system in which neutrons are slowed down without much absorption until they reach thermal energies and are then mostly absorbed by uranium rather than by another element. It remains an open question, however, whether this holds for a system in which hydrogen is used for slowing down the neutrons.

In such a system the absorption of neutrons takes place in three different ways: The neutrons are absorbed at thermal energies, both by hydrogen and uranium, and they are also absorbed by uranium at resonance before they are slowed down to thermal energies. Our result is independent of the ratio of the concentrations of hydrogen and uranium, insofar as it shows that, for thermal neutrons, the ratio of the cross section for neutron production and neutron absorption in uranium is greater than one, and probably about 1.5. What fraction of the neutrons will reach thermal energies without being absorbed will, however, depend on the ratio of the average concentrations of hydrogen and uranium. Since there is an appreciable absorption even far from the center of the resonance band, it follows that the fraction of neutrons absorbed by uranium at resonance will increase with decreasing hydrogen concentration. This has to be taken into account in discussing the possibility of a nuclear chain reaction in a system composed essentially of uranium and hydrogen. A chain reaction would require that more neutrons be produced by uranium than absorbed by uranium and hydrogen together. In our experiment the ratio of the average concentration of hydrogen to uranium atoms was 17 to 1, and in the experiment of von Halban, Joliot and Kovarski this ratio was 70 to 1. At such concentrations the absorption of hydrogen in the thermal region will prevent a chain reaction. By reducing the concentration of hydrogen one would obtain the following effect: On the one hand a larger fraction of those neutrons which reach thermal energies will be absorbed by uranium; on the other hand fewer neutrons reach the thermal region due to an increased absorption by uranium at resonance. Of these two counteracting factors the first is more important for high hydrogen concentrations and the second is more important for low hydrogen concentrations. Starting with high hydrogen concentrations, the ratio of neutron production to total neutron absorption will thus first rise, then pass through a maximum, and, as the hydrogen concentration is decreased, thereafter decrease. We attempted to estimate the quantities involved from the information available about resonance absorption in uranium[5–7] and from the observed net gain of 0.2 in the number of neutrons in our experiment. The effect of the absorption at resonance turns out to be so

[5] Meitner, Hahn and Strassman, Zeits. f. Physik **106**, 249 (1937).

[6] v. Halban, Kovarski and Savitch, Comptes rendus **208**, 1396 (1939).

[7] H. L. Anderson and E. Fermi, Phys. Rev. **55**, 1106 (1939).

large that even at the optimum concentration of hydrogen it is at present quite uncertain whether neutron production will exceed the total neutron absorption. More information concerning the resonance absorption of uranium as well as more accurate measurement of some of the values which enter into our calculation are required before we can conclude whether a chain reaction is possible in mixtures of uranium and water.

We wish to thank Dr. D. W. Stewart, of the Department of Chemistry, and Mr. S. E. Krewer, for advice and assistance in carrying out some of these experiments. We are much indebted to the Eldorado Radium Corporation for enabling us to work with large quantities of uranium oxide in our experiments, and to the Association for Scientific Collaboration for the use of the photo-neutron source and other facilities.

LETTERS TO THE EDITOR

Prompt publication of brief reports of important discoveries in physics may be secured by addressing them to this department. Closing dates for this department are, for the first issue of the month, the eighteenth of the preceding month, for the second issue, the third of the month. Because of the late closing dates for the section no proof can be shown to authors. The Board of Editors does not hold itself responsible for the opinions expressed by the correspondents.

Communications should not in general exceed 600 words in length.

Some New Reactions in Light Nuclei with High Energy Protons

Reaction processes in the simplest nuclear systems have the most hope of being understood in the light of theory, but as yet, even in this restricted part of the field of nuclear physics, not by any means all reactions possible with energies and sources now available have been observed, much less studied. In this note are reported some recent investigations in this region.

1. It was noticed that many materials when bombarded by high energy protons from the Princeton cyclotron gave a 21-minute period, apparently from a common contaminant. The following observations indicate that the reaction in question is N^{14} (H^1, He^4) C^{11}: (*a*) Recoil nuclei collected in nitrogen on platinum or lead gave the characteristic period. (*b*) Positrons are emitted. (*c*) The period coincides with that of C^{11} as determined by other observers. (*d*) The activity behaves chemically like carbon. Recoils were collected on paper and the paper burned in an atmosphere of O_2. When the products of combustion were bubbled through a solution of $Ca(OH)_2$, the activity appeared in the precipitate, which presumably was $CaCO_3$.

The excitation function, Fig. 1, was determined from the initial intensity of the 21-minute period observed on a series of equally spaced aluminum foils traversed by the beam in air. (After bombardment for 18 minutes in air with 5.7-Mev protons, the activity on a foil is due to F^{18} only to the extent of 1.4 percent. Aluminum itself is inactive with this proton energy.) The unavoidable range distribution in the proton beam has, of course, some effect on the shape of the excitation curve. In the figure, therefore, the limits determined by an analysis of the beam are indicated.

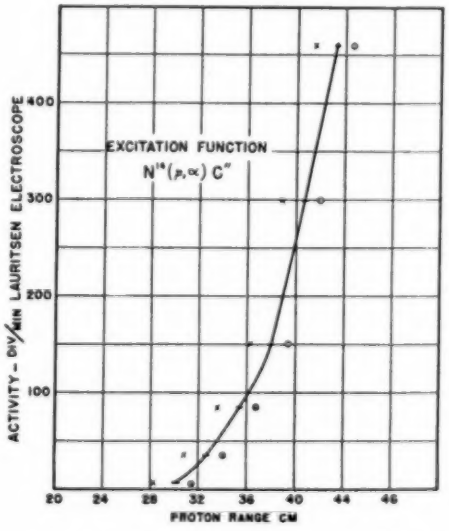

FIG. 1. Activity of C^{11} recoils *versus* proton range. Circles—maximum range of proton beam. Crosses—mean range of beam. Curve drawn through points corresponding to extrapolated range. Correction made for straggling. No correction applied for recoil of compound nucleus.

2. When boron was bombarded with 5.9-Mev protons, a very intense C^{11} activity was observed. The reaction B^{10} (p, γ) C^{11} is well known, but the C^{11} activity was so great that it is difficult to account for it by the (p, γ) reaction alone. The thick-target excitation function for such a resonance process rises only moderately with energy. It seemed plausible therefore to ascribe a large part of the activity to B^{11} (p, n) C^{11}. To test this hypothesis an observation on the neutrons released by this reaction was made. With a clean lead target for a "control" experiment the average initial activity observed in a silver detector after the neutrons were slowed down in paraffin was 29.9 $\pm$0.5 divisions per minute per microampere. Under similar conditions with a target of amorphous boron mechanically pressed into lead, the detector activity observed was 45.2 $\pm$0.8 divisions per minute per microampere. Neutrons might also be produced in the reaction B^{10} (p, n) C^{10}. Nothing is known about C^{10}, however. No strong period corresponding to this isotope of over a few seconds' half-life was observed; a weak period could have been obscured by the C^{11} activity. Since the threshold for the B^{11} (p, n) C^{11} reaction is about 3.5 Mev, whereas the B^{10} (p, n) C^{10} reaction has an expected threshold[1] at about 5 Mev, and considering the relative abundances of the boron isotope, it seems safe to conclude that most of the neutrons observed come from B^{11}.

3. A strong 2.5-minute activity has been produced in silicon by bombardment with 5.8-Mev protons, and is assigned to the reaction Si^{30} (p, n) P^{30}. It is of some interest to remark that no evidence for the reaction Si^{29} (p, α) Al^{26} was obtained, although the proton energy was far above the anticipated threshold.

The writer wishes to express his appreciation for the hospitality of the Palmer Physical Laboratory, and to record his indebtedness to members of the cyclotron group for their cooperation, without which this work could not have been done.

WALTER H. BARKAS*

Palmer Physical Laboratory,
Princeton, New Jersey,
July 13, 1939.

* Member, The Institute for Advanced Study, Princeton, New Jersey.

[1] H. A. Bethe, Phys. Rev. **55**, 439 (1939).

Re-Measurement of the Energies Released in the Reactions Li^7 (p, α) He^4 and Li^6 (d, α) He^4

The energies released in the reactions Li^7 (p, α) He^4 and Li^6 (d, α) He^4 were measured in 1935 by Oliphant, Kempton, and Rutherford.[1] They used a variable pressure air absorption tube which was calibrated with the precisely measured natural alpha-particles from ThC′. They obtained 17.06 ± 0.06 Mev for the Li^7 reaction and 22.06 ± 0.07 Mev for the Li^6 reaction. These values, slightly revised by Livingston and Bethe,[2] have been used by Allison,[3] together with the precise results on the beryllium-proton reactions, obtained by electrostatic analysis,[4,5] to set up masses for several of the lightest atoms.

Recently Bethe[6] has reinterpreted the 1935 Cavendish result on Li^6, raising it to 22.21 Mev, and Oliphant[7] has stated that the correct value may well lie outside the limits specified in the Cavendish result.

We have therefore repeated the earlier work, using an absorption cell in much the same manner. The use of thin collodion windows on the cell instead of mica, the use of thin instead of thick targets, and the prevention of the formation of oil films on the targets differentiated our work from the earlier attempts. Also the higher voltage available for the bombarding beam gave higher yields of disintegration particles and made possible the use of smaller apertures through which they were counted. Several runs were made on different targets of LiF for a period extending over several weeks. In the case of Li^6 a separated target produced in the mass spectrograph by L. H. Rumbaugh was used and gave results no different from the LiF targets. We obtained 17.28 ± 0.03 Mev for the Li^7 reaction and 22.20 ± 0.04 for the Li^6 reaction.

These new values may now be used in connection with our electrostatic analyzer results to give $Li^6 = 6.01682 \pm 0.00011$, $Li^7 = 7.01784 \pm 9$, $Be^8 = 8.00766 \pm 15$, $Be^9 = 9.01486 \pm 13$. These are based on the usual values of H, D and He^4.

Our results confirm Bethe's revision of the Li^6 reaction energy release, and our masses agree closely with those of Bethe-Barkas.[8] The question of the stability of Be^8 is now undecided by these masses, but on the Gamow theory of alpha-particle decay we may predict a minimum lifetime of 10^{-16} second for this nucleus.[9]

A detailed account of this investigation is being submitted for publication by one of us. The progress of this work was greatly aided by a grant from the American Philosophical Society.

SAMUEL K. ALLISON
LESTER S. SKAGGS
NICHOLAS M. SMITH, JR.

Ryerson Physical Laboratory,
University of Chicago,
Chicago, Illinois,
July 13, 1939.

[1] M. L. E. Oliphant, A. R. Kempton, Lord Rutherford, Proc. Roy. Soc. London **A149**, 406 (1935).
[2] M. S. Livingston and H. A. Bethe, Rev. Mod. Phys. **9**, 371 (1937)
[3] S. K. Allison, Phys. Rev. **55**, 624 (1939).
[4] S. K. Allison, L. S. Skaggs and N. M. Smith, Jr., Phys. Rev. **54**, 171 (1938).
[5] L. S. Skaggs, Phys. Rev. **56**, 24 (1939).
[6] H. A. Bethe, private communication. See also W. H. Barkas, Phys. Rev. **55**, 691 (1939), reference 13.
[7] M. L. E. Oliphant, private communication.
[8] W. H. Barkas, Phys. Rev. **55**, 691 (1939).
[9] H. A. Bethe, Rev. Mod. Phys. **9**, 71 (1939), Table XXX, p. 167.

Investigation of Boron by Slow Neutrons

A cloud chamber investigation[1] of the B^{10} (n, α) disintegration appeared to indicate an asymmetrical distribution with respect to the plane perpendicular to the incident neutron direction. In these preliminary observations only 75 disintegrations were observed, of which 45 occurred in the forward direction and 30 in the backward. A fuller investigation has now been made by means of an ionization chamber, and the results demonstrate that the distribution is symmetrical.

W. E. GOOD
R. D. HILL

Department of Physics,
University of Illinois,
Urbana, Illinois,
July 5, 1939.

[1] Goldhaber, Hill, Kruger and Stallman, Phys. Rev. **55**, 1117 (A) (1939).

Disintegration of Deuterium by Protons and p-n Reactions in Light Gaseous Elements

Neither of the homologous reactions,

$$H^1 + H^2 \rightarrow 2H^1 + n^1, \quad (1)$$

$$n^1 + H^2 \rightarrow H^1 + 2n^1, \quad (2)$$

have heretofore[1] been observed, in spite of the importance to be attached to such simple disintegrations which may be treated theoretically with considerable rigor, and consequently may provide additional information concerning nuclear interactions.

The binding energy of the deuteron[2] is 2.17 Mev and therefore the threshold of the reactions (1) and (2) should be reached with protons or neutrons of 3.25 Mev. The present report is to record an experiment designed to detect reaction (1).

A chamber was constructed so that gases could be used as targets for the proton beam from the Princeton cyclotron. The lead lining of the chamber was electrically insulated so that it could also be used as a Faraday collector for the protons which entered through a one-mil aluminum window. Steps were taken to minimize the neutron background caused by bombardment of internal parts of the cyclotron itself. Neutrons generated by disintegrations in the chamber were slowed down in paraffin and measured with a silver detector. Observations were taken when the target was deuterium under one atmosphere pressure, and also normal hydrogen under the same conditions. With the normal hydrogen in the chamber the average initial activity of the detector was 0.238 ± 0.004 div./sec. per microampere. When the chamber contained deuterium the activity was 0.623 ± 0.004 div./sec. per microampere.

With the same geometrical arrangement the neutrons produced in O_2, N_2, CO_2 and A, at one atmosphere pressure in each case, were also observed. Some experiments on the efficiency of the collector in the presence of the various gases indicated that in some cases the apparent proton current was affected somewhat by ionization in the gas. Except for the isotopes of hydrogen the comparison between gases can therefore be only semi-quantitative. Consequently it can only be said that from O_2, N_2 and C the neutron emission is

considerably less than from D_2, the neutrons presumably coming from p, n reactions in the rare isotopes. From argon the neutron emission is larger, about the same as from D_2, giving evidence for the reaction A^{40} (p, n) K^{40}.

We may estimate the absolute cross section for the reaction (1) using the observed ratio of neutrons from deuterium to those from oxygen. DuBridge *et al.*[3] have obtained the absolute cross section and excitation function for O^{18} (p, n) F^{18} at somewhat lower energies than those used in these experiments. We have obtained a rough excitation curve for the reaction at higher energies and have joined this smoothly to the curve obtained by the authors cited. We are thus able to obtain the absolute cross section by referring to this curve. For protons of 5.1 Mev the cross section is found to be about 1.4×10^{-26} cm². However, because of the uncertainties involved in the estimate, only the order of magnitude of the cross section can be said to be known with certainty.

This cross section is too large to be accounted for by a secondary process, *viz.* H^2 (H^2, n^1) He^3, which takes place when elastically recoiling deuterons traverse the deuterium gas.

Princeton University,
Princeton, New Jersey,
July 12, 1939.

WALTER H. BARKAS*
MILTON G. WHITE

* Member, The Institute for Advanced Study, Princeton, New Jersey.
[1] See, however, Lewis *et al.*, Phys. Rev. **45**, 242 (1934), **45**, 497 (1934).
[2] H. A. Bethe, Phys. Rev. **53**, 313 (1938).
[3] DuBridge, Barnes, Buck and Strain, Phys. Rev. **53**, 450 (1938).

X-Ray Fluorescing Coefficient and the Orientation of a Zinc Crystal

The intensity of the diffuse scattering of x-rays from an anisotropic crystal such as zinc is a function of the orientation angle ψ, which is the angle that the line bisecting the angle between the forward direction of the scattered rays and the backward direction of the incident rays makes with the c axis. So also is the intensity of a Bragg reflection from zinc a function of this angle ψ. The variation in both cases is due (a) to the anisotropy in the thermal vibrations of the atoms in the crystal and (b) to the distortion of the electron cloud around the atom. It seemed worth while to test whether the fluorescence coefficient might also be a function of ψ.

Approximately monochromatic rays ($\lambda=0.71$A) were obtained by passing x-rays from a molybdenum target tube through a zirconium filter. These rays fell at a glancing angle θ on the surface of a zinc crystal and the intensity of the secondary rays was measured in the direction ϕ by means of an ionization chamber and electrometer. The secondary rays consisted of fluorescent and scattered rays, the former being much more intense than the latter. We tested the intensity from a (0002) face ($\psi=0°$) of a crystal and compared this with the intensity from a $(10\bar{1}0)$ face ($\psi=90°$) of a second crystal. With $\phi=60°$, θ was given values between 20° and 40°; with $\phi=40°$, θ was given values between 12° and 28°. In order to separate the fluorescent rays from the scattered rays (including a possible small Bragg reflection at $\theta=\phi/2$), a thickness 0.025 cm of aluminum was transferred from the primary beam to the secondary beam. When in the secondary beam, this thickness cuts out practically all of the fluorescent radiation. Subtraction of the intensity reading when the aluminum is in the secondary beam from that when it is in the primary beam gives the intensity due to the fluorescent rays. In all cases we found that $(I_\phi, \theta)_{\psi=0°} = (I_\phi, \theta)_{\psi=90°}$ to within one percent.

We next passed θ through the value 8°15′, which is the position for first-order reflection of $\lambda=0.71$A from the (0002) planes. We thought that, due to extinction coming into play, there perhaps would be a change in the intensity of the fluorescent rays at $\theta=8°15'$. We found no such change.

We finally conclude that the coefficient of x-ray fluorescence (K characteristic rays) is not a function of the orientation of an anisotropic crystal such as zinc.

O. J. BALTZER
G. E. M. JAUNCEY

Wayman Crow Hall of Physics,
Washington University,
St. Louis, Missouri,
July 3, 1939.

Superstructure in Fe Ni_3

In a paper just published Leech and Sykes[1] report the detection by x-rays of superstructure in Fe Ni_3 in specimens which had been heated at 490°C, for times from 50 to 150 hours, and cooled very slowly to 370°C. In some previous experiments[2] I was unable to find superstructure in this alloy after heating at 425°C for 100 hours. I have made another test in which a specimen containing 73.8 percent nickel was heated at 490°C for six days and then cooled to 440°C in fourteen days. This specimen gave superstructure lines with sixteen hours' exposure to x-rays, thus confirming the results of Leech and Sykes.

Sykes and Jones[3] have shown that, when a quenched specimen of the alloy Cu_3Au is heated, lowering of resistance first occurs at the same temperature at which ordering becomes sufficient to be detected by x-rays. It is interesting to point out that this is apparently not the case for Fe Ni_3; Dahl[4] has reported that with heat treatments of one hour duration the resistance of the quenched alloy begins to decrease at about 250°C and that of the hard-worked alloy at 100°C, both reaching a minimum resistance at 425°C. My first x-ray experiments upon Fe Ni_3 in which order was not detected were made upon specimens heated at 425°C, to coincide with this minimum point. The specific heat curve given by Leech and Sykes for quenched specimens of Fe Ni_3 begins to show its first dip due to partial ordering at about 360°C with a minimum at 425°C, and it is possible that slower heating might lower both of these temperatures considerably. These data indicate that most of the decrease of resistance upon heating is due to order over distances too short to be detected by x-rays, although it is not clear that the effect in the cold-worked alloy can be entirely accounted for in this manner.

F. E. HAWORTH

Bell Telephone Laboratories,
New York, New York,
June 30, 1939.

[1] P. Leech and C. Sykes, Phil. Mag. Ser. 7, **28**, 742 (1939).
[2] F. E. Haworth, Phys. Rev. **54**, 693 (1938).
[3] C. Sykes and F. W. Jones, Proc. Roy. Soc. **A157**, 213 (1936).
[4] O. Dahl, Zeits. f. Metallkunde **28**, 133–38 (1936).

On the Sensitivity of Photographic Emulsions for Electrons Between 50 and 100 kev

Because the papers published[1-5] up to now contain little information about the relative sensitivities of different photographic emulsions for electrons with speeds of 50 to 100 kev, the author believes it useful to describe some measurements made by him in this field.

One classification of emulsions, by Knoll and v. Borries,[5] has been established for exposure times of 10^{-8} to 10^{-7} second. The present measurements were made for exposures of 10^{-3} to 1 second. They indicate only relative values, not absolute sensitivities. The objective is to permit the choice of the best emulsion for electron microscopy, or similar purposes, so that the relative amount of backening obtained with different emulsions, rather than the absolute ratio of blackening to incident charge, is the factor of importance. Therefore a standard emulsion has been chosen and all the blackening values measured with reference to this standard emulsion.

The experimental procedure was as follows: The different emulsions to be compared were cut in strips and placed side by side in a cassette. The emulsions which had to be compared were exposed to the electron beam simultaneously with the standard emulsion and developed and fixed together. This procedure does not give directly either absolute blackening curves or the variation of sensitivity as a function of the electron velocity. If these functions are to be determined, the absolute value of sensitivity of at least one of the emulsions must be determined as a function of the intensity of incident beam and velocity.

The comparison was made by using the electron microscope described in previous articles,[6] removing the specimen holder from the object chamber. The coil currents may be adjusted so that an area of uniform current density of 60-mm diameter is obtained in the photographic chamber. After having exposed the emulsions for the first time for a short duration, the cassette containing them is displaced several millimeters and a second, longer, exposure is superimposed. By repeating this procedure several times, a series of blackenings is obtained. Fig. 1 shows the appearance of the exposed emulsions. This procedure presupposes the Bunsen-Roscoe law to be valid for electrons, which seems to be established by a great number of experimenters.

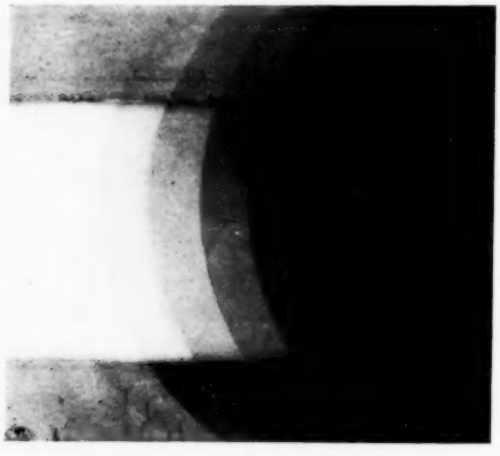

FIG. 1. Appearance of photographic emulsions exposed to electrons.

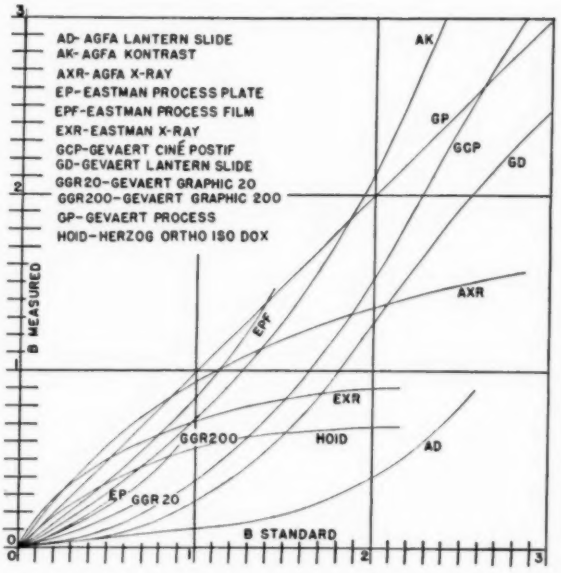

FIG. 2. Comparison of blackening of emulsions.

The measurement of the blackening was accomplished by means of an improvised microphotometer consisting of a microscope with a barrier layer cell substituted for the eyepiece. Fig. 2 shows results obtained for the blackening of the measured emulsion as a function of the blackening of the standard emulsion. As standard the Gevaert Process Plate has been chosen. The blackening of this necessarily appears in the curves as a straight line at 45° to the axis.

This comparison seems to show that for a low value of blackening x-ray films are more sensitive than any other type of emulsion chosen. On the other hand, if we desire higher values of blackening, the process type emulsions are more suitable. It is thus not possible to order emulsions according to their relative merit, as the latter depends on the range of blackening covered.

L. MARTON

Collingswood, New Jersey,
June 29, 1939.

[1] C. D. Ellis and G. H. Aston, Proc. Roy. Soc. **A119**, 645 (1928).
[2] A. Becker and E. Kipphan, Ann. d. Physik **10**, 15 (1931).
[3] H. Schaffer, Archiv f. Elektrotech. **26**, 313 (1932).
[4] B. v. Borries, Thesis Berlin 1932, Forschungsheft 3 der Studiengesettschaft f. Hochstspannungsanlagen, Berlin, 1934.
[5] B. v. Borries and M. Knoll, Physik Zeits. **35**, 279 (1934).
[6] L. Marton, Bull. Acad. Belg. Brux. **21**, 606 (1935).

THE AMERICAN INSTITUTE OF PHYSICS

INCORPORATED

ADMINISTRATIVE STAFF

HENRY A. BARTON, *Director*

MADELINE M. MITCHELL, *Publications Manager*

Office: 175 Fifth Avenue, New York, New York

JOURNALS

THE PHYSICAL REVIEW
REVIEWS OF MODERN PHYSICS
JOHN T. TATE, *Editor*
J. W. BUCHTA, *Assistant Editor*

JOURNAL OF APPLIED PHYSICS
ELMER HUTCHISSON, *Editor*

THE JOURNAL OF THE OPTICAL SOCIETY OF AMERICA
THE REVIEW OF SCIENTIFIC INSTRUMENTS
F. K. RICHTMYER, *Editor*

JOURNAL OF THE ACOUSTICAL SOCIETY OF AMERICA
FLOYD A. FIRESTONE, *Editor*

THE JOURNAL OF CHEMICAL PHYSICS
HAROLD C. UREY, *Editor*
JOSEPH E. MAYER, *Assistant Editor*

THE AMERICAN PHYSICS TEACHER
DUANE ROLLER, *Editor*

GOVERNING BOARD

For The American Physical Society:

JOHN T. TATE, *Chairman*
University of Minnesota

GEORGE B. PEGRAM, *Secretary*
Columbia University

KARL T. COMPTON
Massachusetts Institute of Technology

For The Optical Society of America:

E. C. CRITTENDEN
National Bureau of Standards

A. C. HARDY
Massachusetts Institute of Technology

W. B. RAYTON
Bausch & Lomb Optical Company

For The Acoustical Society of America:

FLOYD A. FIRESTONE
University of Michigan

HARVEY FLETCHER
Bell Telephone Laboratories

WALLACE WATERFALL
The Celotex Corporation

For The Society of Rheology:

WHEELER P. DAVEY
Pennsylvania State College

MELVIN MOONEY
United States Rubber Products, Inc.

R. L. PEEK, JR.
Bell Telephone Laboratories

For The American Association of Physics Teachers:

PAUL E. KLOPSTEG
Central Scientific Company

FREDERIC PALMER, JR.
Haverford College

F. K. RICHTMYER
Cornell University

The American Institute of Physics is a membership corporation of which five societies are the founding members. These five societies are the principal national societies devoted to pure and applied physics in America. Their names, and those of their representatives who form the Governing Board of the Institute, are given above. The principal work of the Institute is the publication of journals sponsored by the societies or by itself. The names and the editors of the journals are also listed above.

The broad purpose of the Institute is to represent, in all matters of wide or common interest, the five thousand or more members and subscribers associated with the Founder Societies and the journals. It aims to advance the science and profession of physics, and to promote cooperation between pure research, the applied sciences and the industries. To achieve these aims, it is greatly in need of an endowment and is empowered by law to administer grants and funds of any kind.

CONTENTS

PHYS. REV. 56 (1939) AUGUST 1

East-West Symmetry of the Cosmic Radiation at Very High Elevations Near the Equator and Evidence that Protons Constitute the Primary Particles of the Hard Component . . . . . THOMAS H. JOHNSON AND J. GRIFFITHS BARRY 219

Angular Dispersion of the Cosmic Radiation in the Upper Atmosphere Resulting from Deflections of Low Energy Particles in the Earth's Magnetic Field . . . T. H. JOHNSON 226

Further Experiments on the Recoil of the Nucleus in Beta-Decay . . . . . H. R. CRANE AND J. HALPERN 232

Delayed Gamma-Rays from Uranium Activated by Neutrons . J. C. MOUZON AND R. D. PARK 238

On the Total Scattering of X-Rays from Crystals . . . . . G. G. HARVEY 242

On Alleged Discontinuities in the Diffuse Scattering of X-Rays from Crystals at Small Angles . . . . . G. G. HARVEY 247

Nuclear Five-Body Problem . . . . . WARREN A. TYRRELL, JR. 250

Dissociation of Propane, Propylene and Allene by Electron Impact . . . . . J. DELFOSSE AND WALKER BLEAKNEY 256

Collision Cross Sections for D-D Neutrons . . W. H. ZINN, S. SEELY AND V. W. COHEN 260

Concentration of Isotopes by the Evaporative Centrifuge Method . . . . . J. W. BEAMS AND C. SKARSTROM 266

Regularities in the Third Spectrum of Thorium . . . . . R. J. LANG 272

7.4μ Fundamental Vibration of Methyl Chloride . ALVIN H. NIELSEN AND HARALD H. NIELSEN 274

Space Charge and Field Waves in an Electron Beam . . . . . SIMON RAMO 276

Neutron Production and Absorption in Uranium . . . . . H. L. ANDERSON, E. FERMI AND LEO SZILARD 284

Letters to the Editor:

Some New Reactions in Light Nuclei with High Energy Protons . . . . WALTER H. BARKAS 287

Re-Measurement of the Energies Released in the Reactions Li^6 (p, α) He^4 and Li^6 (d, α) He^4 . . . . . SAMUEL K. ALLISON, LESTER S. SKAGGS AND NICHOLAS M. SMITH, JR. 288

Investigation of Beryl by Slow Neutrons . . . . . W. E. GOOD AND R. D. HILL 288

Disintegration of Deuterium by Protons and p–n Reactions in Light Gaseous Elements . . . . . WALTER H. BARKAS AND MILTON G. WHITE 288

X-Ray Fluorescing Coefficient and the Orientation of a Zinc Crystal . . . . . O. J. BALTHER AND G. E. M. JAUNCEY 289

Superstructure in Fe Hi . . . . . F. E. HAWORTH 289

On the Sensitivity of Photographic Emulsions for Electrons Between 50 and 100 kev . L. MARTON 290

LANCASTER PRESS, INC., LANCASTER, PA.